An Investigation of the Relationship Between Total Non-Methane Organic Carbon and the sum of speciated Hydrocarbons and Carbonyls Measured by Standard GC/FID: Validation and Refinement of a New Instrument, and Measurements in the South Coast Air Basin

Agreement No. 98-323

State of California Air Resources Board

Final Report

June 6, 2002

Principal Investigator:

Suzanne Paulson

Researchers:

Christophe Maris

Myeong Chung

Udo Krischke

Atmospheric Sciences Department

University of California at Los Angeles

Los Angeles, CA 90095-1565

DISCLAIMER

The statements and conclusions in this report are those of the University and not necessarily those of the California Air Resources Board. The mention of commercial products, their source, or their use in connection with material reported herein is not to be construed as actual or implied endorsement of such products.

Table of Contents

TABLE OF CONTENTS III

LIST OF FIGURES VI

LIST OF TABLES X

ABSTRACT XI

EXECUTIVE SUMMARY XII

1. INTRODUCTION 1

2. INSTRUMENT DEVELOPMENT 4

2.1 Instrument Overview 4
2.1.1 GC analysis 5

2.2 Major Design Changes During this Period 8
2.2.1 Methanizer and Oxidation Catalyst 8
2.2.1.1 Oxidation Capacity with Current Gas Flows 11
2.2.1.2 Effect of Relative Humidity on TNMOC and the Oxidation Catalyst 12
2.2.1.3 New Methanizer Material 13

2.3 Instrument Blank 15
2.3.1 Technique and Procedure 15
2.3.2 Instrument Modifications and Verification 17
2.3.3 Summary 19

2.4 Smog Chamber Validation Experiments 19
2.4.1 Experimental Description 19
2.4.2 Isoprene Photooxidation 20
2.4.3 m-Xylene Photooxidation 21
2.4.4 □□Pinene Photooxidation 22
2.4.5 Effect of Sample Flow Rate on Recovery of Semivolatile Products 23
2.4.6 Effect of Desorption Temperature on Recovery of Semivolatiles 23

2.5 Behavior of Aerosol Particles in Sampling Lines 24
2.5.1 Materials and Methods 25
2.5.2 Results 26

2.6 Detection Limit and Uncertainties **27**

3. FIELD MEASUREMENT SITES AND INSTRUMENTATION 31

3.1 UCLA **31**

3.2 Burbank **33**

3.3 Instrumentation **33**

3.45 Calibrations and Uncertainties **34**
3.4.1 Total Non-Methane Organic Carbon Analyzer 34
3.4.2 NO_x Analyzer 35
3.4.3 O_3 Analyzer 36
3.4.4 Aerosol Analyzer 36

3.5 Instrumental Setup **36**

3.6 Retention index **38**

4. 1999 FIELD DATA 39

4.1 Methanizer Conversion Rate **39**

4.2 UCLA **40**
4.2.1 Meteorology 40
4.2.2 Trace gases 41
4.2.3 Particles 42
4.2.4 TNMOC and sum of speciated VOC's 44

4.3 Burbank **46**
4.3.1 Meteorology 46
4.3.2 Trace gases 48
4.3.3 Particles 49
4.3.4 TNMOC and sum of speciated VOC's 49
4.3.5 Conclusion 53

4.4 Estimation of Air mass Age in the UCLA and Burbank Data **53**
4.4.1 Identification of Peaks in Speciated VOC's Chromatograms 54
4.4.2 Use of Aromatics to Estimate Photochemical Aging 54
4.4.3 Aromatic ratios and Air Mass Age 55
4.4.3.1 UCLA Aromatic Data 55
4.4.4 VOC/NO_x Ratios and Ozone 59

5. 2000 FIELD CAMPAIGNS 64

5.1 Measurements at UCLA During September and October **65**

5.2 December Measurements **81**

5.3 Discussion **88**
5.3.1 Cloudy and Clear Days 88
5.3.2 Weekend Effect? 91
5.3.3 Correlations of TNMOC/sum of speciated VOC's Ratio and VOC's with Winds, O_3, and NO_x 92
5.3.4 Nighttime O_3 96
5.3.5 Aromatic Ratios 96
5.3.6 VOC Speciation and [TNMOC]/[∑SP] 101
5.3.7 C_2-C_6 Hydrocarbons 104

5.4 Conclusions **105**

6. DIESEL BUS STUDY 107

6.1. Introduction **107**

6.2. Sample Collection **107**

6.3. Results and Discussion **107**
6.3.1 Calibration Standard 108
6.3.2.1 Unburned Diesel Fuel 109
6.3.3 Drive Cycle Results 109
6.3.3.1 TNMOC and sum of speciated VOC's 110
6.3.2.3 Speciated Hydrocarbon Concentrations 111
CBD 1 112
6.3.4 Tedlar Bag Measurements 114

6.4 Conclusions **117**

7. GASOLINE VAPOR 119

8. CONCLUSIONS 123

9. REFERENCES 126

10. GLOSSARY 130

List of Figures

Figure 2.1.1 Valve schematic showing flow path for sample acquisition. FC = flow controller, Pd = palladium oxidation catalyst, He/O_2 = 500 ppm O_2 in He mixture. Dotted lines indicate a separate flow path for speciated VOC's; solid lines indicate the TNMOC flow path……. 6
Figure 2.1.2a. Flow schematic for desorption of TNMOC samples with out oxidation. 6
Figure 2.1.2b Flow schematic for desorption of TNMOC samples with oxidation. 7
Figure 2.1.3 Flow schematic for injection in gas chromatograph and subsequent analysis. 7
Figure 2.1.4. Photograph of the instrument, oxidation and reduction catalysts. 8
Figure 2.2.1 Decrease of the methanizer conversion efficiency vs. the number of intervening ambient air samples on 10/12/99.The design of the TNMOC plumbing was altered slightly to avoid introducing O_2 into the methanizer. The current design uses only He to purge the sample from the first to the second trap of the TNMOC channel. 9
Figure 2.2.2: Schematic representation of GC flow scheme during the field experiments (A) and current flow scheme (B). Straight lines: TNMOC channel, dotted lines: Speciated VOC's channel, FC: Flow controller. 11
Figure 2.2.3 Oxidation efficiency of the oxidation catalyst without recharging with He/O_2 during the entire run series. For these experiments, carbon loading in each sample was 18 ppmC, 10-100 times larger than levels in urban ambient air. In practice, the oxidation catalyst is recharged between each run. 12
Figure 2.2.4 Relationship between the relative humidity and the ratio of TNMOC/ Sp. VOC's. The upper panel (a) is data collected during September and October, and the lower panel is data collected during November and December 2000. 13
Figure 2.2.5 Chromatograms of n-hexane calibration of the TNMOC channel in non-oxidation and oxidation mode with Ni and Ru based methanizers. 15
Figure 2.3.6 New design of trap 1. 18
Figure 2.4.1 Concentrations of TNMOC, isoprene and Total speciated compounds as a function of time. 21
Figure 2.4.2 Concentrations of TNMOC, m-xylene and Total speciated compounds as a function of time. 22
Figure 2.4.3 Concentrations of TNMOC, -pinene, and speciated VOC's as a function of time. The flow rate in the sampling line was increased for the last two measurements, and is probably responsible for the relative increase in TNMOC signal. 23
Figure 2.4.4 Measurements of TNMOC, -pinene and sum of speciated VOC's. Runs (measurements) 1-4 were before photooxidation began. Numbers indicate the desorption temperature of trap I. Runs 5-7 and 8-11 were made after 20 minutes and 40 minutes, respectively, of exposure to blacklamps that initiate photochemical oxidation of -pinene. 24

Figure 2.5.1 Transmission of aerosols through a heated 10 m x _" OD Teflon sampling line at different flow rates. Measurement labeled "chamber" were made through a ~0.5 m x _" OD copper sampling line. The total mass measured at the chamber is equivalent to roughly 25 g/m^3. 26
Figure 2.5.2 Transmission of aerosols through a heated 1/8" OD Silco-steel sampling line at different flow rates. Measurement labeled "chamber" were made through a ~0.5 m x _" OD copper sampling line. The total mass measured at the chamber is equivalent to roughly 15 g/m3. 27
Figure 3.1 Half hourly averaged wind direction for (a) sunny (circles) and cloudy (triangles) days during Sept.-Oct. and (b) all sampling days during December. 31
Figure 3.2 Map of the western portion of the Los Angeles air basin. Stars indicate the locations of the measurement sites at Azusa, Burbank and UCLA. Azusa was the subject of measurements in 1997, and is used for comparison in Section 5. 32
Figure 3.3 Map showing location of the Sampling site on the UCLA campus. 33
Figure 3.5.1: Schematic representation of the instrumental setup at Burbank and UCLA during 1999. The flow rates are indicated at several points with arrows, followed by the cumulative residence time for each point. 37
Figure 3.5.2. Flow schematic of the sampling manifold for the field measurements at UCLA during 2000. 38
Figure 4.2.1 Meteorological data at UCLA during the period of the measurements. Zero degrees in wind direction indicates North. 41
Figure 4.2.2: Results of the NO, NO_2, NO_x, and O_3 measurements at UCLA campus during 1999. 42
Figure 4.2.3 TNMOC at UCLA. The sparseness of the data coverage is due to the problems with the methanizer conversion efficiency—points with lower than 80% conversion are not shown. 43
Figure 4.2.4 Sum of speciated VOC's at UCLA. 44
Figure 4.2.5. Hour-of-day averaged mean values of TNMOC and sum of speciated VOC's at the UCLA measurement site. The vertical error bars indicate the span of the measurements at each hour; points with no error bars had only one point. Since the sampling time of the instrument is only 10 minutes, some points that were acquired at different fractions of an hour were binned together, and the horizontal error bars indicates the span of the measurement times. 45
Figure 4.2.6. Plot of the ratio of TNMOC vs. the sum of speciated VOC's for the UCLA data. 46
Figure 4.3.1 Meteorological conditions at Burbank during the period of the measurements. A wind direction of zero indicates North. 47
Figure 4.3.2: Results of the NO, NO_2, NO_x, and O_3 measurements at the Burbank station. 48
Figure 4.3.3 TNMOC concentration data from acquired at the Burbank station. 49
Figure 4.3.4 Sum of speciated VOC's at Burbank. 50
Figure 4.3.5. Hour-of-day averaged mean values of TNMOC and sum of speciated VOC's at the Burbank measurement site. The vertical error bars indicate the span of the measurements at each hour; points with no error bars had only one

point. Since the sampling time of the instrument is only 10 minutes, some points that were acquired at different fractions of an hour were binned together, and the horizontal error bars indicates the span of the measurement times. 51
Figure 4.3.6. Plot of the ratio of TNMOC vs. the sum of speciated VOC's for the Burbank data. 52
Figure 4.3.7. Plot of TNMOC/sum of speciated VOC's ratio vs. time of day for Burbank. 52
Figure 4.4.5 Ln(m&p-xylene/ethyl benzene) vs. TNMOC/sum of speciated VOC's ratio at Burbank. The line indicates linear least squares fit, which has a correlation coefficient (R^2 value) of 0.0.03. 57
Figure 4.4.6 TNMOC/sum of speciated VOC's ratio vs. O_3 at UCLA. The line indicates linear least squares fit, which has a correlation coefficient (R^2 value) of 0.07. 58
Figure 4.4.7 Hour-of-day averaged mean values of TNMOC/NO_X and sum of speciated VOC's/ NO_x ratios vs. Ozone at Burbank. 59
Figure 4.4.8 NO_x vs. O_3 at Burbank. The line indicates linear least squares fit, which has a correlation coefficient (R^2 value) of 0.37. 60
Figure 4.4.9 TNMOC/NO_x vs. O_3 at Burbank. The line indicates linear least squares fit, which has a correlation coefficient (R^2 value) of 0.37. 60
Figure 4.4.10 Sum of speciated VOC's/NO_x vs. O_3 at Burbank. The line indicates linear least squares fit, which has a correlation coefficient (R^2 value) of 0.41. 61
Figure 4.4.11 Hour-of-day averaged mean values of TNMOC/NO_X and sum of speciated VOC's/ NO_x ratios vs. Ozone at UCLA. 62
Figure 4.4.12 NO_x vs. O_3 at UCLA. The line indicates linear least squares fit, which has a correlation coefficient (R^2 value) of 0.32. 62
Figure 4.4.12 TNMOC/NO_x vs. O_3 at UCLA. The line indicates linear least squares fit, which has a correlation coefficient (R^2 value) of 0.38. 63
Figure 4.4.13 TNMOC/sum of speciated VOC's ratio vs. O_3 at UCLA. The line indicates linear least squares fit, which has a correlation coefficient (R^2 value) of 0.22. 63
. 63
Figure 5.1.2 TNMOC, sum of speciated VOC's, TNMOC/sum of speciated VOC's, NO, NO_2, NO_x, O_3, and the vertical temperature profile from Miramar for cloudy days in September-October 2000. 73
Figure 5.1.3 Comparison of the trends of meteorological data for clear weekdays and weekends. 74
Figure 5.1.4. Trends of O_3, NO_x and total non-methane hydrocarbon concentrations ([TC]), TNMOC/sum of speciated VOC's ratio and residence time (calculated from ln([xylene]/[ethylbenzene])) versus time of day for clear weekdays and weekends. 76
Figure 5.1.5. Trends of O_3, NO_x concentrations (average per hour) versus time of day for clear weekdays in September-October period from AQMD data. 77
Figure 5.1.6 Comparison of the trends of meteorological data for cloudy weekdays and weekends. 78

Figure 5.1.7. Trends of O_3, NO_x and total non methane hydrocarbon concentrations ([TC]), TNMOC/sum of speciated VOC's ratio and residence time (calculated from ln([xylene]/[ethy lbenzene])) versus time of day for cloudy weekdays and weekends. 80
Figure 5.1.8. Trends of O_3, NO_x concentrations (average per hour) versus time of day for cloudy weekdays and weekends in September-October period from AQMD data. 80
Figure 5.2.1 TNMOC, sum of speciated VOC's, TNMOC/sum of speciated VOC's, NO, NO_2, NO_x, O_3, and the vertical temperature profile from Miramar for Sundays and Wednesdays in November-December 2000. 85
Figure 5.2.2. Comparison of the trends of meteorological data for weekdays and weekends in November-December period. 86
Figure 5.2.3. Trends of O_3, NO_x and total non methane carbon concentrations ([TC]), [TC]/[SP] ratio versus time of day for weekdays and weekends in November-December period. 87
Figure 5.2.4. Hourly averaged AQMD O_3 and NO_x concentrations versus time of day for clear weekdays measurement days in November-December. 88
Figure 5.3.1 Diurnal averages for TNMOC/sum of speciated VOC's ratio, TNMOC and sum of speciated VOC's for cloudy and clear days. Error bars show the full range of observations. Points without error bars have only 1 or 2 data points averaged. 91
Figure 5.3.2 TNMOC vs. sum of speciated VOC's for clear and cloudy conditions. 91
Figure 5.3.3 Correlations between TNMOC/sum of speciated VOC's ratio and O_3, wind direction and wind speed for clear and cloudy days in September-October and all days in November-December. 95
Figure 5.3.4 Relationship between O_3 and TNMOC/sum of speciated VOC's ratio for September-October data collected between 5 and 8 AM. 96
Figure 5.3.5 Correlations for aromatic compounds with themselves, O_3, and Excess TNMOC. 100
Figure 5.3.6 a-d. Sample chromatograms and VOC classifications for two measurements on 9/15/00. The two upper plots had sum of speciated VOC's = 472 ppbC, and the lower plots are for sum of speciated VOC's = 124 ppbC. 103
Figure 5.3.7 Evolution of percents of VOC classifications by time of day for high ozone days in Sept. – Oct. 2000. 104
Figure 5.3.8 a) Correlation between percent of aromatics and oxygenates and TNMOC/ sum of speciated VOC's ratio, b) Correlation between percent of aromatics and oxygenates and O_3. 104
Figure 5.3.9 Ratio of the C_2-C_6 hydrocarbons concentration sampled at –100°C to C_2-C_6 hydrocarbons concentration sampled at –60°C versus TNMOC/sum of speciated VOC's ratio (concentrations are normalized to toluene concentration; each C_2-C_6 hydrocarbon concentration at -60°C is an average of 2 analysis performed before and after the analysis at sampling temperature of –100°C). 105
Figure 6.3.1 Unburned diesel vapor chromatogram. 109
Figure 7.1 Gasoline vapor chromatogram. 120

List of Tables

Table 2.2 Leak Check Procedure 16
Table 2.3 Blank Carbon dioxide levels and Reproducibility 18
Table 2.4 Variability of Trapped Ambient CO_2 in the TNMOC Channel During 9-12/2000 29
Table 2.5 Estimated Detection Limits and Uncertainties 30
Table 3.1: Instruments deployed during the field measurements at Burbank and UCLA, 1999-2000 34
Table 4.1 Concentration ranges and averages of O_3, NO_x, TNMOC, and speciated VOC's at UCLA and Burbank. 39
Table 4.2 Average Ozone, NO_x and VOC Levels at UCLA and Burbank 53
Table 5.3.1 Averages and Ranges for VOC's and Ozone on Clear and Cloudy Days During September-October 90
Table 5.3.2 Average Ratios for Summer and Winter, Weekends and Weekdays, and Clear and Cloudy Conditions 92
Table 5.3.3 OH Rate Coefficients and Atmospheric Lifetimes for Common Aromatic Compounds. 97
Table 5.3.4 Correlation Coefficients for Aromatic Compounds, O_3, and Excess TNMOC. 98
Table 5.3.2 Data Analyzed for Oxygenates, Aromatics, Alkanes and Alkenes 101
Table 6.1 Results from CARB Emissions Testing Group Matheson Gas Products (MGPI) Cylinder. 108
Table 6.2 Summary of TNMOC and sum of speciated VOC's measurements from the 1998 New Flyer Transit Bus, MTA#3007; Detroit Diesel EC50 Engine; License#1017104, running with ECD1 fuel, tested at the CARB Heavy Duty Diesel Testing Facility located at the MTA in downtown Los Angeles. 110
Table 6.3 Speciated Hydrocarbon Concentrations in Diesel Exhaust Samples 112
Table 6.4 Tunnel blank results for 4/18-4/20 113
Table 6.5 Speciated Hydrocarbon Concentrations Normalized to Decane 114
Table 6.6 Summary of UDDS Tedlar bag and *in situ* analyses, shown in Figure 6.3.2. 115
Table 7.1 Gasoline Vapor Measurements 119
Table 8.1 Summary of TNMOC/sum of speciated VOC's Ratios for All Measurement Series 124

Abstract

Here we describe development of a new instrument to measure the airborne total non-methane organic carbon concentration (TNMOC), and the ratio of this value to the sum of speciated volatile organic carbon (VOC's) measured by standard gas chromatography. The approach is to make a measurement that minimizes sample contact, cryo-trapping whole air samples with minimal trapping of carbon dioxide, carbon monoxide and methane. Samples are processed by an oxidation catalyst to generate carbon dioxide that is measured as TNMOC. Simultaneously, a standard speciated VOC's measurement is made with the same instrument. The ratio of the TNMOC and speciated VOC's measurements provides the "excess VOC's", or that not detected by routine monitoring techniques. Measurements of ambient air were made in West Los Angeles, Burbank and Azusa. Fresh pollution sources including gasoline vapor and diesel exhaust were tested as well. These sources are, not surprisingly, measured well by the standard analysis approach, and had 5-20% "excess" VOC's. The Burbank site, which is surrounded by freeways and light industrial sources had only 10 % excess VOC's, as did UCLA during winter when there is minimal photochemistry. In contrast, between 25 and 45% of the VOC's were unmeasured by the standard technique at the UCLA and Azusa sites during summer. The dominant source of the unmeasured VOC's appears to be air that has been aged for more than 12 hours, possibly for a day or more.

Executive Summary

The formation of ozone and other oxidants in urban and rural areas remains a persistent problem that affects both the public health and economic vigor of many areas in California. Oxidant formation results from the photochemistry of organic compounds in the presence of nitrogen oxides. The organic component begins mainly as biogenic and anthropogenic non-methane hydrocarbons. These compounds are progressively oxidized to carbon monoxide and carbon dioxide over periods of hours to weeks. The variety of primary hydrocarbons (i.e., containing only carbon and hydrogen) and their oxidation products is large. While separate techniques exist to measure groups of compounds (e.g., C_2-C_8 hydrocarbons with some carbonyls, or alcohols, or organic nitrates, etc.) no techniques to assess the total loading of non-methane organic carbon (TNMOC) have been widely applied in the atmosphere. The goal of this project is to determine the relationship between the total non-methane organic compounds and the sum of the speciated hydrocarbons and carbonyls measured by standard techniques. The primary scientific motivations are two: first, how much reactive organic carbon is in the air? How close to standard measurements come to reporting this total? Second, what happens to the multifunctional products of the photo-oxidation reactions of emitted hydrocarbons; do they stay in the gas phase or are they removed to surfaces?

The technique to measure TNMOC centers on a cryogenic separation (on an inert surface) of reactive carbon from the carbon oxides and methane. After separation, the isolated organic material is oxidized to carbon dioxide, allowing quantification. The sample comes in contact only with a sampling tube and heated valve before passing through the primary trap. The target TNMOC condenses, while carbon monoxide, methane and most of the carbon dioxide pass through. Next, the primary trap is briefly purged with helium to remove residual carbon oxides and methane. In the second step, the trap is rapidly heated; and a helium/oxygen mix sweeps the desorbed TNMOC into an oxidation catalyst where it is converted to carbon dioxide. The carbon dioxide is focused in a second trap, desorbed, reduced to methane and quantified with a flame ionization detector. Assuring that all relevant classes of compounds are detected at 100% is crucial to a TNMOC analyzer. Under an earlier contract, we determent that under normal operating conditions all aldehydes and alcohols tested trap at 100%; including formaldehyde, and that there is no interference from water. During this contract period, we established that the organic carbon in the particulate phase (which we do not filter) contributes less than 2% to the TNMOC.

A second air sample is collected simultaneously in a parallel trap under identical conditions, and this sample is analyzed for individual hydrocarbons and a few other organic components. Taken together, these individual compounds make up the "volatile organic compounds" (VOC's) that are measured by standard techniques. This sample is transferred directly to the focusing trap, and from there it is directed into a gas chromatograph. The speciated channel may also be used to determine individual VOC concentrations. This analysis is very similar to the Photochemical Assessment Monitoring Station (PAMS) hydrocarbon analysis, and it has performed well in intercomparisons with PAMS type measurements.

Dozens of smog chamber experiments have been carried out to investigate the oxidation chemistry and ozone formation from hydrocarbons. Few of these experiments can account for 100% of the reacted carbon as products, and less than 40% is common. As the starting hydrocarbons become oxidized, their products become progressively less volatile and more polar. Some of the products may

deposit on the walls of the reactor, form aerosols, or deposit in the gas chromatograph or inlet. In a sense, measuring total carbon in a smog chamber experiment is the "acid test" for a TNMOC analyzer. Results show that the TNMOC measurement works well, in detecting greater than 90% of the oxidized products from both m-xylene (C_9), and isoprene (C_5), and it detects roughly 75% of α-pinene (C_{10}) photooxidation products.

The TNMOC analyzer was deployed to make five measurements series during 1999-2001. Three series were collected at the University of California at Los Angeles (UCLA) during August 1999, September-October and November-December 2000, one was collected at Burbank during September 1999, and a final set of measurements were made at the California Air Resources Board's heavy duty truck dynamometer during April 2001. At UCLA and Burbank, nitrogen oxides, ozone, and meteorological data were logged simultaneously with the VOC analyses. Gasoline vapor was also investigated. For the gasoline vapor, a dominant source of VOC's in ambient air, the speciated measurement not surprisingly does an excellent job of detecting most VOC's; the TNMOC/sum of speciated VOC's ratio is only about 1.06 ± 0.02. The TNMOC/sum of speciated VOC's ratio observed for diesel exhaust was 1.2 ± 0.16. The Burbank site (09/15/99-10/12/99), which is located near the intersection of several freeways and in a light industrial area dominated by auto body shops, had an average ratio of 1.1 ± 0.08. Measurements made at UCLA during winter had a TNMOC/sum of speciated VOC's ratio of 1.1 ± 0.06. The excess TNMOC (that portion unmeasured by the speciated channel) was much higher at UCLA during the smog season, averaging 1.41 ± 0.14 and 1.37 ± 0.06 on clear days in 1999 and 2000 respectively and 1.77 ± 0.10 on cloudy days, during 2000. All confidence intervals are twice the standard deviations of the means. In an earlier study we reported a TNMOC/sum of speciated VOC's ratio of 1.3 ± 0.3 for Azusa (09/04/97-09/29/97).

The pattern that emerges form these data is as follows. The source materials, the site dominated by fresh emissions, and wintertime data have ratios close to 1.0, indicating little unmeasured or "excess" VOC's; the speciated measurements seem to underestimate the total organics by 20% or less. This group of measurements includes gasoline vapor, Diesel exhaust, and data from Burbank and UCLA during late November-December. Sites influenced by photochemistry with a smaller contribution from fresh emissions have higher levels of excess organics relative to the standard measurements. This group includes UCLA during August-October and Azusa. The excess organics appear to be associated with air that has been aged for longer periods than the 4-8 hours associated with diurnal ozone formation.

For the data that are influenced by photochemistry, lower average ratios are associated with higher average VOC concentrations. Examination of the NO_x data confirms the contribution of fresh emissions to high VOC concentrations. This together with several other results seems to indicate that much of the excess VOC's comes from carryover from pollutants that have been aged for a day or more. The result that cloudy days have much higher TNMOC/sum of speciated VOC's ratios than do clear days is consistent with this hypothesis because mixing heights are several times higher on cloudy summer and fall days than clear days, thus pollutants stored aloft can mix down to the surface. The aromatics data from the speciated channel show that the TNMOC/sum of speciated VOC's ratio is positively correlated with increased depletion of aromatics with lifetimes longer than several hours. The TNMOC/sum of speciated VOC's ratio is also positively correlated with an increased contribution of oxygenates, and with O_3 in the early morning when O_3 is a tracer for pollutant carryover rather than surface emission control of the VOC concentrations. Pollutant carryover would be expected to make a larger contribution on weekend days than on weekdays, but we do not have a sufficient number of days of data during the smog season to determine a weekend effect.

In summary, the standard measurements significantly underestimate VOC concentrations during the smog season except near fresh emission sources and thus underestimate the VOC/NO_x ratio. The identity and importantly, the reactivity of this unmeasured organic carbon is still to be determined.

1. Introduction

The formation of ozone and other oxidants in urban and rural areas remains a persistent problem that affects both the public health and economic vigor of many areas around the globe. Oxidant formation results from photochemistry of organic compounds in the presence of nitrogen oxides. The organic component begins mainly as non-methane hydrocarbons (NMHC, containing only carbon and hydrogen) from biogenic and anthropogenic sources. These compounds are progressively oxidized to CO and CO_2 over periods of hours to weeks. The variety of primary hydrocarbons and their oxidation products is large. While separate techniques exist to measure groups of compounds (e.g., C_2-C_8 hydrocarbons with some oxygenates, or alcohols, or formaldehyde or organic nitrates, etc.) no techniques to assess the total loading of non-methane organic carbon (TNMOC) have been widely applied in the atmosphere. The goal of this work is to determine the relationship between the total non-methane organic compounds and the sum of the speciated volatile organic compounds (VOC's) measured by standard techniques. The primary scientific motivations are to define the airborne quantity of reactive organic carbon, find how close this quantity is to the standard measurements of VOC's, and address the question of what happens to the multifunctional products of the photo-oxidation reactions of emitted hydrocarbons; do they stay in the gas phase or are they removed to the aerosol phase or surfaces?

A total reactive carbon measurement has an obvious analogy in the total reactive nitrogen (NO_y; all oxides of nitrogen except N_2O) measurement. The NO_y measurement is now widely used in both the troposphere and the stratosphere (e.g., [1-5]). Initial measurements indicated that the total NO_y signal could not be accounted for by the sum of its measurable components [6, 7], which resulted in re-evaluation of the detection and calibration methods for the component compounds (particularly nitric acid) as well as a search for additional species containing oxidized nitrogen [1, 8].

There are several reasons to expect the TNMOC measurement to result in a number that is larger than the sum of the routinely measured VOC's. Loss of oxygenated and semi-volatile compounds in sampling and on columns is well known [9-13], although the extent of the losses is very difficult to quantify. Modeling results indicate that while the initial oxidation step of a hydrocarbon may take place within hours, if our understanding of the relevant processes is correct, complete removal of the partially oxidized fragments should take weeks [14]. Finally, in controlled smog chamber photo oxidations, a standard gas chromatograph with flame ionization detection (GC/FID) measurement can account for much less than 100% of the reacted parent hydrocarbon [15-17].

Several techniques and measurements similar to the proposed TNMOC measurement have been attempted, but as far as we are aware, only one study has been published in the open literature [18]. In addition a 2-dimensional GC technique has been applied to investigate the nature of the many individual hydrocarbons that are hidden in the baseline of an urban gas chromatograph (GC) trace [19]. Measurements of TNMOC in source streams--at typically 10^3-10^4 times ambient concentrations--are routinely measured by EPA Method 25 or similar [20-22]. Method 25 divides a stack sample into

condensable and gaseous fractions. The condensable fraction is oxidized to CO_2, and the gaseous fraction is injected onto a column where CO_2, CH_4, and CO are separated from the NMOC. The column is then back-flushed and the organics are swept into an oxidation furnace and measured as CO_2. The total organic concentration is the weighted sum of these two measurements, with a detection limit of several ppm [22].

Methods for measuring total NMHC's (including a few polar organics) include analyzing an air sample directly with an FID and subtracting CH_4 that has been measured separately. Since CH_4 concentrations are ~1.6 ppmV in the Northern Hemisphere, this method can be applied only in highly polluted areas. A variation uses a GC column to separate the NMHC's from CH_4. Once CH_4 and CO_2 have eluted, the column is back flushed through an FID [23-26]. A drawback of the back-flush method is loss of polar or heavy VOC's in the column itself. A second variation back flushes the column through a series of oxidation and reduction catalysts to convert the trapped NMHC's first to CO_2 and then to CH_4. This is intended to make the instrument response per carbon atom constant; another drawback of the FID approach is that structure and heteroatoms reduce the FID response by variable amounts (e.g., [27]. Other TNMHC methods are based on sorbent traps, an example of which is the Bendix 8202 [28]. While these methods have advantages, they also must contend with issues of recovery of polar compounds from sorbents and the reduced FID signal from molecules that contain heteroatoms.

Roberts and co-workers have developed a variation of the column back-flush approach to make a TNMOC measurement in ambient air [18]. This approach has the advantage of achieving quite low detection limits (~1 ppbv) but may lose semi-volatile compounds to the GC column. Roberts et al. [18] compared their TNMOC concentrations with speciated VOC measurements collected by other instruments nearby to calculate the TNMOC/ speciated VOC's ratio. Since the calibrations, sampling frequencies and averaging times were different, a fair degree of scatter is anticipated, and a systematic error is possible. Measuring in relatively clean air in Boulder, Colorado, and Nova Scotia, Canada, they found differences between TNMOC (which they refer to as "C_y") and the sum of hydrocarbons and carbonyls that were small in absolute terms, averaging 3.8 ± 7.9 ppbC, but were significant in percentage terms. Ratios of TNMOC/ speciated hydrocarbons + carbonyls were 1.36 ± 1, 1.16 ± 0.7, and 1.33 ± 0.4 for samples from air with < 20, 20 _ 03 _ 50, and > 50 ppbv O3 respectively.

Alistair et al. [19] used a 2-dimensional GC technique to investigate the nature of the compounds in the baseline of a standard GC chromatogram, analyzing air samples collected in Melbourne, Australia. By switching sections of the effluent of a primary column onto a second column, they were able to determine the number of compounds hidden in the baseline, estimate concentrations and determine general compound classifications. Instead of ~120 compounds for a standard speciated chromatogram, Alastair et al. [19] found over 550 different species. Most of the "hidden" material they found in had at least 6 carbon atoms, and many of the newly identified compounds were aromatic. Although they reported only small quantity of oxygenates, about 2%, they found a TNMOC/sum of speciated VOC's ratio of ~1.67.

The TNMOC instrument described here has several improvements compared to previous approaches. Samples introduced into our instrument are exposed to only an inlet tube, valve and short length of transfer tubing, and then immediately analyzed.

Water management is not needed. Speciated VOC's are measured with the same instrument, avoiding problems created by comparing different sample inlets and calibrations.

2. Instrument Development

2.1 Instrument Overview

The TNMOC instrument described here collects two samples in parallel. One sample is analyzed as TNMOC (Channel 1) and the second is analyzed as speciated VOC's (Channel 2). Detailed flow diagrams are shown in Figures 2.1.1 (sampling), 2.1.2a,b (transfer) and 2.1.3 (analysis). In step 1, the first traps (I) are cooled to between -55 and -80 °C, depending on the VOC concentration in the sample (Figure 2.1.1). The sample passes through the sampling tube and a heated valve before passing through trap I. The target TNMOC and VOC's condense, while CH_4, CO, and most of the CO_2 pass through. Once the sampling (cryo-trapping) stage is finished, trap I is purged with helium (60 s at 18.2 mL/min) to remove sample gas from the tubing and air space within the trap. In step 2, trap I is rapidly heated (to 140 °C at 100 °C/min). A He/O_2 mix sweeps the desorbed TNMOC in channel 1 into an oxidation catalyst where the organics are converted to CO_2 (180 s at 18.2 mL/min, Figures 2.1.2a). The TNMOC in channel 2 is transferred directly into a focusing trap (II) using 180 s of He at 18.2 mL/min. An advantage of this method is that decomposition or reaction of labile compounds during trapping and heating has no effect on the result in the TNMOC channel, because the trapped organics are immediately oxidized to CO_2. This CO_2 is also focused in a parallel trap II. The type II traps are immersed in lN_2, to concentrate the (~50 mL) volume necessary to thoroughly desorb the contents of trap I into a small plug for the quantification step. Finally the focusing trap (II) is heated in boiling water and the contents are injected into the GC for analysis. The TNMOC, which has been converted to CO_2, flows into column I and is catalytically converted at the end of column I to CH_4 and quantified with an FID.

The TNMOC instrument is built around a dual FID GC (Hewlett Packard 5890-II). Inlet valves (Valco) are attached to an aluminum block maintained at 60-70 °C. Transfer lines, trap tubing and fittings are constructed from deactivated fused silica lined stainless steel (Restek) and are maintained above ambient temperatures with heating tape. Temperature controllers (Omega) maintain heating and cooling of trap I, the methanation and oxidation catalysts and the valve block. Trap II is alternately cooled and heated by immersing it in liquid nitrogen and hot water. Both traps I and II are filled with silanized glass beads and are constructed of 1/4" and 1/8" outer diameter (OD) tubing, respectively. Trap I is cooled from the center with pulses of lN_2 vapor, so that there is a significant temperature gradient along the length of the tube. As a result, the trap's temperature, which is recorded by a thermocouple attached close to the center of the tube, is a relative value. Each time this trap is replaced, the trapping of CO_2 as a function of temperature is determined and a new optimal operational temperature is chosen, typically falling in the range -55 to -80 °C. Mass flow controllers (Unit Instruments) provide stable flows of He, He/O_2, and sample flow.

One of the most interesting aspects of the TNMOC measurement is its comparison to the sum of the speciated VOC's as they are commonly measured. The

ideal way to make this comparison is to acquire two identical samples simultaneously, and process one sample in TNMOC mode and the other in speciated mode, with separate GC columns. The columns used for both TNMOC and Speciated VOC measurements are 60m x 0.32mm ID x 1µm DB-1 (J&W). This column was chosen because the stationary phase (100% methyl polysiloxane) is among the most widely applied in field measurements of VOC's [11, 29, 30], and is used in Photochemical Assessment Monitoring Stations (PAMS) [31].

Ideally, 100% of the NMOC in the air sample stays in trap I, and CO, CO_2, and CH_4 pass through. In practice, CO and CH_4 (boiling points (T_b) of -191.5 and -164 °C, respectively) pass through, while CO_2, with an ambient concentration larger than the TNMOC by a factor of 100-40,000 and a sublimation point of -78.5 °C, traps to a minor degree, while the C_2-C_4 hydrocarbons are not trapped. The TNMOC detection limit is determined not by the absolute amount of atmospheric CO_2 that traps but by its variability. We can achieve trapping of CO_2 equivalent to about 50 ± 10 ppbv in a 500 mL sample. The amount of CO_2 trapped is traded off, however, with the trapping of C_4-C_5 hydrocarbons. The amount of trapped CO_2 is measured continually, and includes CO_2 background caused by the carrier gasses.

The TNMOC instrument can be operated in three modes: 1) *TNMO*C: The sample is oxidized over a Pd-catalyst to CO_2, run on column 1 and analyzed with FID after conversion to methane. 2) *Speciation, column 1*: No oxidation, column 1, methanizer and FID. This mode was necessary to establish the amount of CO_2 captured in trap I to order to correct TNMOC measurements. This mode is not ideal for speciated VOC's due to losses of heavy hydrocarbons in the methanizer. 3) *Speciated VOC's:* No oxidation, column 2 analyzed with FID (no methanizer). This is the standard speciated hydrocarbon analysis.

2.1.1 GC analysis

The column conditions are as follows: Restek-1 capillary column, I.D.: 0.32 mm, L: 60 m, film thickness: 1 µm; Carrier gas flow rate (line 1): 4.9mL/min He; Carrier gas flow rate (line 2): 4.7 mL/min He. Oven temperature program: 1 min @ 0ºC, 0-200ºC @ 10ºC/min, 200ºC for 5 min. FID detector temperatures: Speciated line, 350ºC, Total carbon line, 350ºC.

Table 2.1 Gas flow rates at the FID detector

Gas	Speciated line (mL/min)	Total carbon line (mL/min)
Hydrogen	70	55
Air	325	325
Nitrogen (make up)	40	80

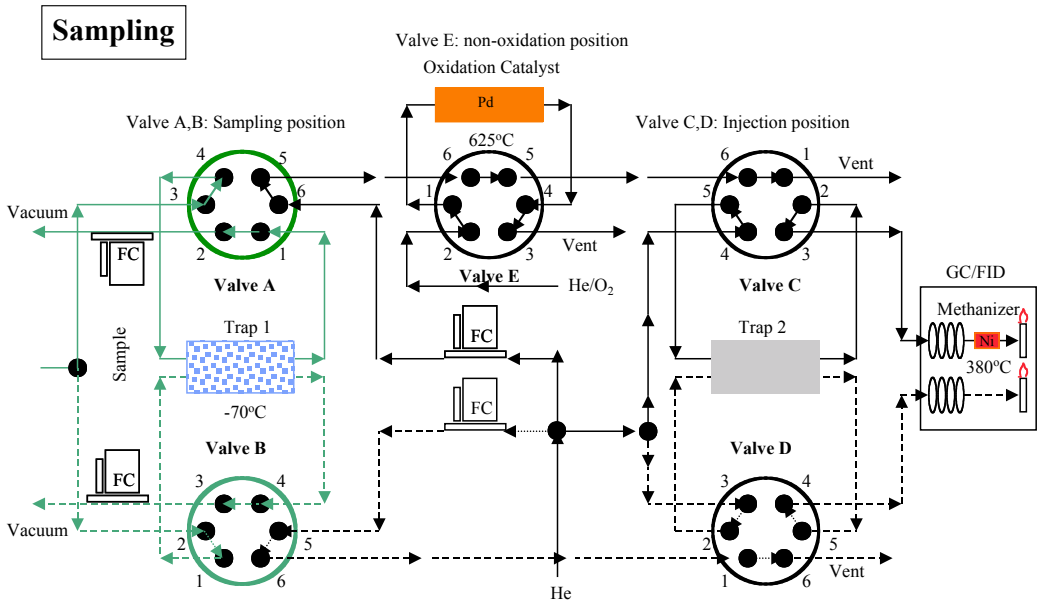

Figure 2.1.1 Valve schematic showing flow path for sample acquisition. FC = flow controller, Pd = palladium oxidation catalyst, He/O_2 = 500 ppm O_2 in He mixture. Dotted lines indicate a separate flow path for speciated VOC's; solid lines indicate the TNMOC flow path.

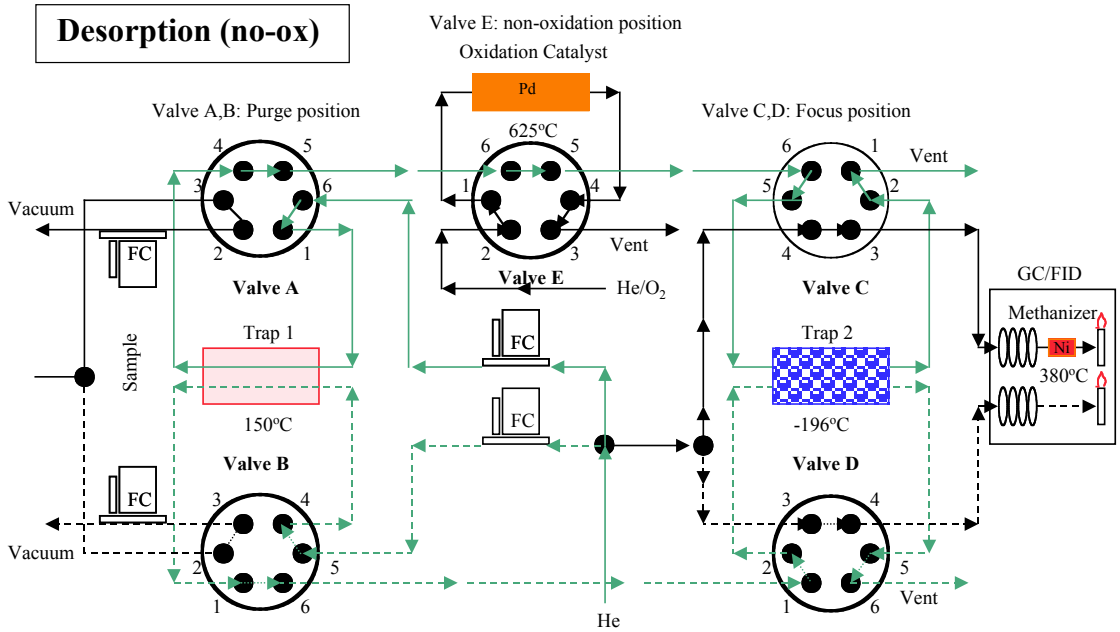

Figure 2.1.2a. Flow schematic for desorption of TNMOC samples with out oxidation.

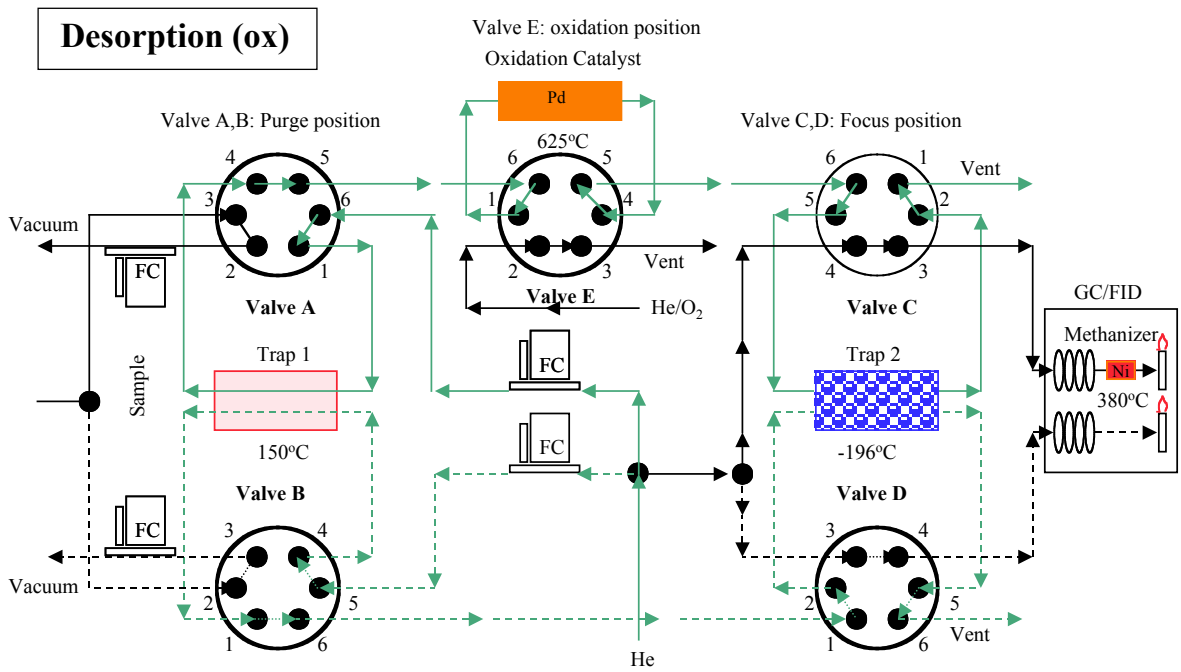

Figure 2.1.2b Flow schematic for desorption of TNMOC samples with oxidation.

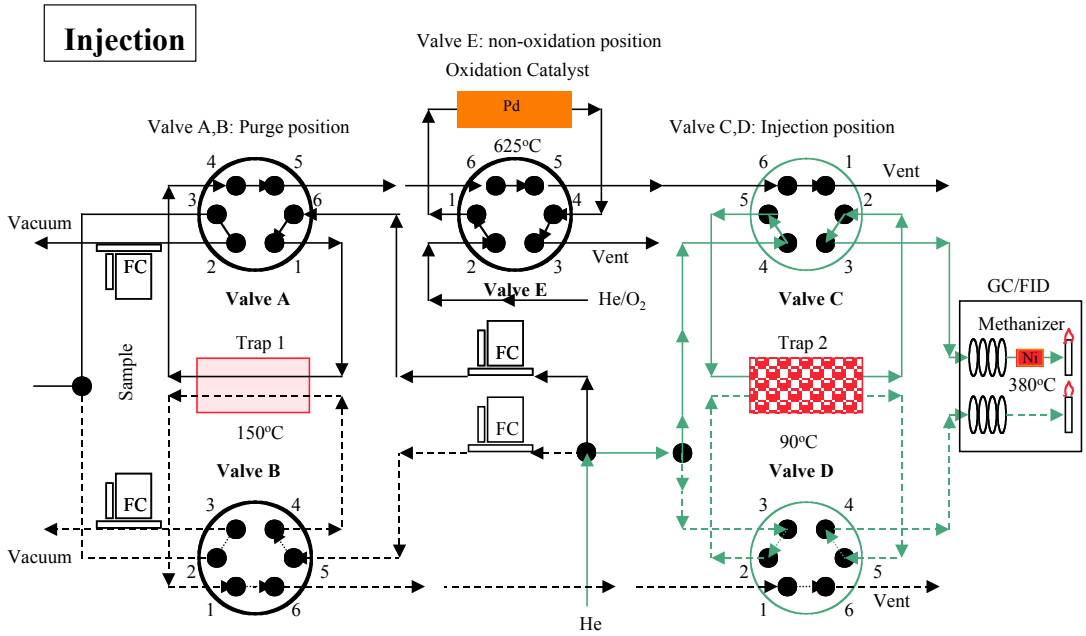

Figure 2.1.3 Flow schematic for injection in gas chromatograph and subsequent analysis.

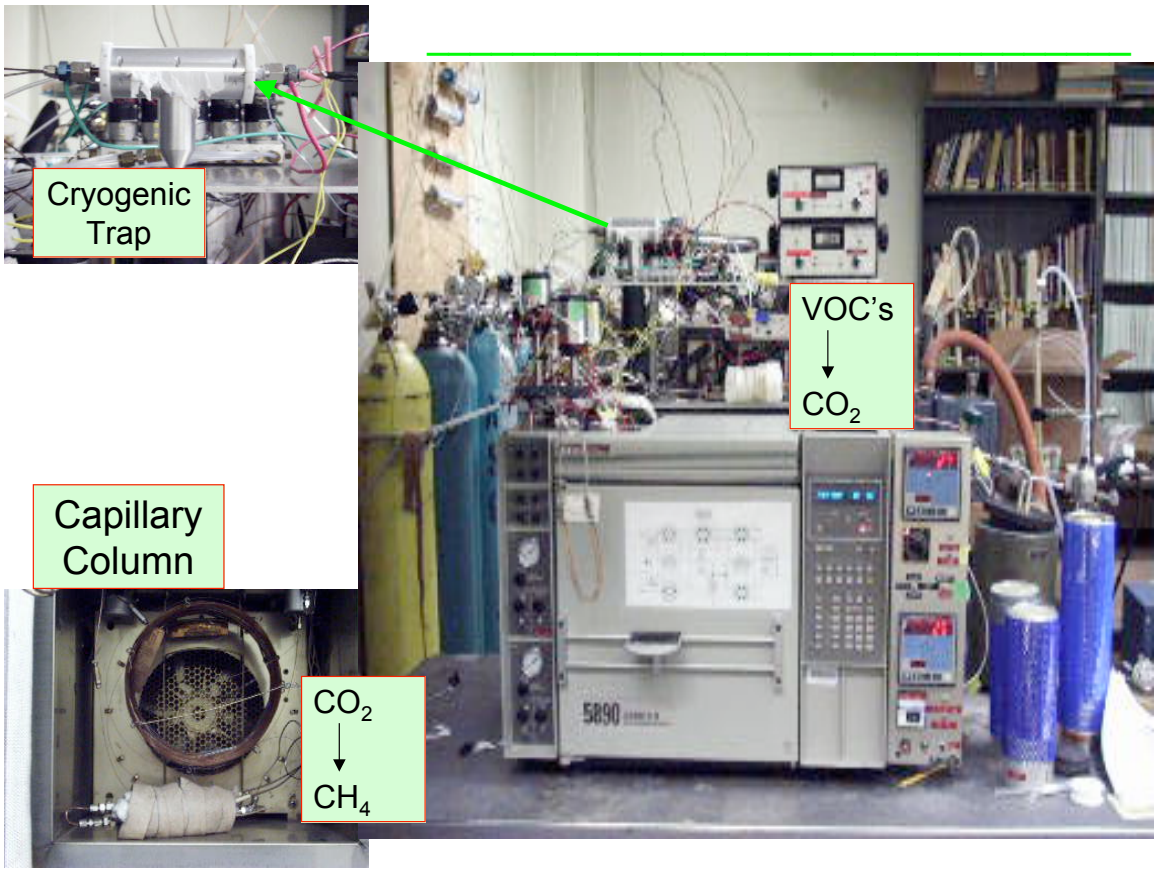

Figure 2.1.4. Photograph of the instrument, oxidation and reduction catalysts.

2.2 Major Design Changes During this Period

Several minor adjustments were made to the instrument during this period to flow rates, zone temperatures, and transfer times, and the values listed above reflect the current operating procedure. More substantial changes to address problems with the instruments blank and the performance and durability of the methanizer are detailed here. These improvements were made after the 1999 field measurements (UCLA and Burbank) and before the 2000 and later field measurements (UCLA and MTA).

2.2.1 Methanizer and Oxidation Catalyst

The field campaigns performed in mid-1999 (at UCLA and Burbank) revealed a rapid reduction of the methanizer conversion rate after performing a limited number of ambient air samples. On 10/12/99 we performed a series of four n-hexane calibrations with 12 interspersed ambient air measurements in order to determine the depletion rate of the methanizer conversion efficiency. The result of this experiment is given in Figure 2.2.1.

This behavior shows characteristics of a poisoning of the catalytic material (Ruthenium). The substances with the greatest potential for this poisonous effect are gaseous sulfur compounds trapped from the ambient air sample and oxygen, which is introduced to the methanizer after the sample is purged from the first to the second cryogenic trap. Due to the fact that the second trap is emerged in lN_2 (Boiling point:

-196°C), and the sample is purged with He/O_2 from the first trap of the TNMOC channel to the second trap, O_2 (Boiling point: –183°C) will be enriched in this trap. After rapid heating, by emerging the second trap in hot water, the trapped O_2 will be injected together with the NMHC to the column and subsequently enter the reduction catalyst.

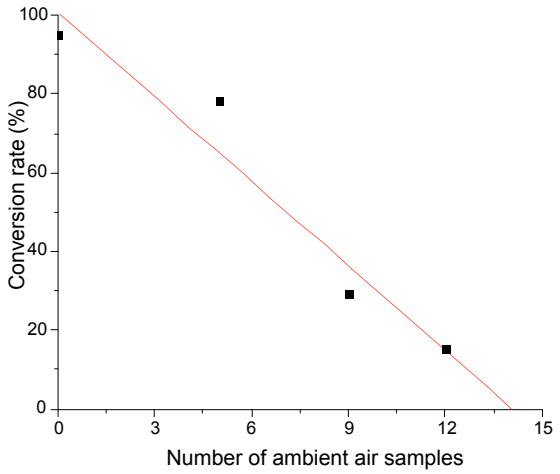

Figure 2.2.1 Decrease of the methanizer conversion efficiency vs. the number of intervening ambient air samples on 10/12/99.The design of the TNMOC plumbing was altered slightly to avoid introducing O_2 into the methanizer. The current design uses only He to purge the sample from the first to the second trap of the TNMOC channel.

It is generally believed that oxidation of hydrocarbons occurs primarily via oxygen that is adsorbed on the surface of the metal catalyst, rather than O_2 in the gas phase. The original design had the He/oxygen continuously flowing over the oxidation catalyst when not in use, and in addition, the transfer gas used to move the sample over the catalyst and into the second trap was also the He/O_2 mix. The new design uses He/O_2 as the transfer gas, thus O_2 is no longer enriched in the second trap. In the oxidation mode, the VOC's are oxidized by the O_2 that is adsorbed on the Pd surface without further O_2 supply from the gas phase. Figures 2.2.2a and 2.2.2b show a flow scheme of the TNMOC instrument with the design used during the field campaigns in 1999 and the current design.

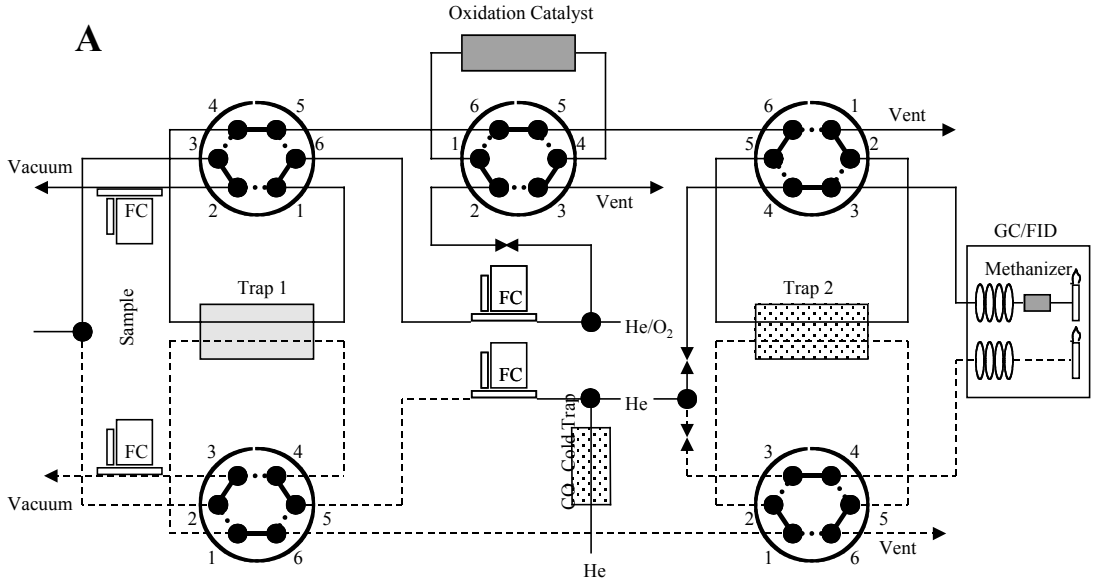
A
Oxidation Catalyst
Vent
Vacuum
FC
Vent
GC/FID
Methanizer
Trap 1
Trap 2
Sample
He/O2
He
CO Cold Trap
Vacuum
He
Vent

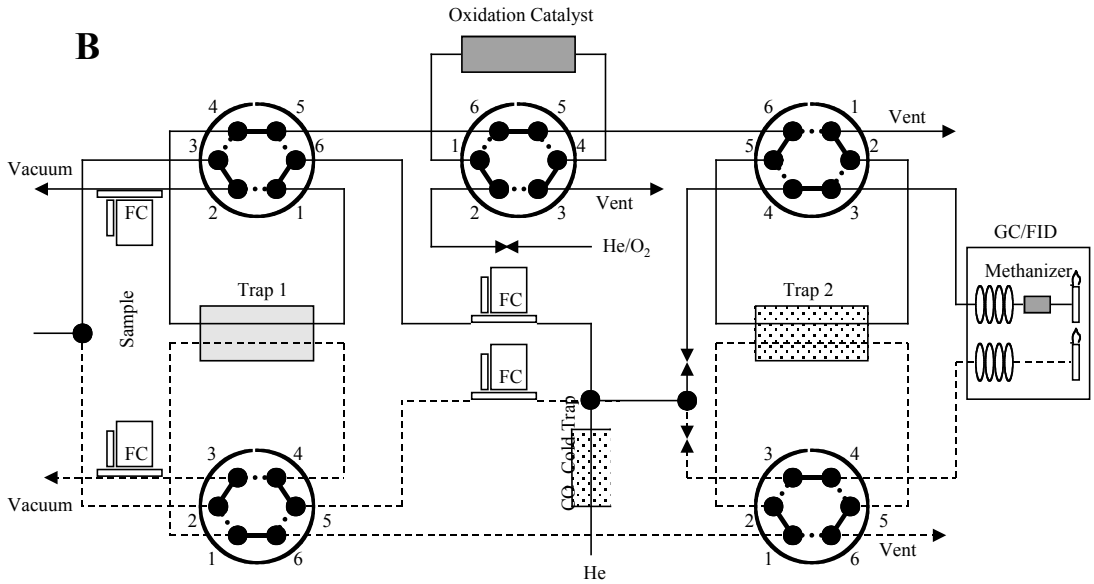

Figure 2.2.2: Schematic representation of GC flow scheme during the field experiments (A) and current flow scheme (B). Straight lines: TNMOC channel, dotted lines: Speciated VOC's channel, FC: Flow controller.

2.2.1.1 Oxidation Capacity with Current Gas Flows

A potential risk of the new design is that the VOC's are not completely oxidized in the oxidation catalyst due to an insufficient supply of O_2. Under normal operation, the oxidation catalyst is purged with He/O_2 for 30-60 minutes between analyses, and repeated runs reveal 100% oxidation. To test the oxidizing capacity of the catalyst with out recharging with He/oxygen, we ran repeated samples without recharging and observed a slight decrease in conversion efficiency (to 92%) over a series of seven n-hexane calibrations (200 ml 1.08 ppmV n-hexane in N_2, Scott specialty gases. Figure 2.2.3 shows the result of the experiment. The total amount of carbon introduced in these tests is equivalent to 18 ppmC in a 500 mL sample, several times larger than hydrocarbon concentrations observed in ambient air, even in Los Angeles. This suggests that because the oxidation catalyst is saturated with fresh O_2 after every oxidation mode run it is reasonable to assume that the oxidation capacity of the catalyst remains unaffected by the new design of the TNMOC instrument.

Several days of ambient air measurements were conducted after the testing of the oxidation capacity to check the performance of the instrument in ambient air. The measurements show no decrease in the conversion rate of the methanizer due to the new design of the instrument. Therefore we expect no further problems with the TNMOC instrument related to a decrease of the methanizer conversion rate due to O_2 interference.

A potential poisoning of gaseous sulfur compounds contained in the ambient air samples cannot be excluded, however, but is most likely to happen only in air samples with a sulfur content of several ppmV. This is a very high value and we do not expect such an effect from regular field measurements in the Los Angeles air basin.

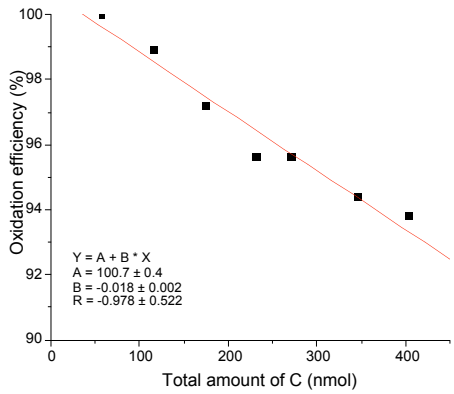

Figure 2.2.3 Oxidation efficiency of the oxidation catalyst without recharging with He/O_2 during the entire run series. For these experiments, carbon loading in each sample was 18 ppmC, 10-100 times larger than levels in urban ambient air. In practice, the oxidation catalyst is recharged between each run.

2.2.1.2 Effect of Relative Humidity on TNMOC and the Oxidation Catalyst

It has been suggested that our oxidation catalyst may be sensitive to water, and potentially release additional CO_2 at high relative humidity (RH). As far as we are aware, there is no evidence for this phenomenon in the literature, however we investigated our data for evidence of this potential bias. Figures 2.2.4a and b show the relationship between the relative humidity and the ratio of TNMOC/ sp. VOC's for the Sept-Oct. data and the December data, respectively. No correlation between the TNMOC/ Sp. VOC's ratio and RH is observed in either data set. In the summer data set, several higher excess TNMOC levels are associated with RH's between 65 and 80%, and to a lesser degree between 80 and 100% RH. These higher ratios correspond to meteorological conditions with high inversion bases and more vertical mixing, which typically occurs during cloudy conditions, and which is discussed in more detail in Section 5.3.1. below.

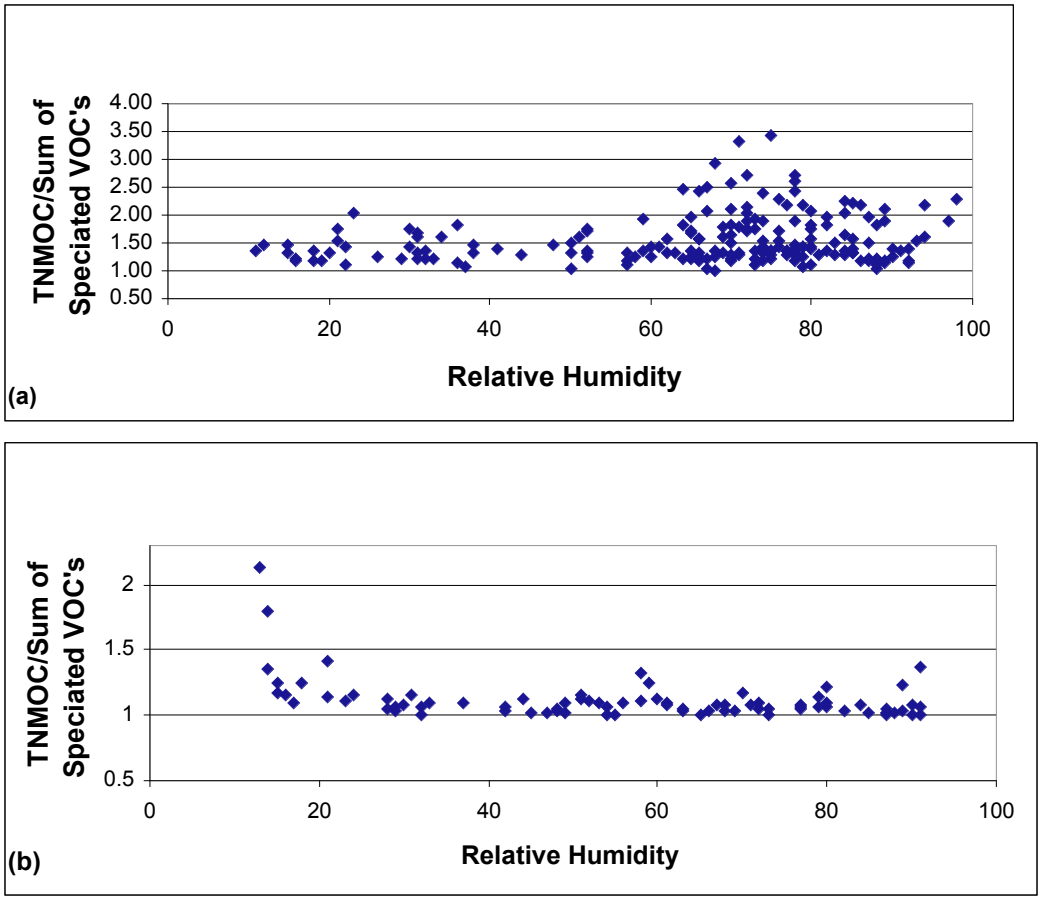

Figure 2.2.4 Relationship between the relative humidity and the ratio of TNMOC/ Sp. VOC's. The upper panel (a) is data collected during September and October, and the lower panel is data collected during November and December 2000.

2.2.1.3 New Methanizer Material

Despite the fact that the Ru based methanizer works well after the improvements we made, there are some unsatisfying features about this specific methanizer design:

i. *Methanizer-to-Methanizer Reproducibility*: Although with the new flow design, methanizers should work for several months, they still need to be replaced from time to time. While we can build methanizers in the laboratory that have desirable characteristics in terms of chromatographic quality, backpressure, and conversion efficiency, it sometimes requires several attempts.

ii. *Activation procedure*: The Ru based methanizer requires a rather lengthy activation procedure that includes an initial cleaning step by heating the methanizer to 700°C under flowing O_2 for four hours followed by an activation step, which is performed at 300°C under flowing H_2 for another four hours. The total time of the activation process (including cooling and heating) is approximately 9 hours, which leads to a total production time of at least 10 - 11 hours if the methanizer is made from scratch. A shorter

production time is desirable considering the fact that a methanizer has a finite lifetime and might need replacement during a field campaign.

iii. *Interference susceptibility*: Methanizers with Al_2O_3 supported metal are usually less sensitive to be poisoned due to the fact that the Al_2O_3 provides a large insensitive adsorption surface to trap potentially poisoning substances. This will lead to a longer lifetime of the methanizer during daily use while performing field measurements. Unfortunately there is no Al_2O_3 supported Ru commercially available in the right mesh size to replace the currently used pure Ru metal.

For these reasons a commercially available methanizer (SRI Instruments, Torrance, CA) was tested on its performance in the TNMOC instrument. This methanizer consists of a ca. 12 cm long $^1/_8$" OD stainless steel tube filled with Al_2O_3 supported Ni. The methanizer activation process is comparably short, requiring only heating for one hour with a H_2 flow of 10 ml/min at the manufacturers recommended operational temperature of 380°C. Even if this methanizer was originally designed for the use with packed columns its performance in the TNMOC instrument, which is equipped with capillary columns, is excellent. The methanizer has a very low backpressure, an excellent chromatographic quality and meets the manufacturers given conversion rate of 95 – 98%, we measured 96 ± 2% in the temperature range of 350 – 400°C.

The chromatogram shown in Figure 2.2.5 shows the results for a lab-built Ru methanizer together with results for the commercial Ni catalyst. Some tailing of the n-hexane peak is observed for the Ru catalyst. As can be seen, the chromatographic quality of the commercial methanizer is very good and it causes almost no peak tailing. This will lead to smaller integration errors and successively to a better precision of the instrument due to a better reproducibility of the calibration. The excellent chromatographic quality of the commercial methanizer is also shown in the CO_2 peak of the oxidation mode chromatogram. Ru based methanizers usually result in stronger tailing of the CO_2 peak (not shown). The better behavior of the Ni based methanizer will therefore lead to a better precision of the TNMOC measurements.

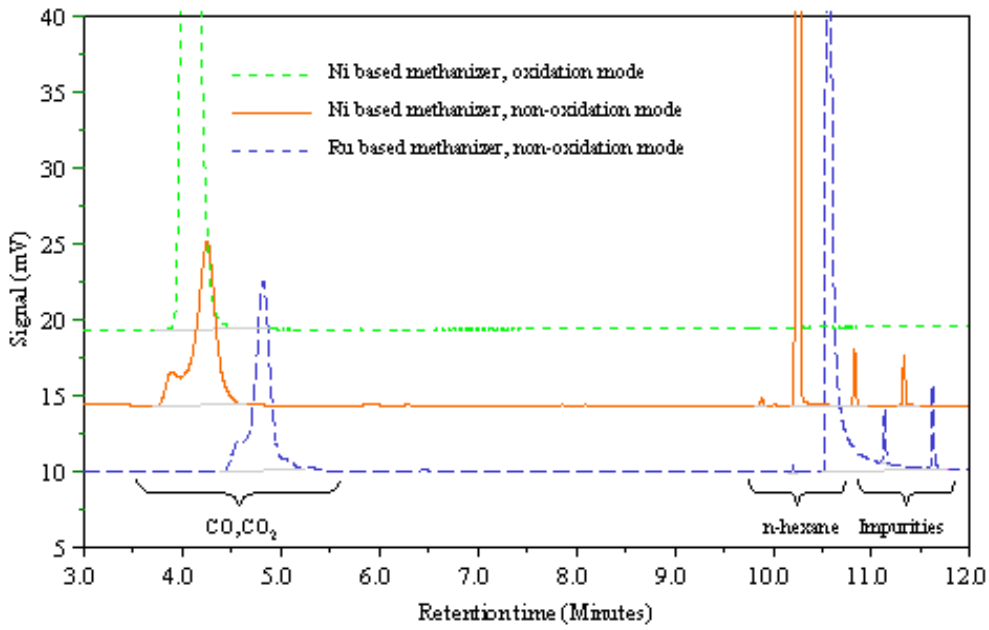

Figure 2.2.5 Chromatograms of n-hexane calibration of the TNMOC channel in non-oxidation and oxidation mode with Ni and Ru based methanizers.

The commercial Ni methanizer appears to have a long lifetime, although it is too early to tell. It was installed at the end of January 2000 and was run almost daily with both ambient air and calibration gas samples, and shows no signs of subsidence

In conclusion, the use of the commercial Ni based methanizer will likely improve the performance of the TNMOC instrument significantly. This methanizer type shows excellent performance in all three important criteria (reproducibility, activation procedure, and interference susceptibility) and is therefore the preferable and more economic choice.

2.3 Instrument Blank

2.3.1 Technique and Procedure

The procedure to check for very small leaks consists of placing a few drops of volatile solvent (pentane) on the connections. If there is a leak, pentane is detected by the FID detector. One or more connections can be tested together during each checking procedure. The instrument is checked step-by-step according to the detailed procedure shown in Table 2.2. The column oven was programmed to run isothermally at 50ºC. When all connections are tight, a zero carbon dioxide signal is observed for parts 2, 3, 4 and 5.

Table 2.2 Leak Check Procedure

Experimental procedure	Instrumental parts tested
Part 1 Valves C and D are switched to the injection position.	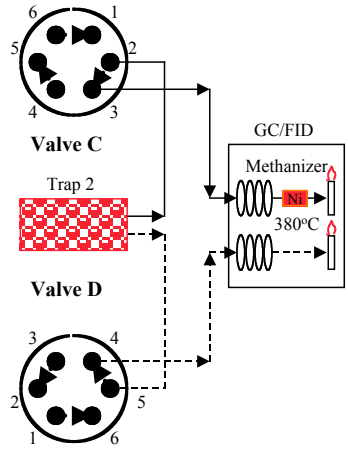 Valve C, D: injection position
Part 2 Trap 2 is immersed in liquid nitrogen and valves C and D are to the injection position. Trap 2 is immersed in boiling water 3 min after introducing a few pentane drops and GC analysis is started.	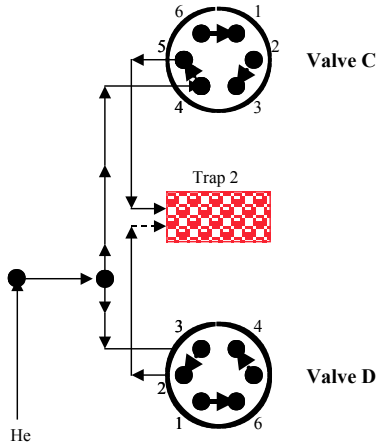 Valve C, D: injection position
Part 3 Valves A, B and valves C, D are in the purge and the focus position respectively. Trap 2 is immersed in liquid nitrogen and trap 1 is at a temperature of 140ºC. 3 min after putting pentane on the connections, valves C and D are switched to the injection position, trap 2 is immersed in boiling water and GC analysis is started	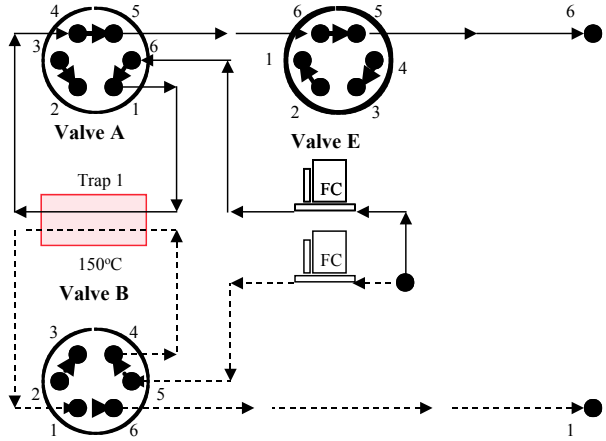 Valve C, D: focus position Valve A, B: purge position

Part 4 Valve E is in the oxidation position. Valves A and C are in the purge and focus position respectively, trap 2 is immersed in liquid nitrogen. 3 min after putting pentane on the connection of the oxidation tube part, valve C is switched to the injection position, trap 2 is immerged in boiling water and GC analysis is started	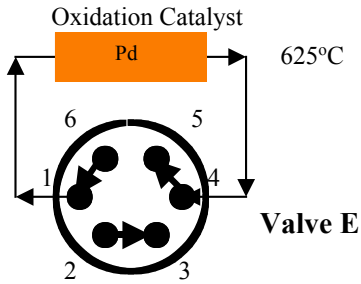 Valve E: oxidation position
Part 5 Valves A and B are in the sampling position and trap 1 is cooled at –100ºC. 3 min after putting pentane on the connection, valves A, B and C, D are respectively switched to the purge and the focus position, trap 2 is immersed in liquid nitrogen. Trap 1 is heated to 140ºC. After 3 min of transfer time, valves C and D are switched to the injection position, trap 2 is immersed in boiling water and GC analysis is started.	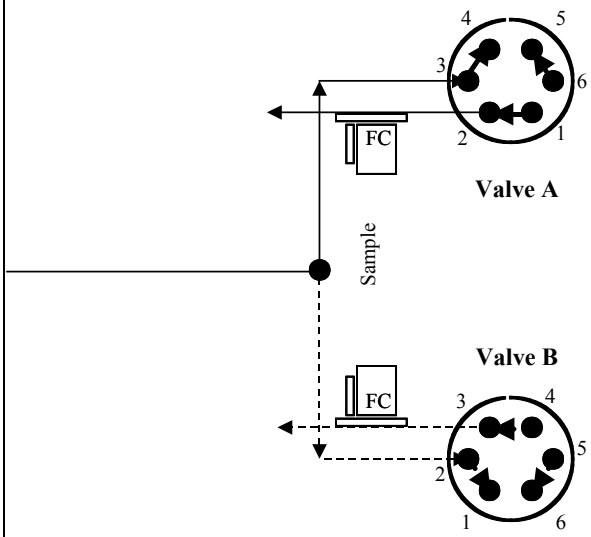 Valve A and B: sampling position

2.3.2 Instrument Modifications and Verification

Many modifications were performed to eliminate tension on the tubing connections within the instrument and to prevent the recurrence of leaks. Finally, a redesigned Trap I was installed (Figure 2.2.6).

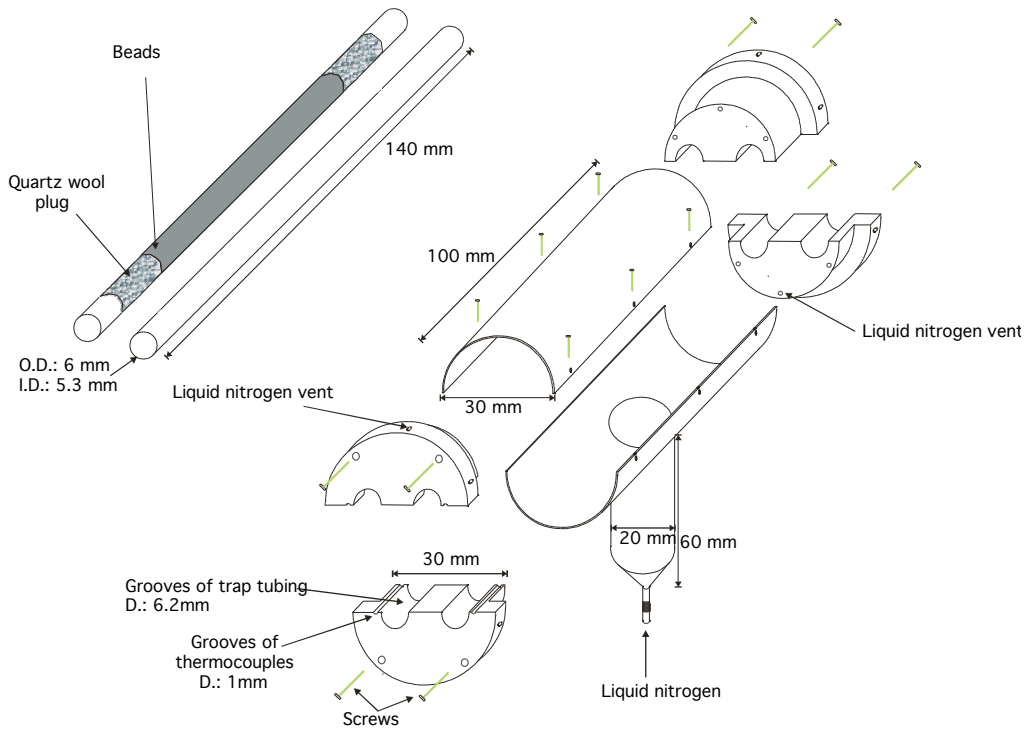

Figure 2.3.6 New design of trap 1.

The new Trap 1 has two main advantages: 1) it can be opened if there are problems (thermocouples or tubing connections begin to leak), 2) the new shape of trap 1 promotes more homogenous cooling of trap tubing by using a five times larger diameter tubing to deliver liquid nitrogen.

For the different parts of the instrument (part 2,3 and 4), the carbon dioxide blank level was measured. The oxidation tube and methanizer efficiencies and repeatability were determined by sampling a hexane standard with a concentration of 1 ppmV (table 2.3).

Table 2.3 Blank Carbon dioxide levels and Reproducibility

Mode	Residual CO_2 (area cts)	Hexane (TNMOC channel)* Average ±SD RSD	Hexane (Speciated channel)* Average ± SD RSD
Procedure *part 2*	0	-	-
Procedure *part 3*	2	-	-
Procedure *part 4*	9	-	-
Whole procedure/ no oxidation	12	- 1513±5 - 0.3%	- 1300±3 - 0.2%
Whole procedure/oxidation	-	- 1507±3 - 0.2%	- 1301±3 - 0.2%

*Area counts for 228 mL of 1 ppmV (6.0 ppmC) of n-hexane.

The background CO_2 signal of the different instrumental parts can be considered negligible with respect to that of the total of non-methane organic compounds analyzed. For the total carbon mode, hexane responses with and without oxidation are very similar (difference less than 1%). We can conclude that the oxidation tube and methanizer have efficiencies better than 99 %. Repeatability for both lines is very good, and the FID response is slightly higher for the TNMOC line, likely due to the different configuration of gas flows due to the methanizer located just before the FID on Channel 1.

2.3.3 Summary

The result of the improvements undertaken during this quarter is a very stable instrument. The carbon blank is less than 10 ppbC. The detection limits are about 50 pptC and 10 ppbC for the speciated and TNMOC channels, respectively. The instrument performed very well throughout the 2000 field measurements.

2.4 Smog Chamber Validation Experiments

The target compounds for this instrument include polars, light oxygenates, semi-volatile compounds emitted from biogenic and anthropogenic sources [11, 32, 33] and the oxygenated and/or nitrated compounds that form when hydrocarbons are oxidized in photochemical smog reactions. The performance of the instrument has already been tested with a variety of individual compounds and mixes of known composition including light, polar oxygenates, aliphatic and aromatic hydrocarbons and mono-terpenes. A more stringent test was proposed as part of this project; a laboratory version of an aged air mass experiment. Smog chamber experiments of representative hydrocarbons generate some of the highly polar and semi-volatile compounds that are generated in ambient air. Also, because some of the target reactive compounds have unknown identities, testing their collection and recovery presents obvious problems. A good surrogate source for these "unknown" compounds is a smog chamber where hydrocarbon photooxidation projects may be generated. "Carbon balance" is not attainable with a standard GC-FID in this type of experiment due to the oxygenated and nitrated photooxidation products carbon (e.g., [34, 35]), however the TNMOC measurement should be able to detect more of the reacted.

2.4.1 Experimental Description

Smog chamber experiments were conducted in a 1.4 m^3 Teflon chamber. The chamber was surrounded by variable intensity UV lights (Silvania Blacklights, 40W, F40/350BL). Reactants were added in the zero air stream (Thermo Environmental) as the chamber was filled. A Teflon mixing fan was used while the chamber was filled and for about 5 minutes before each sample was withdrawn. The initial concentrations were about 0.5 ppm and from 0.8 ppmC to 3.5 ppmC for NO and hydrocarbons, respectively. Some NO_2 forms in the process of filling the chamber via the reaction:

$$2\,NO + O_2 \rightarrow 2\,NO_2 \qquad (1)$$

NO and NO_2 were monitored throughout the experiments using a Thermo Environmental Instruments, Inc., Model (14B/E) chemiluminescence NO - NO_2 - NO_x analyzer. Ozone was monitored by a Dasibi Environmental Corporation (Model 1003RS) ozone analyzer. A 10 m length of heated 1/4" Teflon tubing was used as the sample line for the TNMOC instrument. Samples were withdrawn at 0.7 (α-pinene) or 1.3 (isoprene and m-xylene) L/min with a pump attached to the downstream end of the sample inlet. A sample flow of 50 mL/min was drawn from this line into the TNMOC instrument. Initial concentrations of reactants were measured in TNMOC mode and speciated VOC's mode. When the initial concentrations were stable, the blacklamps were turned on to generate a simulated "urban" atmosphere. In these smog chamber experiments, the hydrocarbon reacts with OH, O_3 and NO_3. Concentrations of reactants were measured in parallel in TNMOC mode and speciated VOC's modes.

2.4.2 Isoprene Photooxidation

Figure 2.3.1 shows the results of an isoprene photooxidation experiment. Concentrations in TNMOC mode, isoprene concentration from speciated VOC's mode, total speciated VOC's concentrations including isoprene and products, are plotted as a function of photolysis time. The average initial isoprene concentration was 2.7 ppmC, and the initial concentration of NO_x was 460 ppb. Prior to beginning of photooxidation experiment, trapping efficiency of isoprene was measured as a function of trap I temperature. Isoprene was completely trapped in trap I at –70 C, the operational temperature. At the end of the experiment, the O_3 concentration had reached 112 ppb and the NO_x had decreased by 30%. The isoprene had decreased to 31% of its original value, the speciated VOC's to 56%, and TNMOC to 88% of its initial value. The true TNMOC value in this experiment was expected to be 90-94% of its original value due to a) some carbon being completely oxidized to CO or CO_2 (4-8% for this run) b) formation of propene from the reaction of isoprene with O_3 (roughly 2%), and c) deposition to the walls of the chamber, which should be negligible for isoprene, but will be several percent for products that have four or five carbons and one or more hydroxy, carbonyl, nitrate or acid group. Estimates of a) and b) are based on the oxidation mechanism of isoprene [16]. These results show that the TNMOC instrument has done an excellent job of detecting the products of isoprene oxidation, which are known to include formaldehyde, methylglyoxal, methylvinylketone, methacrolein, 3-methylfuran, epoxides and several 5-carbon hydroxycarbonyls [16, 36].

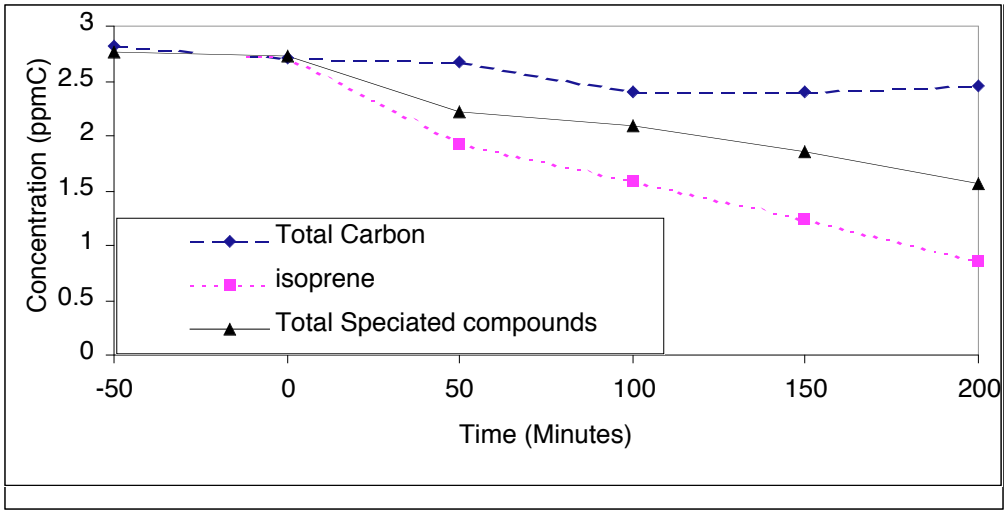

Figure 2.4.1 Concentrations of TNMOC, isoprene and Total speciated compounds as a function of time.

2.4.3 m-Xylene Photooxidation

Figure 2.3.2 shows the results of a m-xylene chamber experiment. The average initial m-xylene concentration was 3.0 ppmC, and the initial concentration of NO_x was 560 ppb. The O_3 concentration reached a maximum of 129 ppb 60 minutes into the run, and decreased to 75 ppb by its completion. By the end of the run, the NO_x had decreased by 75%, the m-xylene had decreased to 38% of its original concentration, the speciated VOC's was 40% of its original value, and TNMOC was 84% of the initial value. The true TNMOC value in this experiment was expected to decrease 88-94% of its initial value due to a) some carbon being completely oxidized to CO or CO_2 (2-6% for this run) b) formation of aerosols (from 1-4%) [37], and c) deposition to the walls of the chamber, which should be less than 1% for m-xylene, but will be several percent for all products that retain the majority of the carbon backbone. The TNMOC instrument has done a very good job of detecting the products of m-xylene oxidation, which include formaldehyde, and a number of oxygenated and nitrated 8-carbon products [23, 38]. It is particularly impressive that almost none of the products of m-xylene photooxidation make it through the standard GC-FID analysis, yet they are almost completely detected by the TNMOC measurement.

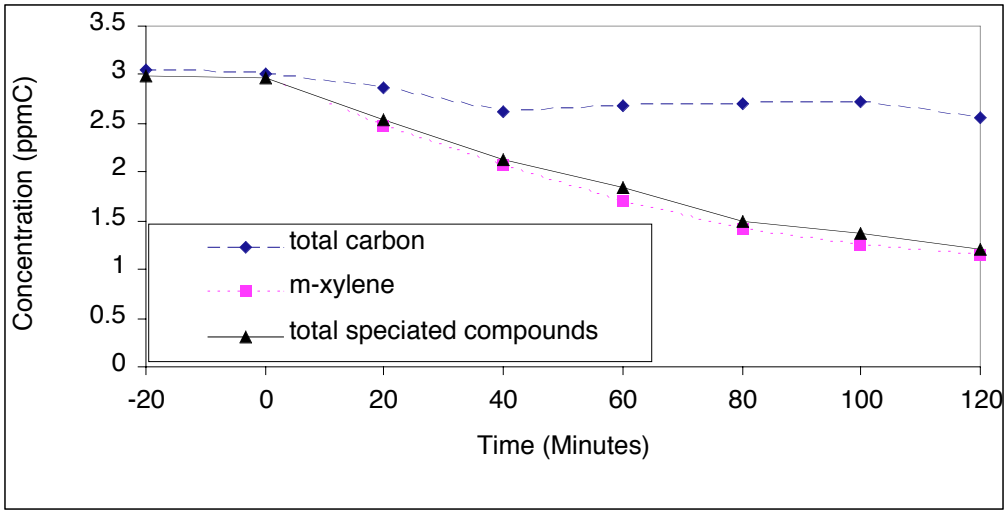

Figure 2.4.2 Concentrations of TNMOC, m-xylene and Total speciated compounds as a function of time.

2.4.4 ▯▯Pinene Photooxidation

Figure 2.3.3 shows the results of an ▯-pinene chamber experiment. The initial concentrations of ▯▯pinene and No_x were 1.9 ppmC and 780 ppb, respectively. The O_3 concentration had reached 116 ppb by the time the run was terminated. By the end of the run, the NO_x had decreased by 30%, ▯-pinene had decreased to 9% of its original value, the ▯ speciated VOC's was 13% of its original value, and TNMOC was 31% of the initial concentration. The true TNMOC value in this experiment was expected to decrease to 80%-92% of its original value due to a) some carbon being completely oxidized to CO or CO_2 (2-4% for this run) b) formation of aerosols (from 5-10%) [39], and c) deposition to the walls of the chamber, which should be a few percent for ▯-pinene, and will probably be more than 10 percent for products of ▯-pinene oxidation, which include such semi-volatile compounds as pinonaldehyde, pinonic acid, norpinonaldehyde, norpinonic acid, and pinic acid, 2-hydroxy-3-nitratepinane and 3-oxo-2-nitratepinane [40, 41]. The expected aerosol yield is higher than that reported below for our aerosol measurements (section 3), however because we allowed the aerosols to "age" for several hours before making measurements, most of the mass had already deposited at the wall. Although the performance of the TNMOC instrument was very good for both the isoprene and m-xylene oxidation products, clearly many of the products of ▯-pinene oxidation are not recovered at 100%. Losses in the sampling line and in the desorption step from Trap I are described below.

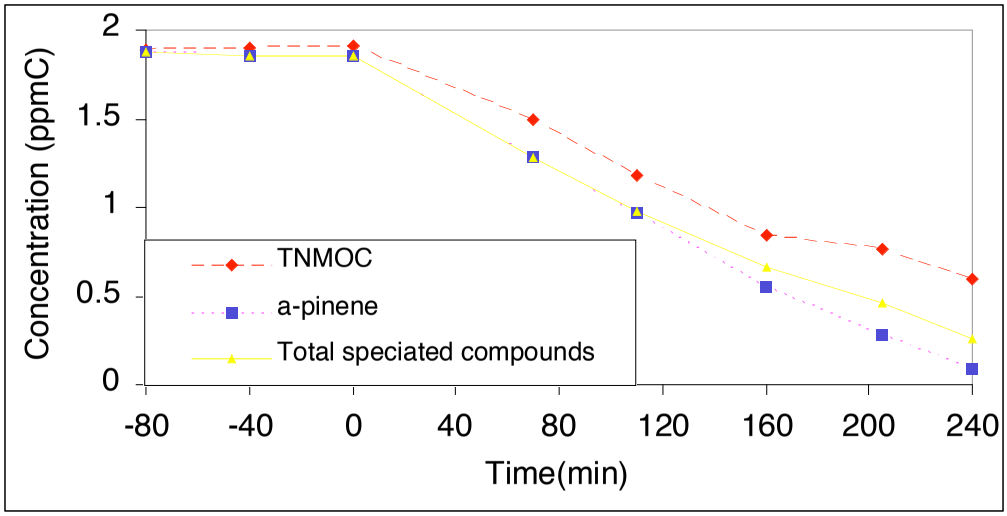

Figure 2.4.3 Concentrations of TNMOC, α-pinene, and β speciated VOC's as a function of time. The flow rate in the sampling line was increased for the last two measurements, and is probably responsible for the relative increase in TNMOC signal.

2.4.5 Effect of Sample Flow Rate on Recovery of Semivolatile Products

Examination of the data in Figure 2.3.3 shows a change in slope for the TNMOC signal for the last two measurements. For these runs, the flow rate in the Teflon sampling line was increased from 0.67 L/min to 1.3 L/min and 2 L/min for the second to last and last measurement, respectively. Clearly some of the losses of semivolatiles were in the sample line itself, although increasing the flow rate only improved the recovery somewhat. Measurements were also made for the products of isoprene photooxidation (not shown), but in this case the lights were turned off so that the mixture was fairly stable. A similar trend was observed – the recovery was lower (by about 10%) with flow rates below 1.3 L/min, and reached a maximum of 1.3 L/min or higher flow rates. 1.3 L/m was used for the isoprene and m-xylene experiments.

2.4.6 Effect of Desorption Temperature on Recovery of Semivolatiles

The desorption temperature of trap I was also considered. Figure 2.3.4 shows results of concentrations of α-pinene, TNMOC, and β speciated VOC's for an αβpinene photooxidation with different Trap I desorption temperatures. Runs 1-4 are the initial values, 5-7 after 20 minutes, and 8-11 after 40 minutes. The concentrations of αβpinene and β speciated VOC's were essentially independent of desorption temperature in trap I. After the αβpinene had reacted down to 46% of its initial concentration, a desorption temperature of 100 C gave a TNMOC value that was 63% of the initial concentration, while increasing the desorption temperature to 150 C increased the TNMOC to 78% of the initial value, very close to the lower limit of the expected range for the true value

(~85-95%), indicating that between 65 and 83% of the photooxidation products were recovered. While increasing the Trap I desorption temperature even further is an obvious next step, 150 °C is currently the maximum temperature for Trap I. Since this time, we have performed our desorption at 150 °C.

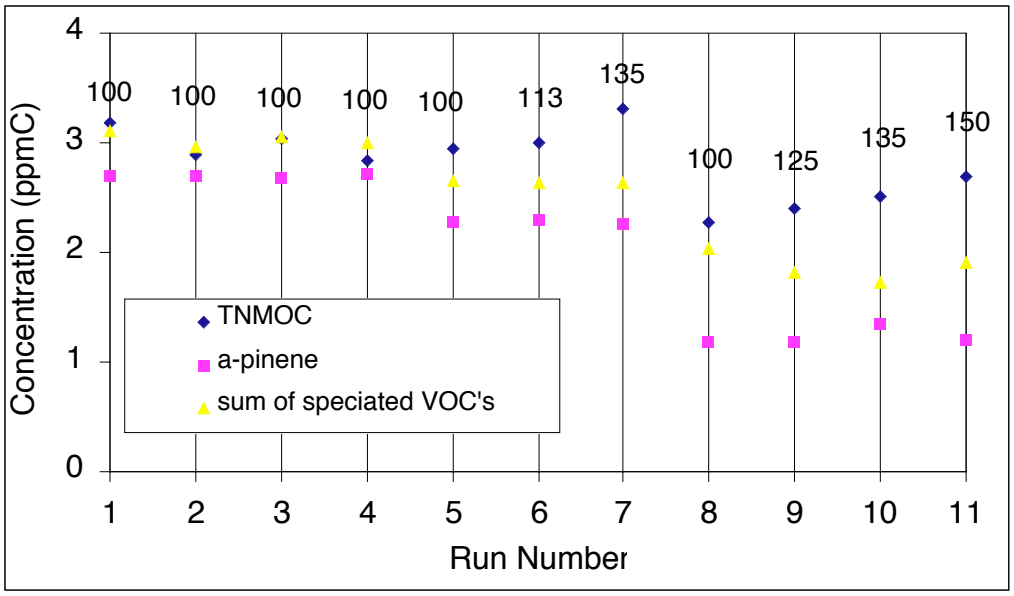

Figure 2.4.4 Measurements of TNMOC, α-pinene and sum of speciated VOC's. Runs (measurements) 1-4 were before photooxidation began. Numbers indicate the desorption temperature of trap I. Runs 5-7 and 8-11 were made after 20 minutes and 40 minutes, respectively, of exposure to blacklamps that initiate photochemical oxidation of α-pinene.

2.5 Behavior of Aerosol Particles in Sampling Lines

The goal of the TNMOC measurement is to measure reactive organics in the gas phase. The organic carbon in the aerosol phase is usually much smaller than that contained in the gas phase, but nevertheless, aerosol organic carbon would preferably be excluded from the TNMOC measurements. A particle filter could be attached to the sample inlet, but this would add a potentially interactive surface to the sample train, and potentially produce such undesirable effects as adsorbing semivolatiles or desorbing aerosol organic carbon. While the exact contribution of aerosols to the total carbon measurement is difficult to quantify, a rough estimate can be made. Polluted air might contain up to 20 $\mu g/m^3$ of aerosol phase organic carbon, although 5 $\mu g/m^3$ is more typical [42, 43]. To convert this to an equivalent gas-phase concentration (ppbC), the following calculation is made:

$$\left(\frac{1\mu g\ \text{aerosol carbon}}{1\,m^3}\right)\left(\frac{1\ \text{mol}}{12\,g\ C}\right)\left(\frac{10^{-6}\,g}{1\,mg}\right)\left(\frac{6.02\bullet 10^{23}\ \text{molec.}}{1\ \text{mol}}\right)\left(\frac{1\,cm^3\ \text{air}}{2.46\bullet 10^{19}\ \text{molec.}}\right)\left(\frac{10^{-6}\,m^3}{1\,cm^3}\right) = 2\ \text{ppbC} \qquad (1)$$

Since the concentration of gas phase organics in urban air range from 200-1000 ppbC, the limits of the aerosol contribution is from < 1 to 20%. 20% is an upper limit because high levels of organic aerosols are more frequently associated with higher levels of pollution, and thus with high levels of TNMOC. A typical contribution of aerosol to TNMOC is expected to be less than 5%. In addition, some aerosols are almost certainly lost in the sampling lines and valves upstream of the sampling device and aerosols that penetrate to Trap I may not be measured quantitatively as TNMOC, thus the contribution of aerosol organic carbon to the TNMOC measurement is almost certainly very small. To characterize the fate of aerosols in our system, we investigated aerosol transmission through our sampling lines.

2.5.1 Materials and Methods

Aerosol measurements were made both directly at the source of the aerosols and at the end of the sampling line to the TNMOC instrument. For these initial studies, losses in the final 1/16" outer diameter (OD) transfer line and valve that are upstream of Trap I were not tested. Measurements were conducted with a laser aerosol spectrometer manufactured by Particle Measuring Systems (model LAS-X), which is capable of measuring particles in the size range 0.1-3 μm. The instrument measures laser light scattered by the aerosol particles as they pass through the laser beam. The scattered energy is reflected by a mirror in the chamber towards a photomultiplier tube, which converts the signal into a voltage. The voltage is proportional to the size of the aerosol particle. In this way, the spectrometer records both size and number counts. The air samples are drawn into the spectrometer via an inlet tube and an internal pump, with a constant sample flow of 1.2 cm^3s^{-1}. The composition of the tube itself may be changed, although the diameter of the inlet tube, 0.125" OD, is fixed.

Ambient air is the ideal source for aerosols, but has the drawback that ambient aerosol number densities and size distributions vary on a short time scale. When ambient air proved difficult to interpret, samples were generated by photolyzing mixtures of α-pinene/NO_x in our smog chamber. Shown here are two experiments with initial concentrations of α-pinene at 400 ppb. Since the focus of the measurements was on the relative losses of particles in our sampling lines, after the lights were turned on for a few hours, the aerosols generated from the oxidized hydrocarbons were allowed to "age" for from 4-20 hours, resulting in a relatively stable (albeit small) aerosol population.

2.5.2 Results

Representative results for experiments with Teflon and Silco-steel sample lines are shown in figures 2.4.1 and 2.4.2, respectively. In both cases data was collected first at the chamber (10 minute sampling interval), then at the end of the sampling line at different flow rates (2 five minute intervals each), and then again at the chamber. Measurements at the same position and flow rate were averaged.

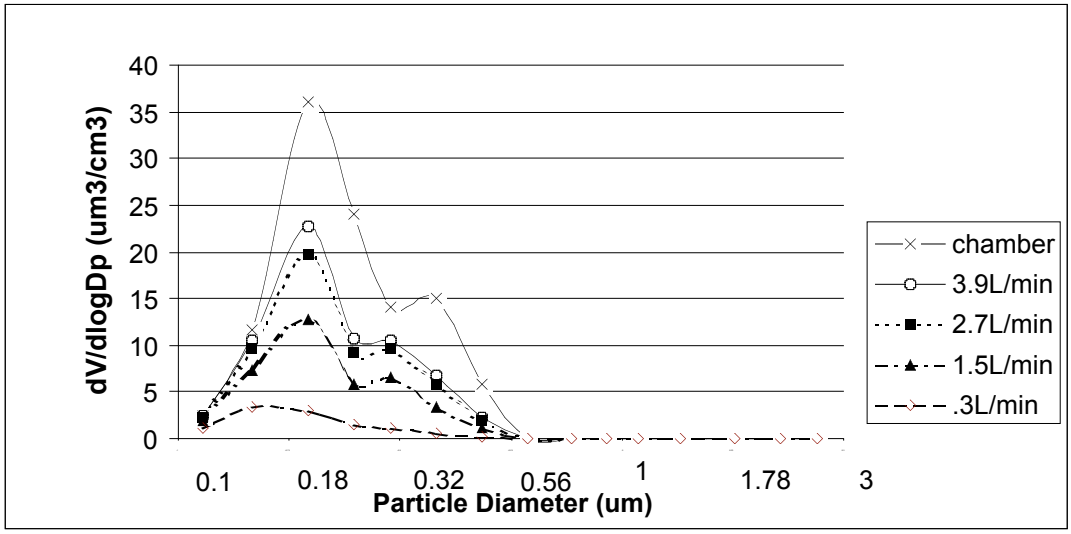

Figure 2.5.1 Transmission of aerosols through a heated 10 m x _" OD Teflon sampling line at different flow rates. Measurement labeled "chamber" were made through a ~0.5 m x _" OD copper sampling line. The total mass measured at the chamber is equivalent to roughly 25 $\mu g/m^3$.

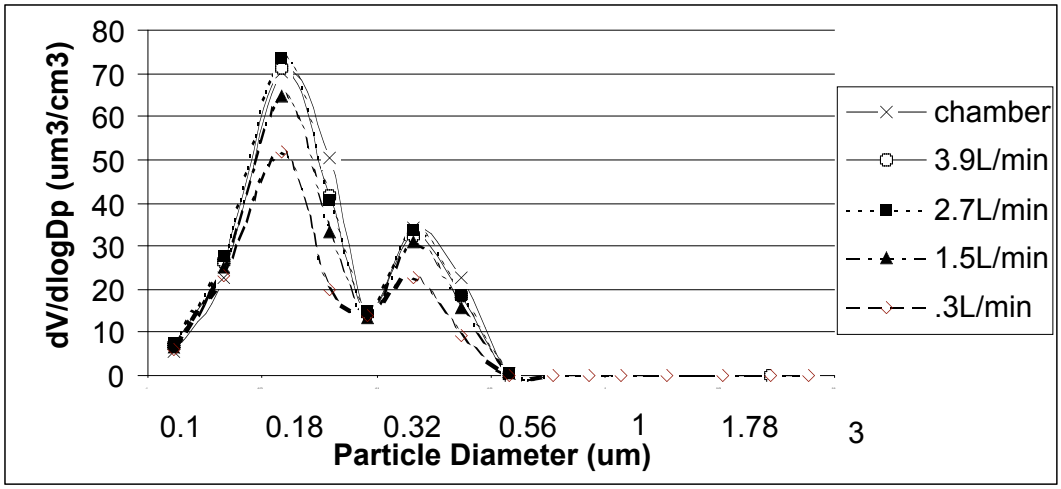

Figure 2.5.2 Transmission of aerosols through a heated 1/8" OD Silco-steel sampling line at different flow rates. Measurement labeled "chamber" were made through a ~0.5 m x _" OD copper sampling line. The total mass measured at the chamber is equivalent to roughly 15 g/m3.

It is apparent from both plots that the aerosols generated in the chamber are smaller than that typically observed in ambient air. These small particles are lost in the Teflon sampling line more readily than in the Silco-steel sampling line, although transmission through both of the lines is significant at the higher flow rates that are favored based on the studies of TNMOC recovery in chamber experiments discussed above. Small particles are transported to the walls of the tube by diffusion, and thus the losses should be inversely proportional to the residence times in the tubes [43]. The residence times in the Teflon tube at the same flow rate are about 6 times those of the Silco-steel tube, and the aerosol losses are roughly proportional to this difference. It is interesting to note that the TNMOC measurements made together with these measurements did not increase when the flow rate in the sampling line was increased above 1.3 L/min, even though transmission of aerosols did. This hints that aerosols are being removed either between the sample line and trap I, or in Trap I itself, but in any case may not be measured as TNMOC. Although not addressed by these measurements, it is possible that lager aerosol particles are lost at much higher rates due to inertial impaction on the walls of the sampling tube [43]. Application of these results to the field measurements is discussed in Section 4.

2.6 Detection Limit and Uncertainties

The discussion that follows refers to the instrument as it performed as of 2000, and how it performs at the present time. As for many instruments, detection limits and uncertainties for the both the TNMOC and speciated channels and the ratio of the two are variable, since some sources of uncertainty are absolute, while others are proportional to the size of the measurement.

Since the TNMOC channel produces a single, isolated peak, integration of the signal is straightforward. The reproducibility of the calibration gas measurements (n-

hexane) is ± 3 % for measurements repeated with in a few days, and ± 5 % over the whole 2000 sampling period. Oxidation and reduction catalysts are very stable, and conversion rates are not differentiable from 100%. For the TNMOC channel, both the detection limit and the uncertainties are determined primarily by the subtraction of the trapped ambient CO_2, which is the dominant source of potential error. With trap 1 held at a temperature of -60°C of trap 1, 0.01% - 0.05% of ambient carbon dioxide was trapped depending on the sample volume. One to four measurements without oxidation were performed daily to determine the contribution of trapped ambient CO_2 to the TNMOC signal by running ambient air samples without the oxidation catalyst in line. During the 2000 measurements at UCLA, the following data were collected to determine the precision of the trapped ambient CO_2 values. We used two sample sizes; 570 and 1140 mL. 1140 mL was the default, and 570 mL was used on days with high humidity to avoid FID flameout due to water. The 1 variability for the different types of measurements is from ± 5 to 16 ppbC, but does not depend on the sample size, and the overall 1 variability for all measurements is 11 ppbC. These values somewhat overestimate the uncertainty from this source because on any single day, the measurements are more reproducible than they are over periods of weeks. The detection limit of the TNMOC channel is then three times the standard deviation of the trapped ambient CO_2, or about 35 ppbC. The uncertainty is given by the standard deviation itself, and is equivalent to about 10 ppbC. The very lowest TNMOC concentrations we have measured are 35 ppbC, at the detection limit, and clearly these points are fairly uncertain. Average TNMOC levels even on cloudy days are 6 times greater than this, so that uncertainty from this channel is about ± 5% from the CO_2 measurement and ± 7% when combined with other sources of error. Clearly there is the possibility that despite our inlet, some compounds are still not detected by the TNMOC channel. Such possible compounds are not included in this estimate

Table 2.4 Variability of Trapped Ambient CO_2 in the TNMOC Channel During 9-12/2000

Period	Sample Volume (mL)	n	$[CO_2]$* Average ± SD (ppbC)	$[CO_2]$ min. (ppbC)	$[CO_2]$ max. (ppbC)	[TC] Average ±SD (ppbC)	[TC] min. (ppbC)	[TC] max. (ppbC)
Sunny 09/12/00-10/09/00	1140	15	49±14	36	86	329±178	91	835
	570	5	129±8	121	142			
Cloudy 09/12/00-10/09/00	1140	10	54±8	41	64	205±120	68	620
	570	8	115±13	84	126			
11/30/00-12/20/00	1140	11	59±5	50	69	269±172	35	889
	570	2	126±16	115	137			

* Calculated as an equivalent concentration in the volume sampled. Above a minimum volume of several mL, approximately the same absolute quantity of CO_2 is trapped regardless of sample volume.

Measurements and quantification of individual hydrocarbons are reasonably straightforward. Our detection limit for individual VOC's is 10-20 pptC if the compound is well resolved on the chromatogram. The reproducibility for the n-hexane standard is ± 2%,but a realistic value for the uncertainty for most compounds in ambient air is ± 10–20%.

The uncertainty of the sum of speciated VOC's channel is the most difficult to estimate. Clearly if an air sample contained 100 individual compounds with a total concentration of 1 ppbC, this would be very difficult to measure. Ambient air tends to contain several dominant peaks, however, all of which are far above their detection limit at total concentrations 25 ppbC, the lowest concentrations we have encountered. Keeping in mind that the purpose of this instrument is to provide some measure of the organics present in ambient air that are not measured by the standard GC techniques (i.e. PAMS measurements), the minor components that get lost in the baseline should not be reported in this channel (but must be in the TNMOC channel), so a 1 ppb detection limit is reasonable. The uncertainty in this measurement is key, however. Deriving a sum of speciated VOC's is straightforward if the baseline is very flat, but less so the more congested it becomes. Standard integration programs are naturally oriented toward quantifying individual compounds, and tend to draw the baseline toward the base of the clearly defined peak. In contrast, we draw our baselines so that there is a straight line below the entire chromatogram, beginning at where the baseline starts to rise, and ending at the point where peaks cease to appear. In this way, we tend to *overestimate* the quantity of carbon in this channel so as to *underestimate* the TNMOC/sum of speciated

VOC's ratio. How the baseline is integrated has a slightly larger effect on the low concentration points relative to the mid concentration data, and has little impact on the analysis of the highest concentration points. As a result, the of Speciated VOC's measurements carry a + 3-5%,- 10-30% uncertainty.

The uncertainties in the ratio of TNMOC/sum of speciated VOC's is calculated based on the TNMOC and sum of speciated VOC's values.

Table 2.5 Estimated Detection Limits and Uncertainties

	Detection Limit	Uncertainty
TNMOC channel	35 ppbC	±10 –20 ppbC; ± 7% at concentrations over 200 ppbC, increasing below
of Speciated VOC's Channel	1 ppbC	+ 3-5% - 10-30%
Individual VOC's	10 pptC	± 3-20%, depending on separation
TNMOC/SUM OF SPECIATED VOC'S RATIO	—	± 0.05 to ± 0.10 for ratios between 1 and 2, depending on concentration, - 0.1, + 0.5 for ratios above 2

3. Field Measurement Sites and Instrumentation

3.1 UCLA

Measurements were performed on the UCLA campus in the penthouse laboratory of the Math Sciences Building (Figures 3.2 and 3.3). The inlet of the sample line was located at 34.07 N, 118.45 W and at 150 meters elevation, 24 m above local ground level. The inlet of the sampling line is located 1.5 m above the roof of the penthouse lab, and about 5 meters above the roof of the building. UCLA is bordered by residential neighborhoods to the north, east and west, and by a commercial district to the south. The 405 freeway is located approximately 1.5 km west of UCLA, and Wilshire Blvd, a heavily traveled surface street, is located about 1 km to the south. Relatively low concentrations of pollutants may be expected, due to the elevated position of the sample site, its proximity to the shore, limited local sources and the distinctive land-sea wind circulation in this coastal region.

The meteorology at UCLA is reasonably reproducible. Averaged surface winds for 2000 are shown in Figure 3.1; winds for each day are shown in Section 5. During the field measurements during 1999, most days were sunny and clear; during 2000 several days were cloudy. On both sunny and cloudy days the surface wind pattern is similar. At night the wind speeds are low (generally less than 1 m/s) and the prevailing direction is from the N of E. During the day, the prevailing wind is about 210°, or SSW. Between noon and 8 PM, wind speeds range between 1 and 4 m/s, with average maxima of about 2.5m/s at 4 PM (See Section 5). From 5 AM to noon, and 8 PM until 10 or 11 PM are transition times when the wind shifts between day and night regimes.

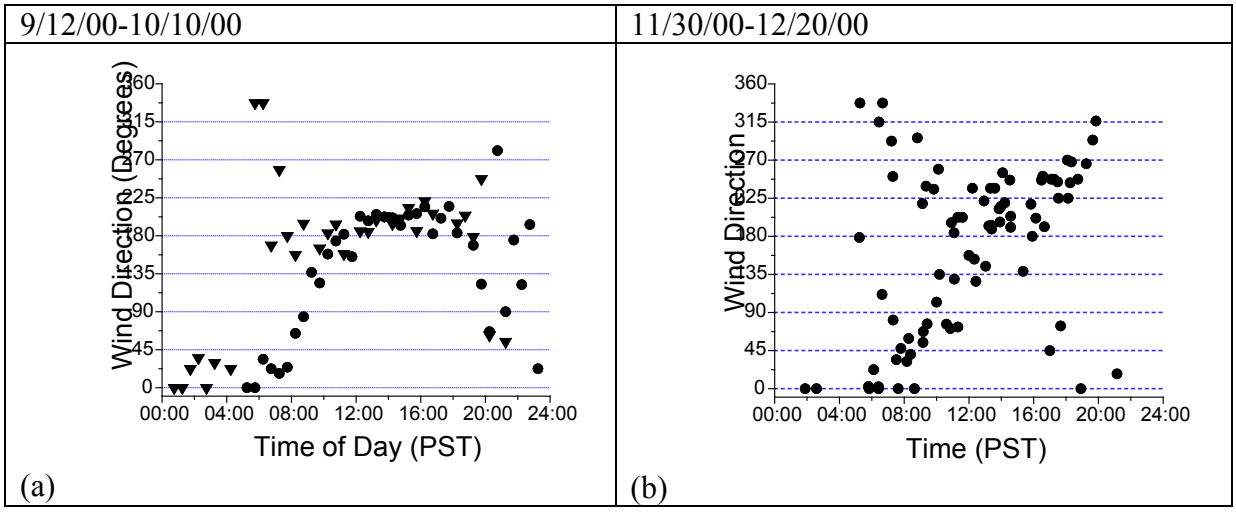

Figure 3.1 Half hourly averaged wind direction for (a) sunny (circles) and cloudy (triangles) days during Sept.-Oct. and (b) all sampling days during December.

The morning transition is key to understanding pollutant concentrations at the UCLA site. Before 5 AM in Sept.-Oct., the wind comes from the North, a hill area with a relatively low population of exclusive homes, separated by a moderately traveled surface street, Sunset Blvd. Between 5 and 8 AM winds are shifty but are still predominantly from the North. At about 8 AM the wind starts to shift in earnest, so that the average wind direction at 8, 9 and 10 AM is about 100, 170 and 200°. Areas to the south and west of the UCLA site experience much higher vehicle traffic and commercial activity. The 405 freeway which runs N-S about 1 km to the south west of the site delivers much higher VOC and NO_x levels to the site once the transition occurs, and typically by 9 AM a NO_x peak is observed. In contrast, the morning NO maxima occurs at 7 AM at the SCAQMD site located 300 m E of the 405 and 150 m S of Wilshire, about 1.5 km from the UCLA site. The morning wind transition occurs a bit later in winter; at 8, 9 and 10 AM, wind is coming from 25, 50 and 80° respectively and result in an even later morning NO_x maximum. Most mornings, there is a small, short-lived spike in the wind speed at around 6 AM, increasing the wind speed from near zero up to 1 or 2 m/s. This spike is not associated with a consistent wind direction, however it is associated with a spike in the calculated residence time and the TNMOC/□ of speciated VOC's ratio (below).

Figure 3.2 Map of the western portion of the Los Angeles air basin. Stars indicate the locations of the measurement sites at Azusa, Burbank and UCLA. Azusa was the subject of measurements in 1997, and is used for comparison in Section 5.

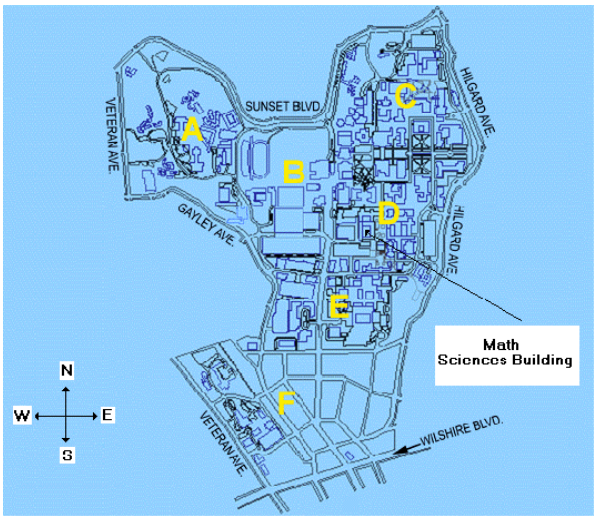

Figure 3.3 Map showing location of the Sampling site on the UCLA campus.

3.2 Burbank

The city of Burbank is located in the San Fernando Valley approximately 20 km NNW of downtown Los Angeles. The measurement site was located in the air monitoring station operated by the SCAQMD (Figure 3.2). The station is located in an one-story building with the sample inlet for the instruments located on top of the roof of this building, about 5 m above ground. The Burbank Station is surrounded by heavily traveled freeways, the closest of which, interstate 5, is about 0.5 km away. The station is located in a mixed residential and light industrial area, and the local industry is dominated by auto body shops. An oil-fired power plant is located to the North East, but only 2.9% of the winds during the period of our field measurements came from the North East, so the expected influence of the power plant is small. Given the strong local sources, concentrations of pollutants may be expected to be high.

3.3 Instrumentation

The measurement stations were equipped with the same set of instruments to measure TNMOC, the sum of speciated VOC's, NO, NO_2, NO_x, O_3, wind-speed, wind-direction, and temperature. Particle number distribution was also measured in 1999. Table 3.1 summarizes the instruments we operated at the stations, together with their respective sample frequencies. A small meteorological station measuring wind speed, direction, and temperature with 1-minute time resolution was deployed (Davis Instruments). A NO_x analyzer (Thermo Environmental model 42) and an ozone analyzer (Dasibi Corporation 1003-RS) were operated continuously, also with 1-minute time resolution. Ozone, NO_x, and meteorological data were archived on a personal computer.

Table 3.1: Instruments deployed during the field measurements at Burbank and UCLA, 1999-2000

Parameter	Instrument	Sampling Period (min.)	Sample frequency (1/h)	Sample volume /flow
TNMOC and VOC's	GC HP 5890 II	10	1-2	500 mL @ 50 mL/min (1999), 570-1140 mL/min @ 50 mL/min (2000)[2]
NO	Thermo Environmental Model 42	1	60	100 mL/min
NO_2				
NO_x				
O_3	Dasibi Model 1003-RS	1	60	2 L/min
Aerosols[1]	PMS	1 (Avg. to 10 min.)	60	200 mL/min
Wind-speed	Davis Instruments Weather Wizard III	1	60	-
Wind-direction				
Temperature				

[1]Not measured in 2000.
[2]In 2000, simultaneous TNMOC and sum of speciated VOC samples were acquired every 30-60 minutes. The sampling acquisition time was between 10 and 20 min, depending on ambient relative humidity. These sampling times correspond to sample volumes of 570-1140 mL. When relative humidity was above 60%, the sample volume was limited to 570 mL in order to prevent flame out of the FID from excessive water.

3.45 Calibrations and Uncertainties

3.4.1 Total Non-Methane Organic Carbon Analyzer

Simultaneous calibration of the TNMOC and speciated VOC channels was performed twice each sample day by using 200 mL samples of 1.08 ppmV n-hexane in N_2 (Scott). The resulting FID calibration factors (Area/ppmC·ml) were used to calculate the concentration of TNMOC and the sum of speciated VOC's from the chromatograms of the ambient air samples. At UCLA, a retention time marker mix was generated by diluting 1000 ppmV $C_1 - C_6$ n-alkanes in N_2 (Scott) down to about 400 ppbV with N_2, and was run daily. At Burbank a mixture of 1 ppmV benzene, toluene, ethyl benzene, o-, m-, p-xylene in N_2 (Scott) was used to establish retention times. These, together with retention time tables obtained from other researchers were used to identify individual peak concentrations (Section 9, Appendix). A small diaphragm pump was used to maintain a flow of 1 Lpm at the TNMOC instrument, from which the 500 mL samples

were drawn at 50 (1999) or 57 (2001) mL/min. The concentrations measured in this campaign always exceeded the detection limit (3σ of the uncertainty due to subtraction of the carbon blank) of about 100 ppbC (1999) or 50-60 ppbC (2000) for the TNMOC channel.

The uncertainties for the TNMOC and Σ speciated VOC's were calculated using propagation of error based on several sources of uncertainty. Potential errors are introduced for the TNMOC data from the following sources: the methanizer conversion efficiency, the n-hexane calibration factor, the CO_2 blank, and the "measurement error," which includes integration error and random errors such as sample size or trapping temperature. For TNMOC at UCLA, the estimates for these errors were 6, 7, 8 and 6 % and for Burbank they were 6, 4, 2, and 6, respectively. For the Σ speciated VOC's channel, errors arise from the calibration factor and from measurement error. For Σ speciated VOC's at UCLA the estimates for these errors were 9 and 3 and for Burbank they were 7 and 3, respectively. Using the standard approach to propagation of errors, we have:

(1) $$\text{total error} = \sqrt{\sigma_n^2},$$

resulting in ± 14 % and 10 % for TNMOC for UCLA and Burbank, respectively, and ± 9 and 8 % for the Σ speciated VOC's at UCLA and Burbank, respectively.

With these estimates for the uncertainty, we can estimate the expected uncertainty in the ratio, TNMOC/Σ speciated VOC's. Again, using standard error propagation, the error for a quotient of the form: is given by:

(2) $$q = \frac{x}{y}$$

is given by:

(3) $$\frac{\partial q}{|q|} = \frac{\partial x}{|x|} + \frac{\partial y}{|y|}$$

Thus the uncertainty for any *individual* TNMOC/Σ speciated VOC's ratio acquired at UCLA during 1999 was ± 23 %, and those from Burbank were ± 18 %. Thus, given these potential sources of error, it is possible that if the true ratio is 1.0, the value we measure could be as low as approximately 0.8 or as high as 1.2. The averages we calculate are fortunately much more robust, since the error is decreased as the square root of the number of observations. Thus the uncertainties in our *averages* are thus ± 4 % for both data sets, excluding atmospheric variability.

At this point no effort has been made to correct this data for the light hydrocarbons that are not trapped in our first trap. This issue will be addressed in the next report.

3.4.2 NO_x Analyzer

The NOx analyzer was calibrated with a 9.75 ppmV NO in N_2 standard (Scott). This standard was diluted to 217 ppbV with ultra zero air (Airgas) and introduced to the

analyzer. Due to the excellent long-term stability of the instrument, the calibration procedure was performed once a week.

3.4.3 O_3 Analyzer

The Dasibi 1003-RS is equipped with an internal UV-lamp to produce O_3. This O_3 is introduced into the detection cell of the analyzer and is used as an internal standard. If the radiant power of the UV-lamp decreases, the calibration is compromised. In addition, the internal calibration cannot account for potential losses of O_3 in the sample line (although these are expected to be small). For this reason our measurements were compared with the results of the nearest SCAQMD O_3 analyzers, which are calibrated frequently by means of an external O_3 master standard. At Burbank, the SCAQMD analyzer was located in the same station, while for UCLA the West Los Angeles station was used, located about 2 km south of UCLA campus, at L.A. County Veterans Administration Hospital grounds about 500 meters east of the intersection of Wilshire Blvd. and Federal/San Vicente Blvd, just west of the 405 freeway. Agreement was very good for UCLA, while the Burbank data has been re-calibrated based on the SCAQMD instrument. For the 2000 measurements, the manufacturer, Dasibi Environmental Company, calibrated the ozone analyzer on April 10, 2000, certifying that the instrument was with in 3% of the calibration value for concentrations in the 9-500 ppb range.

3.4.4 Aerosol Analyzer

Aerosol concentrations were measured with a laser aerosol spectrometer (Particle Measuring Systems model LAS-X). The spectrometer measures particles in the size range from 0.09-3.0 μm, with the instrument being able to detect the particles in the following bins: 0.10-0.13 μm, 0.13-0.17 μm, 0.17-0.22 μm, 0.22-0.28 μm, 0.28-0.33 μm, 0.33-0.43 μm, 0.43-0.54 μm, 0.54-0.69 μm, 0.84-1.0 μm, 1.0-1.2 μm, 1.2-1.6 μm, 1.6-2.0 μm, 2.0-2.5 μm, and 2.5-3.0 μm. The sample was drawn in via an internal pump at a constant flow rate of 1.2 cm^3 s^{-1}. The particle counter is normally calibrated by the manufacturer, and was calibrated in May of 1999.

3.5 Instrumental Setup

The meteorological equipment was installed on the rooftops at both stations to minimize potential architectural influences on the meteorological measurements. The sample manifold for the trace gases was attached to the mounting tripod of the meteorological station and mounted underneath the radiation shield of the temperature sensor to protect it from rainfall and dust. The manifold was made of 10 m x 1/8" (OD) Silcosteel (Restek) tubing, which was heated to about 50°C to prevent losses of semi-volatile and/or polar organic compounds due to adsorption on the inner wall of the tubing. Figure 3.4 shows a scheme of the sampling manifold used in 1999, and Figure 3.5 shows the scheme built for the 2000 measurements.

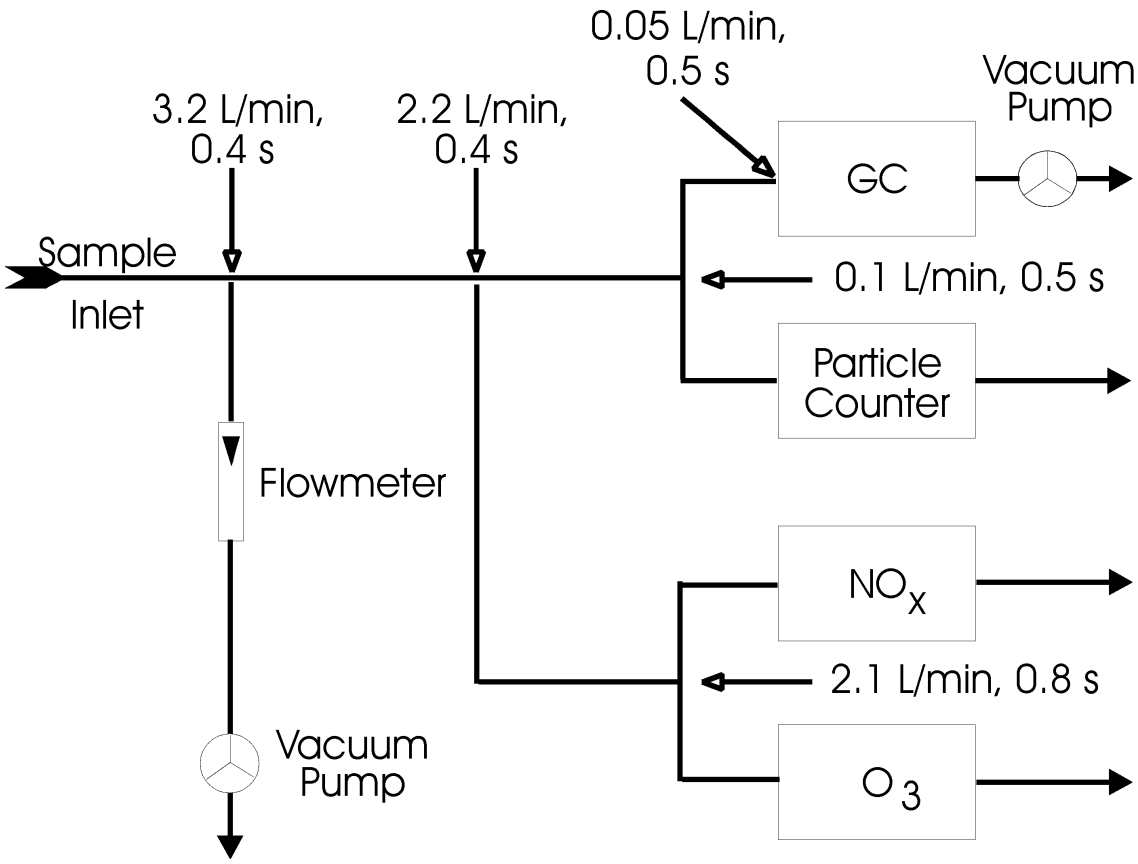

Figure 3.5.1: Schematic representation of the instrumental setup at Burbank and UCLA during 1999. The flow rates are indicated at several points with arrows, followed by the cumulative residence time for each point.

The vacuum pump/flow meter unit was used to maintain a permanent flow of the sample air through the manifold. The total flow was approximately 3.2 l/min, resulting in a residence time of 0.4 s for the air sample in the manifold. The design of the manifold assured that only a minimum of particulate organic matter will reach the first trap of the GC. The particle counter was attached to the same manifold branch as the GC to assess the potential influence of organic particulate matter on the results of the TNMOC and sum of speciated VOC measurements.

The sample inlet used in 2000 was similar in design to that used in 1999, and is shown in Figure 3.5. Ambient air was pumped at 42 L/min through a 14 m, 8 mm ID FEP Teflon tube. The residence time in the tube was 1 s.

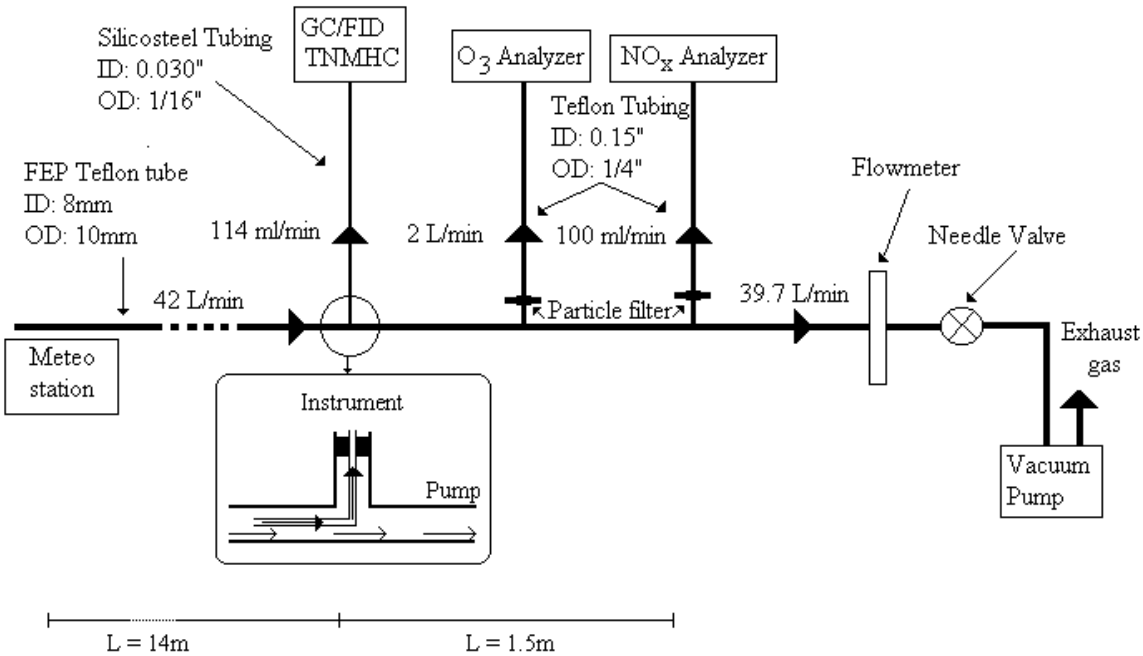

Figure 3.5.2. Flow schematic of the sampling manifold for the field measurements at UCLA during 2000.

3.6 Retention index

Retention index (I) is a measure of the retention of a solute relative to the retention of normal alkanes (straight chain hydrocarbons) at a given temperature and column. Equation E1 is used to calculate retention indices for temperature program conditions. The retention index for a normal alkane is its number of carbons multiplied by 100. For example, n-dodecane (n-$C_{12}H_{26}$) has I = 1200. If a solute has I = 1478, it elutes after n-C_{14} and before n-C_{15}, and it is closer to n-C_{15}. Retention indices normalize instrument variables so that retention data can be compared for different GC systems. Retention indices are also good for comparing retention characteristics for different columns.

Equation E1. Retention indices (IT) for Temperature Program Conditions

$$IT = 100\,[(t_{R(x)}-t_{R(y)}) / (t_{R(z)} - t_{R(y)}] + 100y$$

t_R= retention time
x = solute of interest
y = normal alkane with y number of carbon atoms eluting before solute x
z = normal alkane with z number of carbon atoms eluting after solute x
z-y = difference in carbon number between the two normal alkanes

4. 1999 Field Data

Results of the field campaign are shown in the following paragraphs. The results of the measurements at UCLA will be presented first, followed by the results of the measurements made in Burbank. Averages and ranges for both sites and all measurements except particles are shown in Table 4.1.

Table 4.1 Concentration ranges and averages of O_3, NO_x, TNMOC, and □ speciated VOC's at UCLA and Burbank.

Compound	UCLA		Burbank	
	Average (ppbV)	Range (ppbV)	Average (ppbV)	Range (ppbV)
NO	4.7 ± 9	<dl – 100	43 ± 70	<dl – 410
NO_2	16 ± 8	<dl – 50	53 ± 20	10 – 148
NO_x	21 ± 15	<dl – 140	100 ± 90	7 – 510
O_3	20 ± 15	<dl – 750	15 ± 20	<dl – 93
TNMOC (ppbC)	372 ± 170	120 - 880	2270 ± 600	740 - 4000
□SP (ppbC)	258 ± 100	80 – 520	2060 ± 500	730 - 3000

The detection limits (dl) were:
dl NO_x = 1 ppbV (according to manufacturer)
dl O_3 = 1 ppbV (according to manufacturer)
dl TNMOC = 107 ppbC (3□ of CO_2 blank)

4.1 Methanizer Conversion Rate

During the 1999 measurements we encountered a new and recalcitrant problem with the methanizer performance when the instrument was used for ambient air sampling—this problem did not appear until the instrument was deployed in the field. This methanizer was built with the same method and materials as the methanizer that performed flawlessly during the 1997 SCOS field campaign, but it failed within about 20 measurements in 1999. For this reason n-hexane calibrations were performed at least twice a day to calibrate the conversion rate of the methanizer in order to correct the data. On 10/12/99 we performed a series of four n-hexane calibrations interspersed with 12 ambient air measurements. The results indicate that the decrease of methanizer efficiency is approximately linear, so that at least over a small range the n-hexane calibrations can be used to correct the TNMOC values for loss in conversion efficiency. Clearly the uncertainties due to this correction increase for lower conversion rates. Therefore here we report we only measurements with a conversion rate higher 80% for further analysis of the field results. This value represents 65% and 54% of all data collected at UCLA and

Burbank, respectively. The conversion rates were corrected to 100% by the individual conversion rate calibration curves of the specific days.

The reason for this behavior was later determined to be catalyst poisoning by O_2, which is introduced to the methanizer with the air sample or the He/O_2 carrier gas (purging the sample from the first trap to the oxidation catalyst), respectively. We continued measurements in Burbank after experiencing this problem at UCLA in hopes that a local source (i.e. a Chemistry Department fume hood exhaust) might be the source of the problem, but this was clearly not the case. The solution to the problem is discussed in Section 2.2 above.

4.2 UCLA

4.2.1 Meteorology

Figure 4.1.1 shows the wind-speed, wind-direction and temperature at UCLA during the period of the measurements. The data indicate that the measuring site at UCLA is subject to a pronounced land-sea wind circulation pattern with predominantly southerly winds during day- and northerly winds at nighttime. The wind-speeds show a strong diurnal variation with highest values (2.5 – 4 m/s) found around noon. During nighttime the wind-speed decreases to approximately 0.5 m/s. The temperatures also show strong diurnal variations with daily maxima of 22-29 °C and daily minima of 12-17 °C.

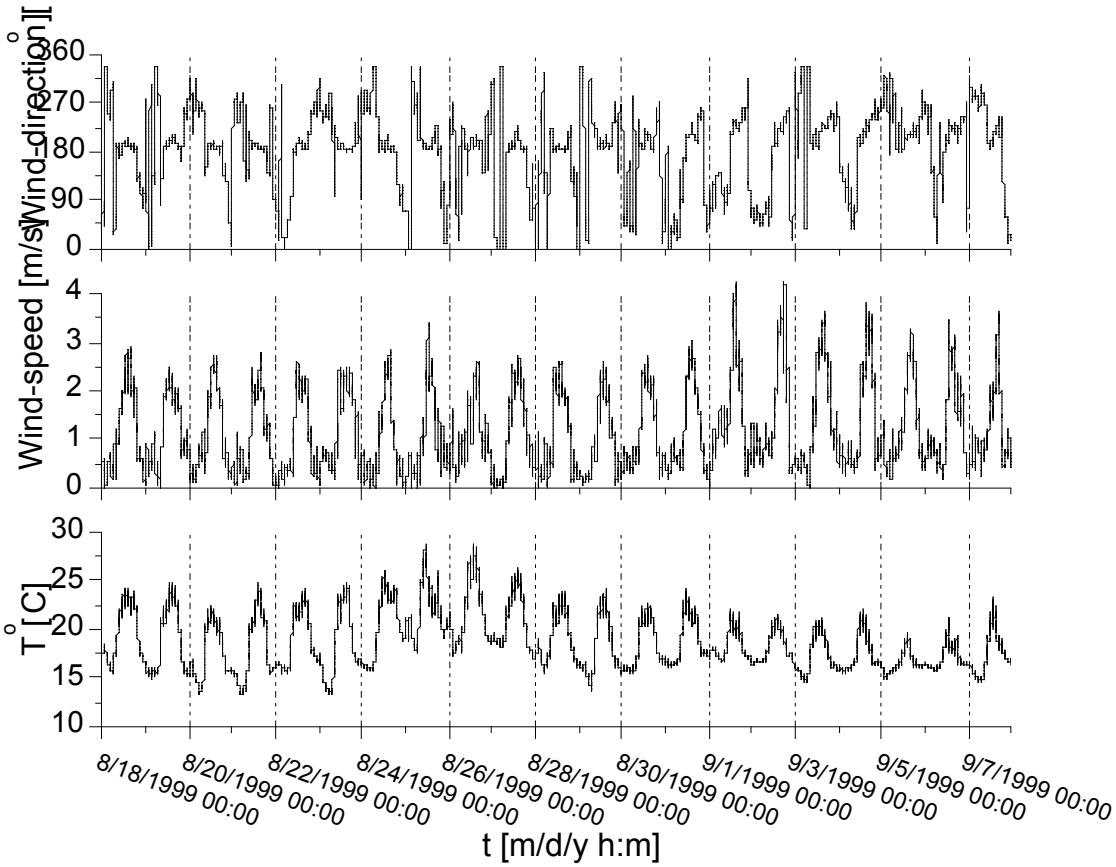

Figure 4.2.1 Meteorological data at UCLA during the period of the measurements. Zero degrees in wind direction indicates North.

4.2.2 Trace gases

Figure 4.2.2 shows the results of the NO, NO_2, NO_x, and O_3 measurements at UCLA during 1999. O_3 shows a distinctive diurnal variation with the highest values occurring in the early afternoon (14:00 –16:00 h) with daily maxima of about 70 ppbV. As expected, NO increases in the early morning from low nighttime values, reaching a maximum in mid-morning and decreasing again as O_3 rises in the late morning. The elevated values for NO, NO_2 and NO_x in the morning hours are presumably due to rush-hour traffic coupled with lower mixing rates in the morning. The precise timing of the NO_x maxima at UCLA is discussed in more detail in Section 5. The lower concentrations of NO_x after 09/01/99 coincides with a period of high wind-speeds, lower temperatures, and predominately westerly winds. This may result from a period of very clean conditions at the measuring site most likely due to dilution with clean marine air.

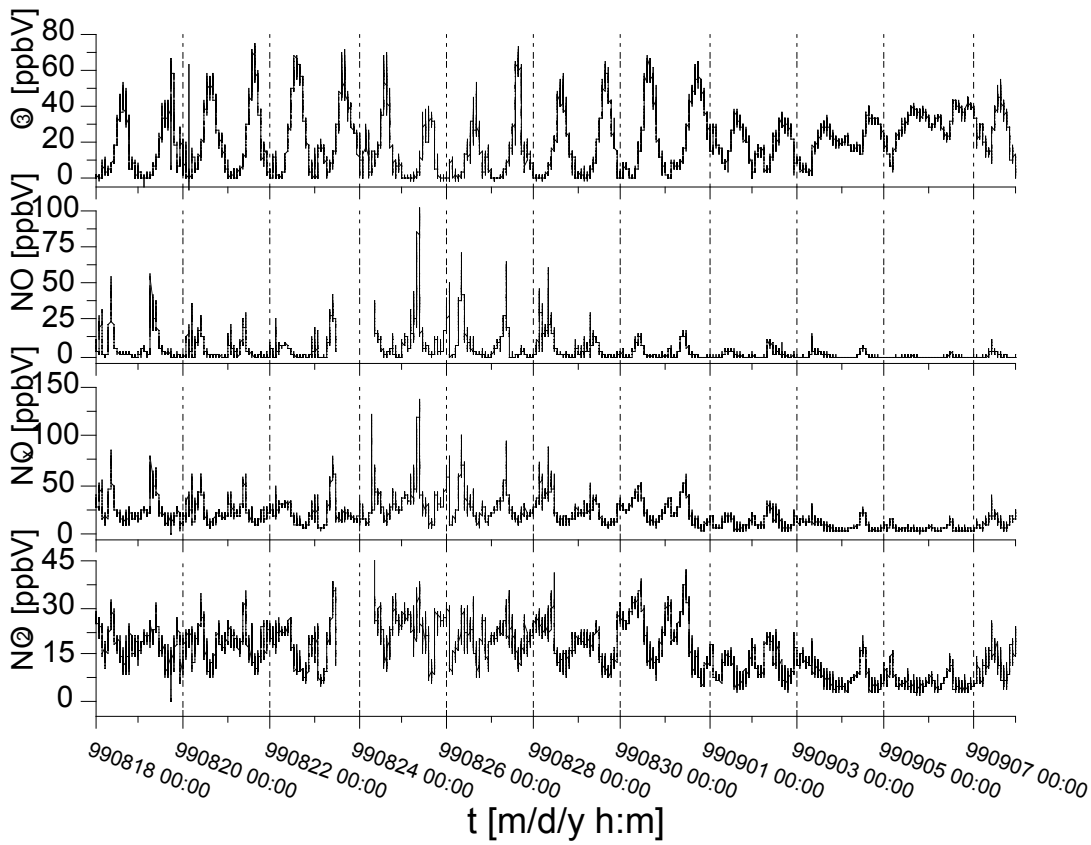

Figure 4.2.2: Results of the NO, NO_2, NO_x, and O_3 measurements at UCLA campus during 1999.

4.2.3 Particles

The goal of the particle measurements was to determine the maximum potential contribution of organic carbon in particles to the TNMOC measurement. Currently we do not filter air samples, but expect some particle losses in the inlet tube. The particle analyzer was set up to draws samples from near the TNMOC instrument at the end of the inlet tube but before the inlet of the GC itself. Data analysis was performed for a limited number of samples with either extreme high or low amounts of carbon present. To obtain the aerosol mass, the following expression was used:

(1) $$\left(\frac{N \cdot \frac{4\pi r^3}{3}}{V_{air}}\right) \cdot \rho \cdot \frac{\mu gC}{m^3} \text{ organic carbon}$$

Here, N is the number of particles counted over the time interval, r is the radius of the particles (assumed to be the median value of the limits of each size bin), V_{air} is the volume of air sampled (720 cm^3 over ten one minute sampling intervals), and ρ is the density of the particles, which is assumed to be 1 g/cm^3. The result of equation (1) can be converted to equivalent ppbC in the gas phase with the following formula:

$$\left(\frac{1\mu g}{m^3}carbon\right)\left(\frac{1mol}{12gC}\right)\left(\frac{10^{-6}g}{1\mu g}\right)\left(6.02\times10^{23}\frac{molec}{mole}\right)\left(\frac{1cm^3 air}{2.46\times10^{19}molec}\right)\left(\frac{10^{-6}m^3}{1cm^3}\right)=2\,ppbC$$

Particle data corresponding to the 10-minute sampling periods of the TNMOC instrument were analyzed and averaged. For the period from 8/27/1999 to 8/28/1999, the highest and lowest TNMOC values were 270 and 470 ppbC, corresponding to 8/27/1999 at 20:35 and 8/28/1999 at 10:33, respectively. For these two points, the total aerosol mass is equivalent to 1.9 % and 1.1 % of the TNMOC value. Furthermore, this calculation assumes that all of the particle mass is due to organic carbon, which is surely not the case. Aerosol organic carbon accounts for 30% of the total mass in Los Angeles on average [43], so that the aerosol carbon reaching our inlet, even if it were completely converted to TNMOC, contributes less than 1% of the TNMOC signal, and can be ignored.

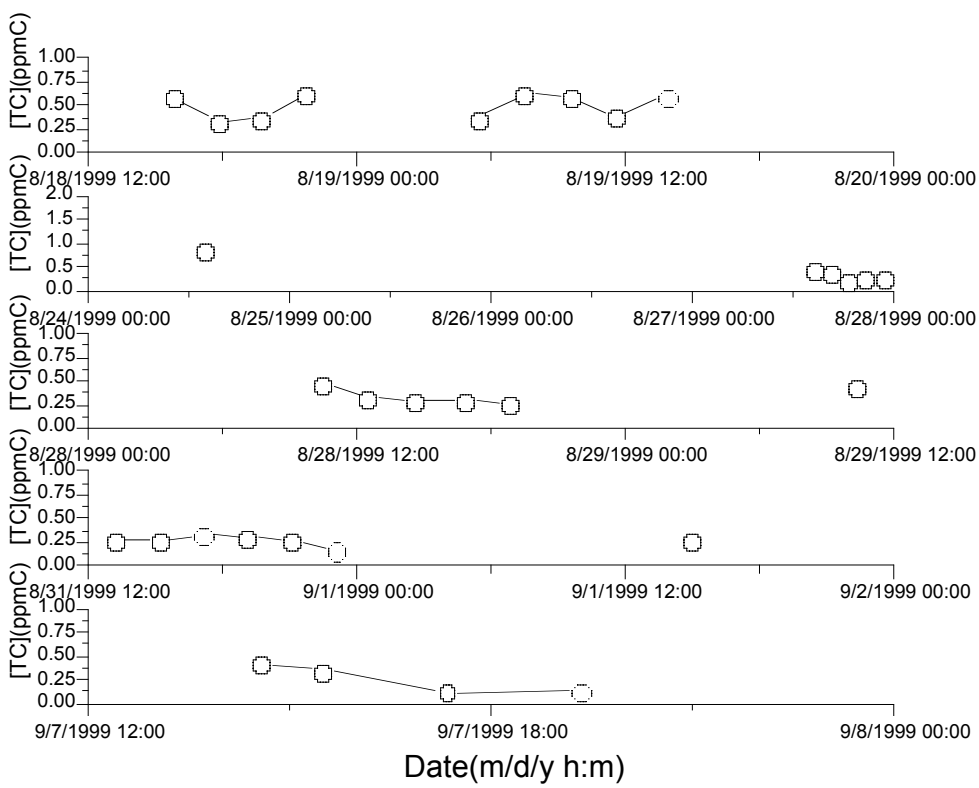

Figure 4.2.3 TNMOC at UCLA. The sparseness of the data coverage is due to the problems with the methanizer conversion efficiency—points with lower than 80% conversion are not shown.

4.2.4 TNMOC and sum of speciated VOC's

Figure 4.2.4 shows the results of the TNMOC and the sum of speciated VOC's measured at UCLA. Both TNMOC and speciated VOC's were quite low at the UCLA site, ranging between 0.19-1.44 ppmC for TNMOC and 0.14-0.57 ppmC for speciated VOC's, with averages of 370 ± 170 and 260 ± 100, respectively, and a sample set of 34 points. As expected, the average TNMOC concentration was greater than that of the sum of speciated VOC's. The magnitude of the excess was perhaps surprising, averaging 40%. .

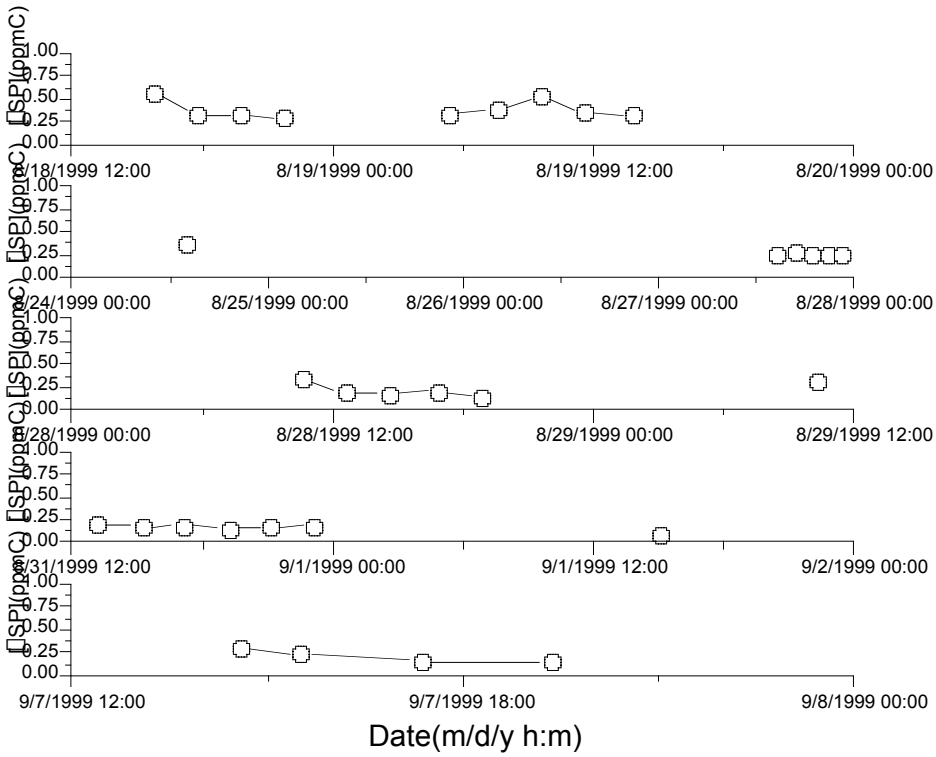

Figure 4.2.4 Sum of speciated VOC's at UCLA.

The average concentration of the TNMOC and sum of speciated VOC's for each hour of day for the UCLA data set is plotted in Figure 4.2.5. The data weakly follows a fairly common diurnal urban organics profile, whereby concentrations rise from the very early morning hours to reach a maximum around 8 or 9 AM, and then slowly decrease. A similar pattern is observed more strongly in our NO_x data.

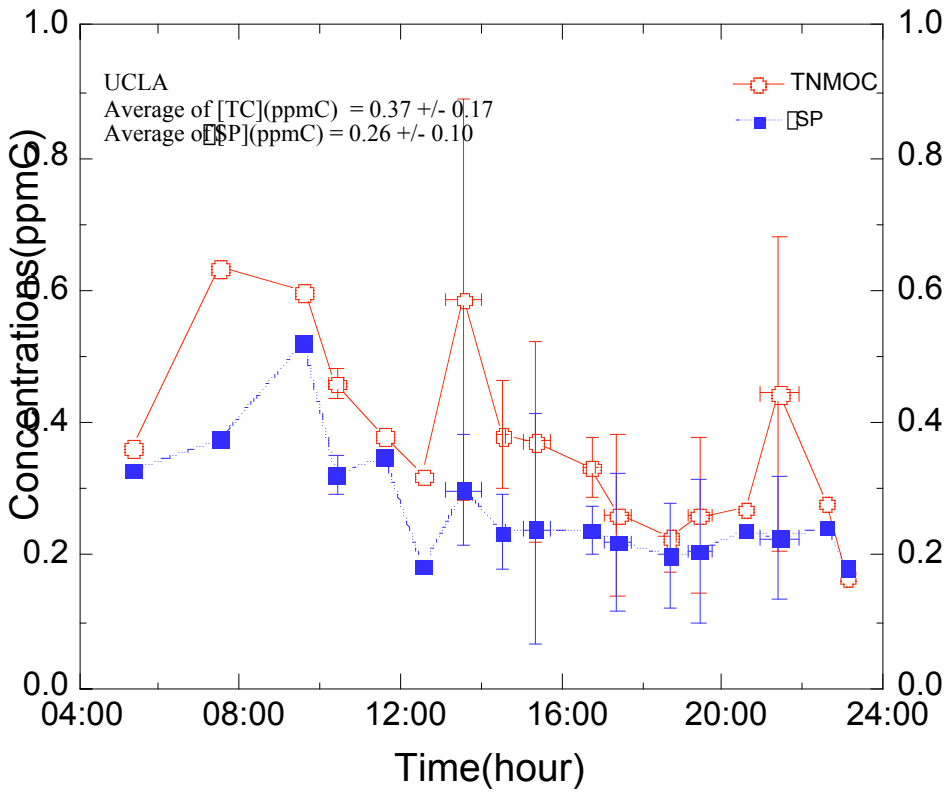

Figure 4.2.5. Hour-of-day averaged mean values of TNMOC and sum of speciated VOC's at the UCLA measurement site. The vertical error bars indicate the span of the measurements at each hour; points with no error bars had only one point. Since the sampling time of the instrument is only 10 minutes, some points that were acquired at different fractions of an hour were binned together, and the horizontal error bars indicates the span of the measurement times.

Figure 4.2.6 shows TNMOC plotted vs. sum of speciated VOC's for UCLA. The average ratio for UCLA was 1.41 ± 0.07 (1σ). A few of the ratios fall below the 1:1 line as expected given the error in the individual measurements, coupled with the atmospheric variability.

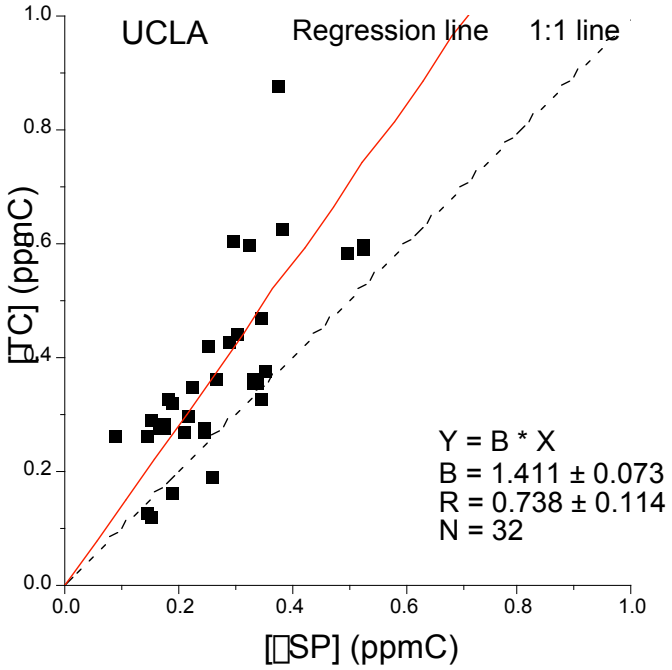

Figure 4.2.6. Plot of the ratio of TNMOC vs. the sum of speciated VOC's for the UCLA data.

4.3 Burbank

4.3.1 Meteorology

Figure 4.3.1 shows the wind-speed, wind-direction and temperature at Burbank during the period of the measurements. Clearly land-sea-wind circulation has little influence the Burbank measurement site; the wind direction is highly variable within the band from about 45 to 315 degrees. The wind-speed shows a strong diurnal variation, however. The maximum wind-speeds, about 2 m/s, occur around noon as they do at UCLA, but are about a factor of two lower. The temperatures show strong diurnal variation with a minimum of about 15°C during nighttime and a maximum of almost 40°C during daytime. The lower wind-speeds, the strong local sources lead to expected higher concentrations of the trace gases at Burbank station.

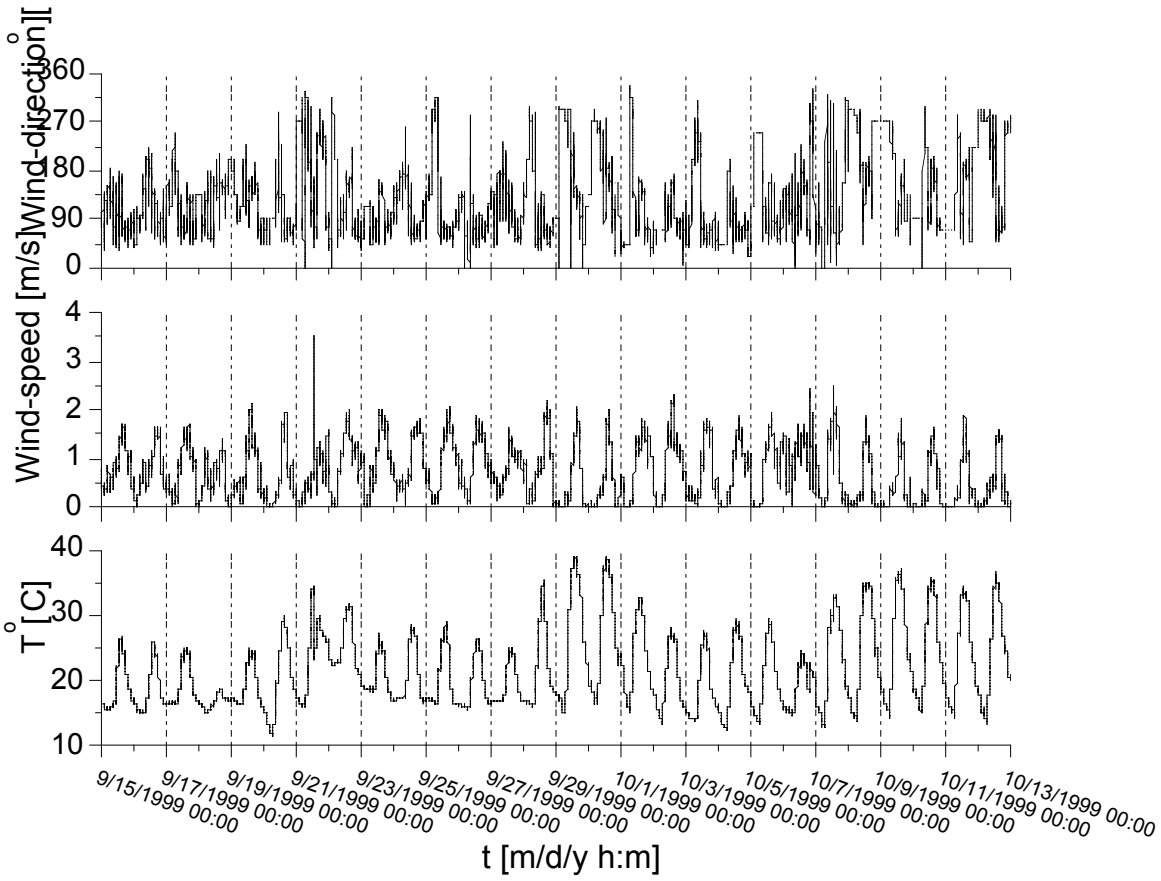

Figure 4.3.1 Meteorological conditions at Burbank during the period of the measurements. A wind direction of zero indicates North.

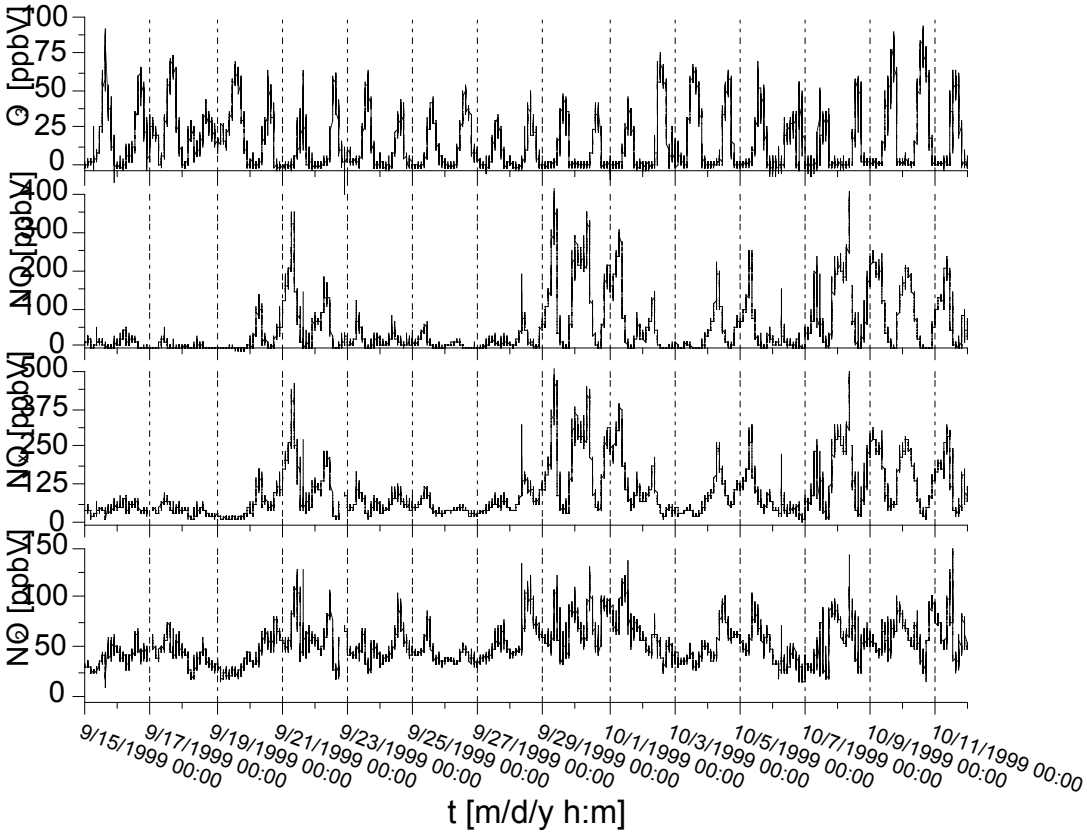

Figure 4.3.2: Results of the NO, NO_2, NO_x, and O_3 measurements at the Burbank station.

4.3.2 Trace gases

Figure 4.3.3 shows the results of the NO, NO_2, NO_x, and O_3 measurements at Burbank. The NO and NO_x measurements show strong diurnal variations with the highest concentrations in the early morning hours. This is most likely due to rush-hour traffic on the heavily traveled freeways around Burbank. Generally the concentrations are much higher than UCLA with averages of NO_x, NO_2, and NO, averaging 4.8, 3.3, 10.1 times higher, respectively than the concentrations measured at UCLA. The very high NO value is consistent with strong local anthropogenic sources. O_3 shows a distinctive diurnal variation with the highest values occurring in the early afternoon (14:00 –16:00 h), similar to UCLA. The highest measured values for O_3 in Burbank are approximately 25% higher than the concentrations measured at UCLA, but still, the maxima did not exceed 100 ppb.

4.3.3 Particles

Particle measurements were made on 9/15/99. For this day, the high and low TNMOC values were 740 ppbC and 2360 ppbC at 10:15 AM and 6:30 PM, respectively. Performing the calculation for these points, the maximum organic carbon contained in the aerosol mass was 4.6 % and 1.4 % of the total, respectively. Again, since the fraction of the total aerosol that is organic carbon is about 30%, this contribution should not exceed 2%.

4.3.4 TNMOC and sum of speciated VOC's

Figures 4.3.3 and 4.3.4 show the results of the TNMOC and sum of speciated VOC's measurements at the Burbank station. The TNMOC at Burbank was ranged from about 0.5 up to 9 ppmC and the sum of speciated VOC's 0.4 to 8 ppmC, with averages of 2.27 ± 0.65 and 2.06 ± 0.51 respectively, factors of 6 and 8 higher than UCLA, respectively. The highest value in both quantities, measured on 09/21/99, coincided with a sudden increase in the NO_x concentration (NO increased from 190 to 310 ppb). The ratios for each data point are included in Figure 4.3.5 with the UCLA data. The average ratio was 1.10, and several of the ratios were less than one. As described above, individual values have uncertainties of about ± 18 %, so that it is not surprising, given that the average value was only 1.1, that some ratios are less than one.

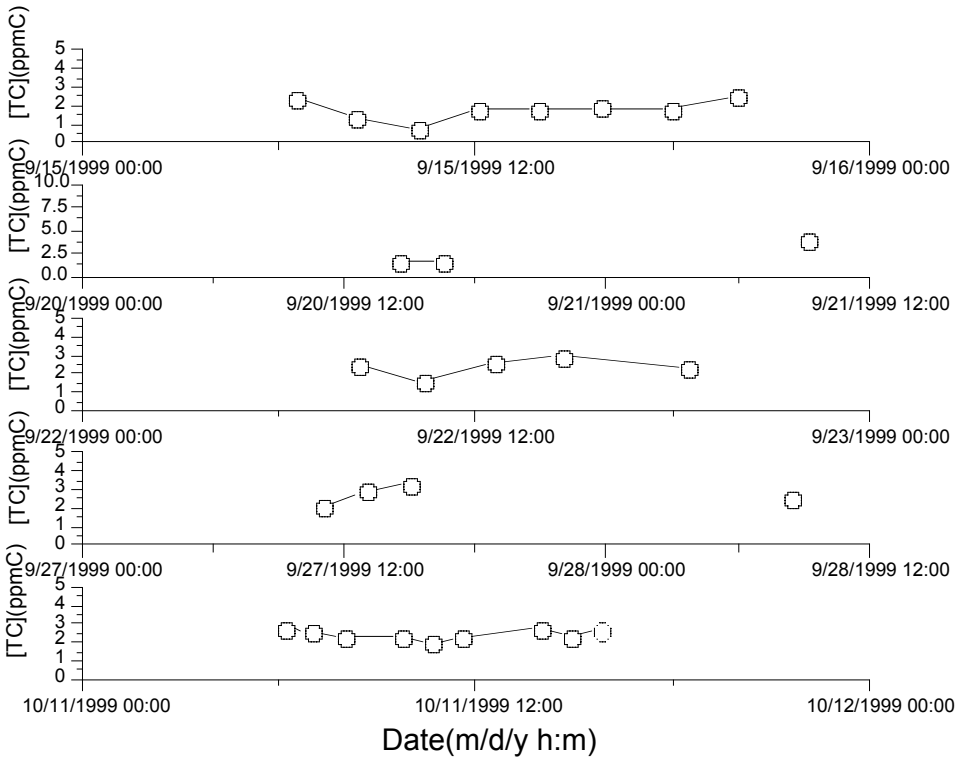

Figure 4.3.3 TNMOC concentration data from acquired at the Burbank station.

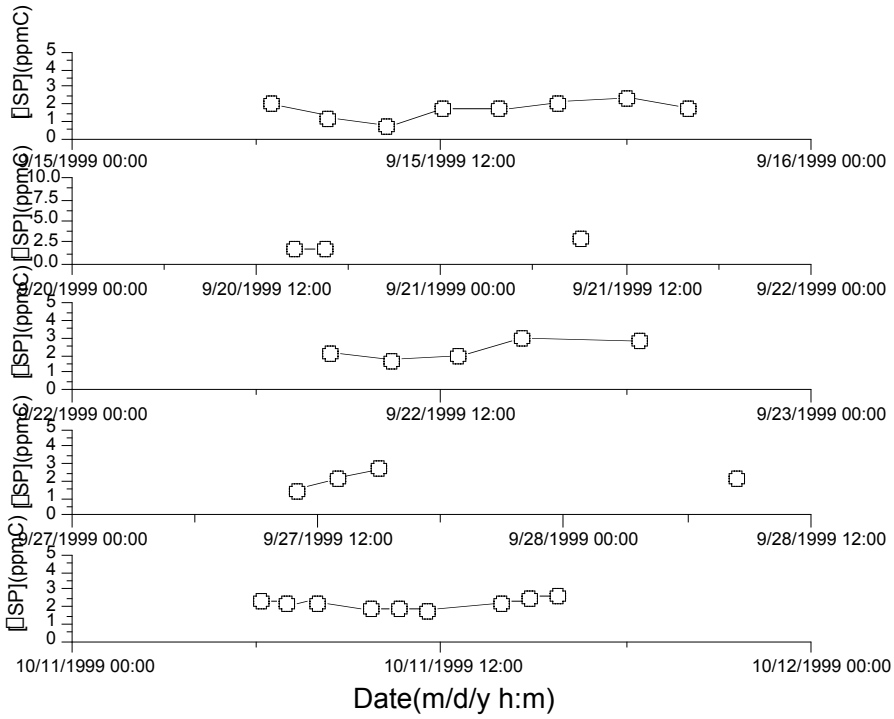

Figure 4.3.4 Sum of speciated VOC's at Burbank.

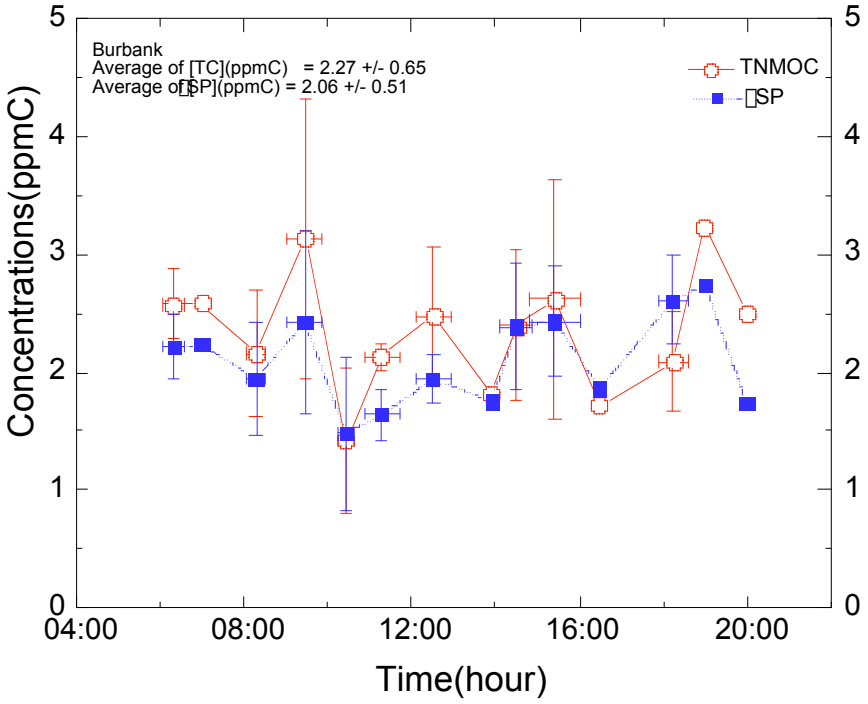

Figure 4.3.5. Hour-of-day averaged mean values of TNMOC and sum of speciated VOC's at the Burbank measurement site. The vertical error bars indicate the span of the measurements at each hour; points with no error bars had only one point. Since the sampling time of the instrument is only 10 minutes, some points that were acquired at different fractions of an hour were binned together, and the horizontal error bars indicates the span of the measurement times.

Figure 4.3.6 shows TNMOC plotted vs. sum of speciated VOC's for Burbank. The average ratio for Burbank was 1.10 ± 0.04 (1σ). Figure 4.3.7 shows the relationship between TNMOC/sum of speciated VOC's ratio and time of day at Burbank. Consistent with other data sets we have collected, there is little if any trend.

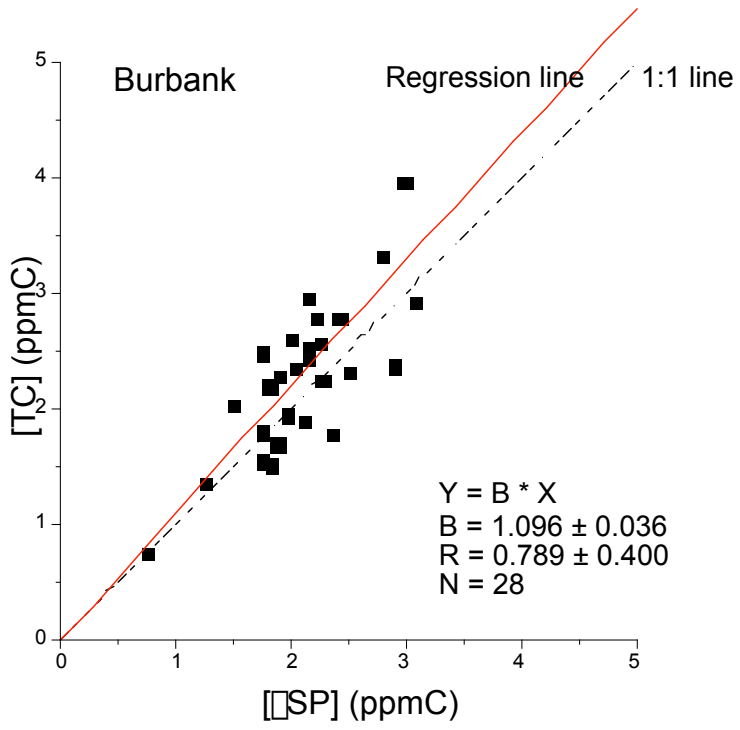

Figure 4.3.6. Plot of the ratio of TNMOC vs. the sum of speciated VOC's for the Burbank data.

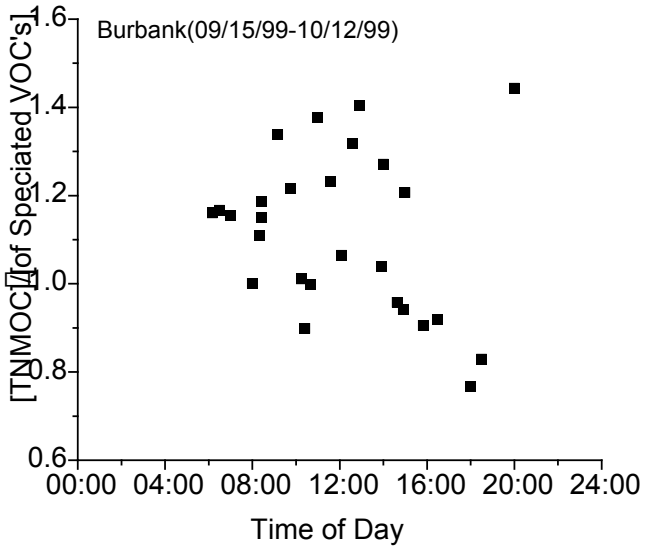

Figure 4.3.7. Plot of TNMOC/sum of speciated VOC's ratio vs. time of day for Burbank.

4.3.5 Conclusion

The much lower pollutant concentrations at UCLA compared to Burbank (for example, TNMOC levels were 360 compared to 2270 ppbC) were accompanied by a higher ratio of TNMOC to sum of speciated VOC's, 1.41 ± 0.07 and 1.10 ± 0.04, respectively. The data acquired in Azusa in 1997 coincides with the same trend, falling between the UCLA and Burbank values on both counts. There the average TNMOC concentration was about 520 ppbC while the ratio was 1.29 ± 0.3.

4.4 Estimation of Air mass Age in the UCLA and Burbank Data

Table 4.2 shows the average concentrations and ratios for NO_x, O_3, TNMOC, Σ speciated VOC's and several aromatics over the entire sampling periods for UCLA and Burbank. As discussed in the last progress report, concentrations of primary pollutants at Burbank were 6-13 times those at UCLA. Burbank is heavily influenced by direct emissions, as evidenced by the high NO concentrations, high VOC levels, and consistent with a low TNMOC/ΣSpeciated VOC's ratio. Further consistent, is that the directly emitted aromatics such as toluene and the xylenes are present at Burbank at levels 10-12 times those at UCLA. TNMOC is only 6 times higher, indicating that the excess TNMOC observed at UCLA is not part of unmeasured primary emissions.

Table 4.2 Average Ozone, NO_x and VOC Levels at UCLA and Burbank

Compound	UCLA	Burbank	Ratio Burbank/UCLA
	Average ± std	Average ± std	
TNMOC (ppbC)	376 ± 167	2298 ± 644	6.1
ΣSP(ppbC)	263 ± 99	2073 ± 513	7.9
Ratio	1.44 ± 0.41	1.11 ± 0.18	-
NO_X (ppbV)	20 ± 13	112 ± 96	5.6
NO (ppbV)	4 ± 8	53 ± 76	13
NO_2(ppbV)	16 ± 6	57 ± 26	3.6
Ozone(ppbV)	30 ± 18	23 ± 22	0.8
Toluene(ppbV)	1.26 ± 0.74	15.73 ± 4.27	12
Ethyl benzene(ppbV)	0.2 ± 0.11	1.97 ± 0.67	10
m,p-Xylene(ppbV)	0.67 ± 0.4	7.60 ± 2.19	11
o-Xylene(ppbV)	0.29 ± 0.18	2.85 ± 0.93	10
[m,p-Xylene]/[Ethyl benzene]	3.33 ± 0.40	3.90 ± 0.27	1.2
Wind Speed(m/s)	1.62 ± 0.91	0.89 ± 0.62	-
Temperature (°C)	20 ± 3	24 ± 6	-
[TNMOC]/[NO_X] (ppbC/ppbV)	23 ± 12	37 ± 29	1.6
[ΣSP]/ [NO_X] (ppbC/ppbV)	16 ± 7	34 ± 29	2.1

4.4.1 Identification of Peaks in Speciated VOC's Chromatograms

The identification of peaks was based on three retention time marker mixtures: 1. A mixture of C_1 - C_6 n-alkanes diluted from a 100 ppmV standard to 100 ppbv/compound was used as a retention time standard at both UCLA and Burbank. 2. A 1ppmV benzene, toluene, ethyl benzene, o-, m-, p-xylene in N_2 (Scott Specialty Gases) was used as an additional retention time standard at the Burbank site. 3. An EPA 52 compound standard that was analyzed in Azusa during the 1997 SCOS study. Reference chromatograms from this standard were used for comparison to the other standards.

4.4.2 Use of Aromatics to Estimate Photochemical Aging

The relative concentrations of the aromatic isomers m&p-xylene and ethyl benzene are presented in this report for estimating average hydrocarbon age in our ambient samples. The ratio of two simultaneously measured species can provide an estimate of photochemical aging, provided (i) these compounds occur in significant concentrations and constant relative proportion in the major anthropogenic sources of hydrocarbons and (ii) the compounds are removed from the atmosphere at significantly different rates by photochemical reactions that follow psuedo-first order kinetics [44, 45]. In this analysis, concentrations of hydrocarbons are not negligible in the diluting air since air that arrives at the stations is a mixture of partially processed air and fresh emissions containing some of the tracer hydrocarbons. Thus, this calculation only provides an estimate of the average degree of photochemical processing.

Ignoring the effect of dilution, the ratio of two hydrocarbons should evolve according to the following equation:

$$\ln([A]/[B]) = \ln([A]_0/[B]_0-(k_A-k_B)[OH])t$$

Where [A] and [B] are m&p-xylene and ethyl benzene concentrations measured at the station and $[A]_0$ and $[B]_0$ are initial m&p-xylene and ethyl benzene concentrations at the source, respectively, [OH] is the mean OH concentration, k_A and k_B are bimolecular reaction rate constants for m&p-xylene and ethyl benzene, respectively, and t is the residence time of air mass. We focus on m&p-xylene and ethyl benzene because their peaks can be reliably quantified, and these aromatics are thought to be emitted in fairly constant proportion (below). M&p-xylene are not separated on a DB-1 column, thus their concentration is combined. Rate constants for m&p-xylene and ethyl benzene are 22.0×10^{-12}, 14.3×10^{-12}, and 7.1×10^{-12} cm^3 $molecules^{-1}$ s^{-1}, respectively [46, 47]. A 12 hour average OH mixing ratio of 5×10^6 molecules cm^{-3} was assumed [43]. Our maximum observed values for the m&p-xylene/ethyl benzene ratio were 3.7-4, in excellent agreement with the value reported for Los Angeles gasoline in 1975 [45] and in ambient air in 1987 [28], and somewhat higher than the 3.4-3.55 range measured in Atlanta by Connor et al. [48]. The reason that these values have remained relatively constant, as gasoline formulas have changed significantly may lie in the fact that the boiling points of all three lie within 3 °C of one another, thus they are not easily separated in the distillation process. Here, a value of 3.7 for the ratio of m&p-xylene to ethyl benzene was assumed to be characteristic of fresh emissions.

4.4.3 Aromatic ratios and Air Mass Age

4.4.3.1 UCLA Aromatic Data

The ratio of m&p-xylene to ethyl benzene at UCLA ranged from 2.5 to 3.7 (ln 2.5 = 0.90 and ln 3.90 = 1.3), reaching a minimum at about 2:00 PM. If we assume that the initial m&p-xylene/ethyl benzene ratio is 3.7 and an OH concentration of $5x10^6$ molec/cm^3, this corresponds to a maximum residence time of about 90 minutes (Figure 4.4.1).

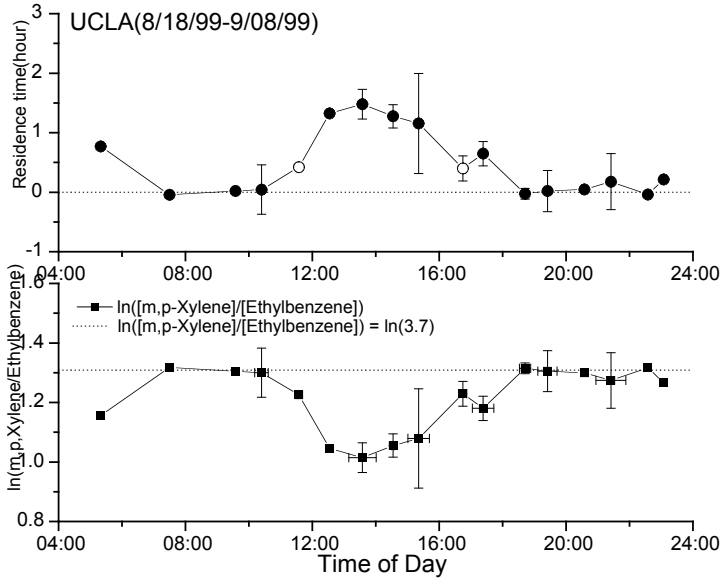

Figure 4.4.1. Hourly averaged mean value of ln(m&p-xylene/ethyl benzene) (lower panel) and the average age the air mass (upper panel) vs. the time of day at UCLA.

There is a weak correlation between a decrease in the ratio of m&p-xylene to ethyl benzene and an increase in the TNMOC/sum of speciated VOC's ratio, indicating that higher TNMOC levels compared to sum of speciated VOC's are observed as the air mass age increases (Figure 4.4.2). Further consistent with this, the TNMOC/sum of speciated VOC's ratio has a somewhat stronger, positive correlation with the O_3 concentration (Figure 4.4.3).

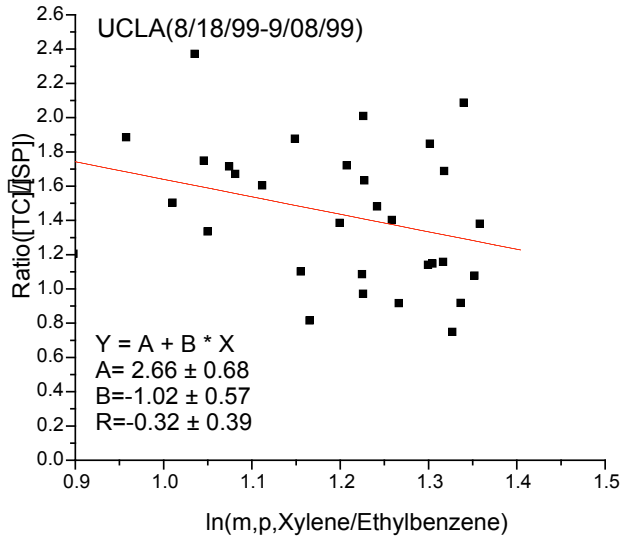

Figure 4.4.2. Ln(m&p-xylene/ethyl benzene) vs. the TNMOC/sum of speciated VOC's ratio at UCLA. The line indicates linear least squares fit, which has a correlation coefficient (R^2 value) of 0.10.

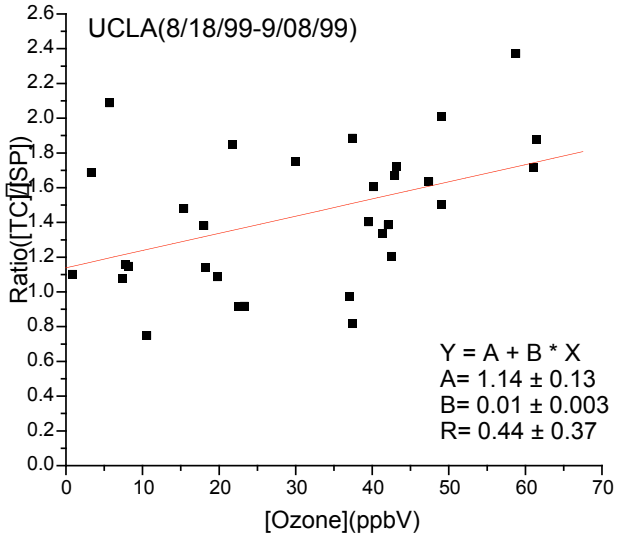

Figure 4.4.3 TNMOC/sum of speciated VOC's ratio vs. O_3 at UCLA. The line indicates linear least squares fit, which has a correlation coefficient (R^2 value) of 0.19.

In contrast with UCLA site, the Burbank was heavily influenced by direct emissions. Indeed, Figure 4.4.4 shows that the m&p-xylene to ethyl benzene ratio remained nearly constant throughout the day. Likewise, the TNMOC/sum of speciated VOC's ratio was uncorrelated with both the m&p-xylene/ethyl benzene ratio and O_3 (Figures 4.4.5 and 4.4.6). It should also be noted that while m&p-xylene/ethyl benzene ratio is as high as 3.9 at Burbank, the maximum values for this ratio at UCLA were 3.7.

This may indicate that UCLA is always exposed to partially aged air, possibly from mixing from aloft.

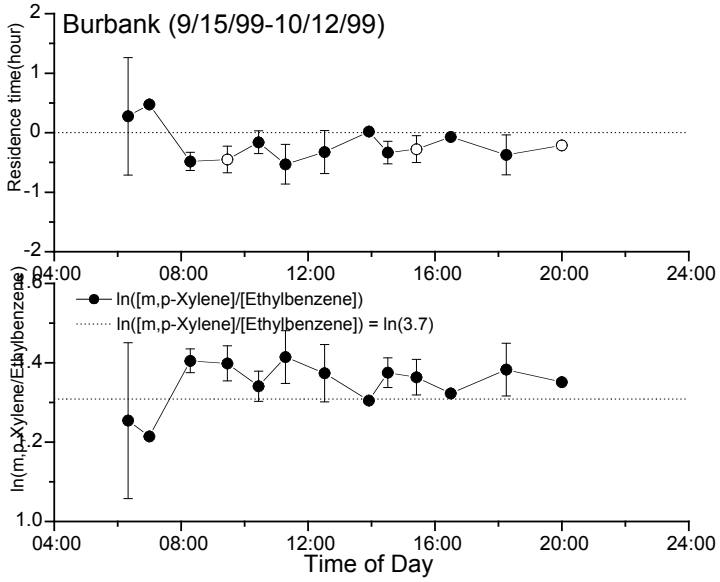

Figure 4.4.4 Hourly averaged mean value of ln(m&p-xylene/ethyl benzene) (lower panel) and the average age the air mass (upper panel) vs. the time of day at Burbank. The dotted line indicates a m&p-xylene/ethyl benzene ratio of 3.7.

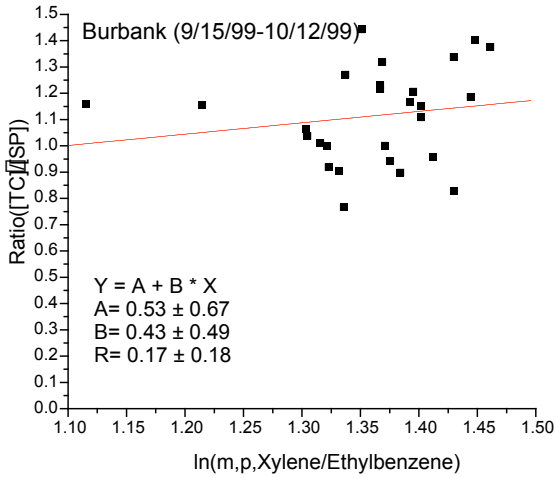

Figure 4.4.5 Ln(m&p-xylene/ethyl benzene) vs. TNMOC/sum of speciated VOC's ratio at Burbank. The line indicates linear least squares fit, which has a correlation coefficient (R^2 value) of 0.0.03.

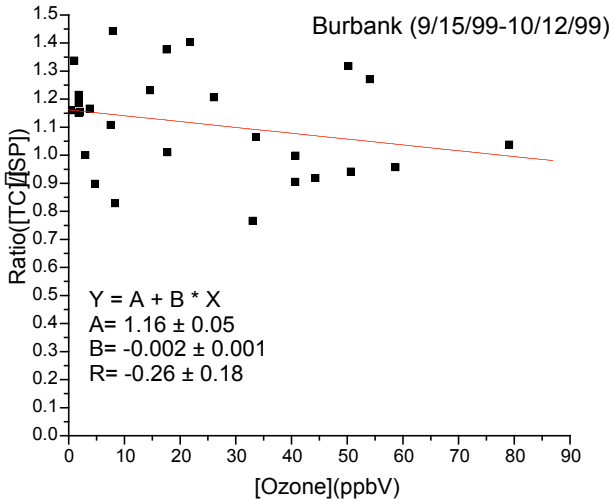

Figure 4.4.6 TNMOC/sum of speciated VOC's ratio vs. O_3 at UCLA. The line indicates linear least squares fit, which has a correlation coefficient (R^2 value) of 0.07.

4.4.4 VOC/NO_x Ratios and Ozone

Figures 4.4.7 and 4.4.8 show the hourly averaged ratios of TNMOC/NO_x and sum of speciated VOC's/NO_x, as well as the ozone concentration for Burbank and UCLA. Much of the variability in the VOC/NO_x ratios is due to fluctuations in the NO_x concentrations, and when NO_x concentrations are high, O_3 concentrations are expected to be low, partly due to the reactions:

$$O_3 + NO \rightarrow NO_2 + O_2$$

$$NO_2 + O_3 \rightarrow NO_3 + O_2$$

The Burbank data show a very close correlation between the VOC/NO_x ratio and O_3 (Figure 4.4.7), for both the TNMOC and sum of speciated VOC's. That the TNMOC and sum of speciated VOC's have the same behavior is expected, since in this data set, TNMOC and sum of speciated VOC's concentrations were nearly equal. Figures 4.4.8-10 show scatter plots for O_3 vs. NO_x, TNMOC/NO_x and sum of speciated VOC's/NO_x, without averaging. NO_x vs. O_3 has a correlation coefficient that is only slightly smaller than the VOC/NO_x vs. O_3 correlations, indicating the NO_x concentration explains most of local variability in O_3.

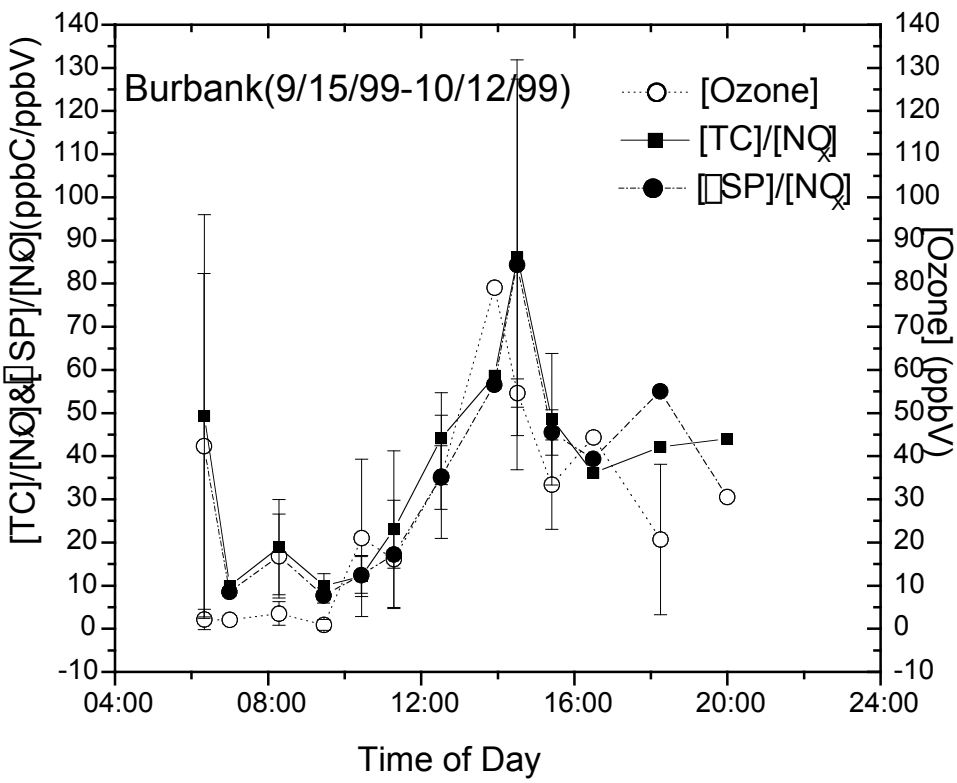

Figure 4.4.7 Hour-of-day averaged mean values of TNMOC/NO_X and sum of speciated VOC's/ NO_x ratios vs. Ozone at Burbank.

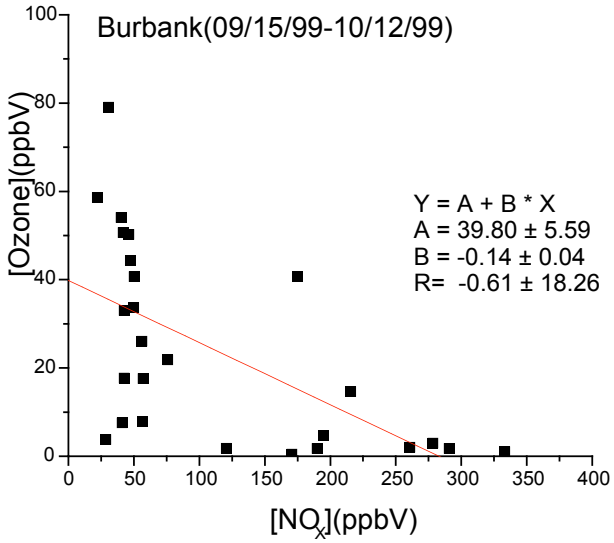

Figure 4.4.8 NO_x vs. O_3 at Burbank. The line indicates linear least squares fit, which has a correlation coefficient (R^2 value) of 0.37.

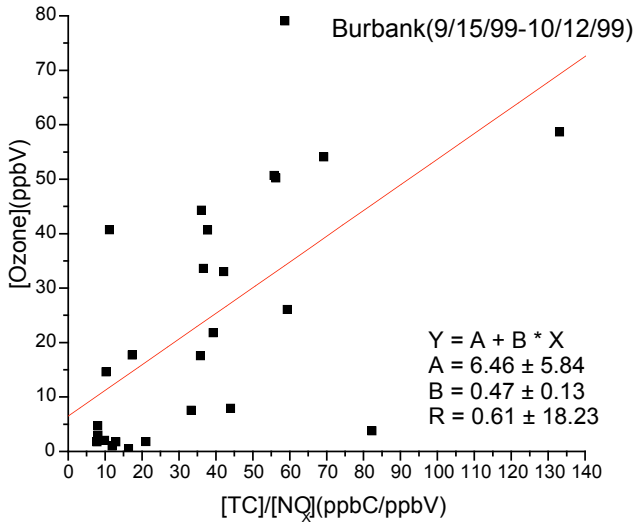

Figure 4.4.9 TNMOC/NO_x vs. O_3 at Burbank. The line indicates linear least squares fit, which has a correlation coefficient (R^2 value) of 0.37.

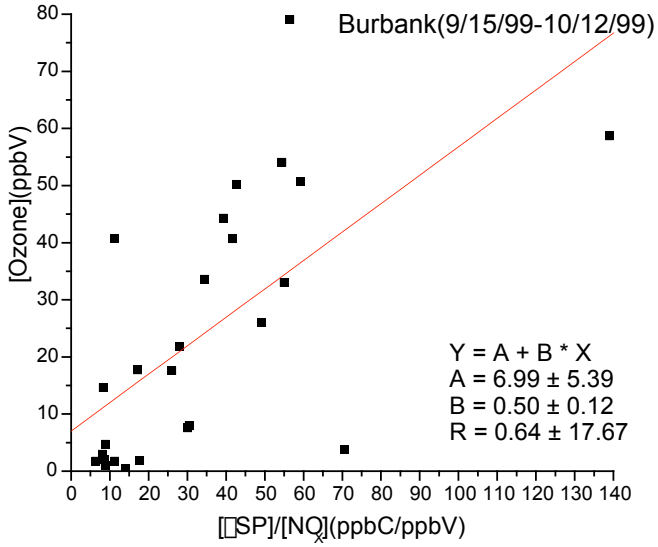

Figure 4.4.10 Sum of speciated VOC's/NO_x vs. O_3 at Burbank. The line indicates linear least squares fit, which has a correlation coefficient (R^2 value) of 0.41.

The UCLA data show an interesting relationship between O_3 and the VOC/NO_x ratio (Figure 4.4.11). Ozone levels are reasonably well predicted by NO_x concentrations (Figure 4.4.12), poorly predicted by the sum of speciated VOC's/NO_x ratio (Figure 4.4.13), and are best predicted by the TNMOC/NO_x ratio.

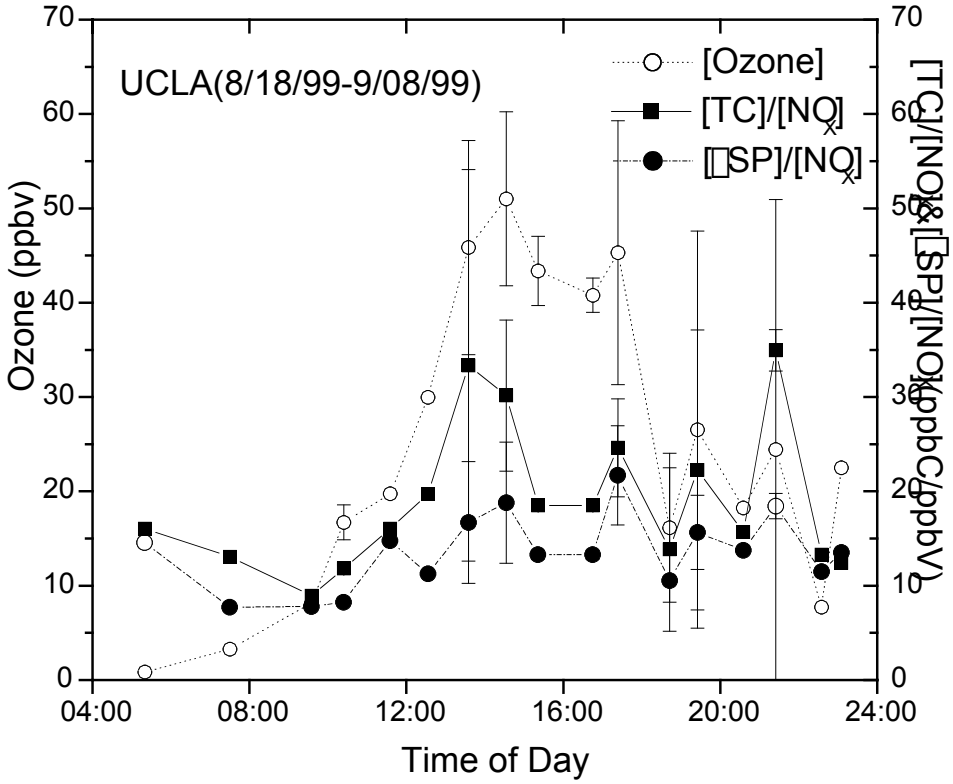

Figure 4.4.11 Hour-of-day averaged mean values of TNMOC/NO_X and sum of speciated VOC's/ NO_x ratios vs. Ozone at UCLA.

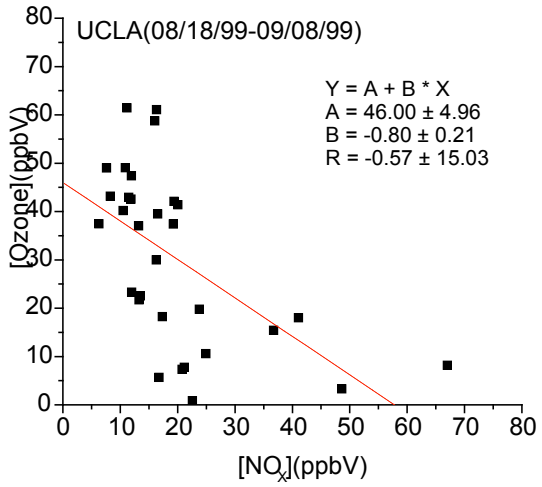

Figure 4.4.12 NO_x vs. O_3 at UCLA. The line indicates linear least squares fit, which has a correlation coefficient (R^2 value) of 0.32.

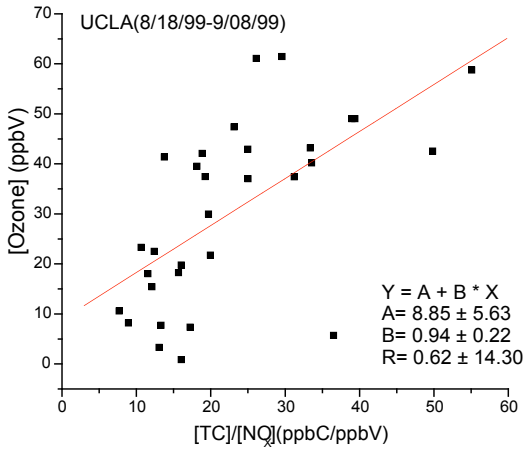

Figure 4.4.12 TNMOC/NO_x vs. O_3 at UCLA. The line indicates linear least squares fit, which has a correlation coefficient (R^2 value) of 0.38.

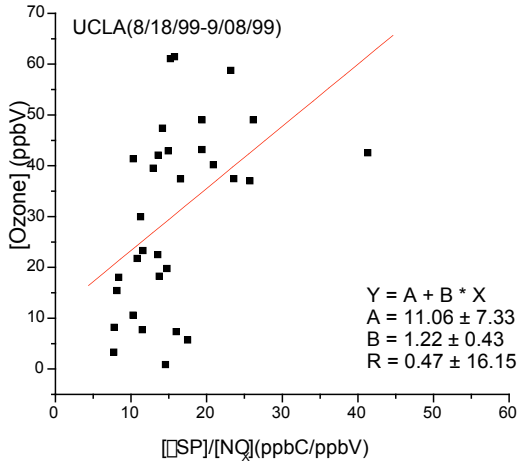

Figure 4.4.13 TNMOC/sum of speciated VOC's ratio vs. O_3 at UCLA. The line indicates linear least squares fit, which has a correlation coefficient (R^2 value) of 0.22.

.

5. 2000 Field Campaigns

In this section, data are presented for individual days and as an aggregate in two sub-sections, September-October and November-December. These sub-sections are followed by sub-section 5.3 that contains correlations and interpretation.

The field measurement days were classified according to prevailing meteorology, as shown in Table 5.1.1. Clear and cloudy designations are based on early morning observations; some cloudy days eventually cleared. All cloudy days have a narrow diurnal temperature range, with extremes of 17 and 23 °C; most cloudy days had only 3-5 °C variation. Clear days had much more warming, with extremes of 15 and 35 °C for the whole data set, and typical variations of about 12 °C. Examination of the sounding data from Miramar, CA reveals that cloudy days have fairly constant vertical temperature profiles that change little over the course of the day, with mixing heights from 600 to 1800 M (below). Clear days have more variable meteorology, but typically show a strong surface inversion at 5 AM developing to mixing heights of 400-600 M later in the day. Cloudy days have significantly higher TNMOC/sum of speciated VOC's ratios than do clear days (Section 5.3).

For this measurement period, the Miramar (SD) soundings are the closest profiles available; the Los Angeles International Airport profiler was not working at that time. The Miramar site is reasonably representative of the meteorology in the region, and is in good agreement (i.e. mixing heights are within 300 m or better) with the LAX data for September of 2001 (not shown). The Miramar site is somewhat more inland than the UCLA site, and might be expected to experience more surface temperature variability, however surface heating at Miramar is remarkably consistent with that observed at UCLA.

Table 5.1.1 UCLA 2000 Sampling Schedule

Weather	09/12/00-10/08/00		11/30/00-12/20/00	
	Weekday	Weekends	Wednesday	Sunday
Clear	09/12/00 09/13/00 09/14/00 09/15/00 09/25/00 09/26/00	09/16/00 09/17/00		
Cloudy	09/19/00 09/20/00 09/22/00 09/27/00 09/28/00	09/23/00 10/07/00 10/08/00	11/30/00 12/06/00 12/13/00 12/20/00	12/03/00 12/10/00 12/17/00

5.1 Measurements at UCLA During September and October

TNMOC, sum of speciated VOC's, TNMOC/sum of speciated VOC's, NO, NO_2, NO_x, O_3, and the vertical temperature profile from Miramar, CA for each sampling day are shown in Figures 5.1.1 and 5.1.2 below. The Miramar site is the closest coastal site that was collecting vertical temperature profiles during this period (above). Data for cloudy days follows that for clear days. Dotted lines in the vertical temperature profile plots indicate mixing heights. It should be noted that even though an O_3 instruments was calibrated shortly before the field measurements, it appears to have an offset of about +13ppb.

Clear Days

09/12/00 09/13/00

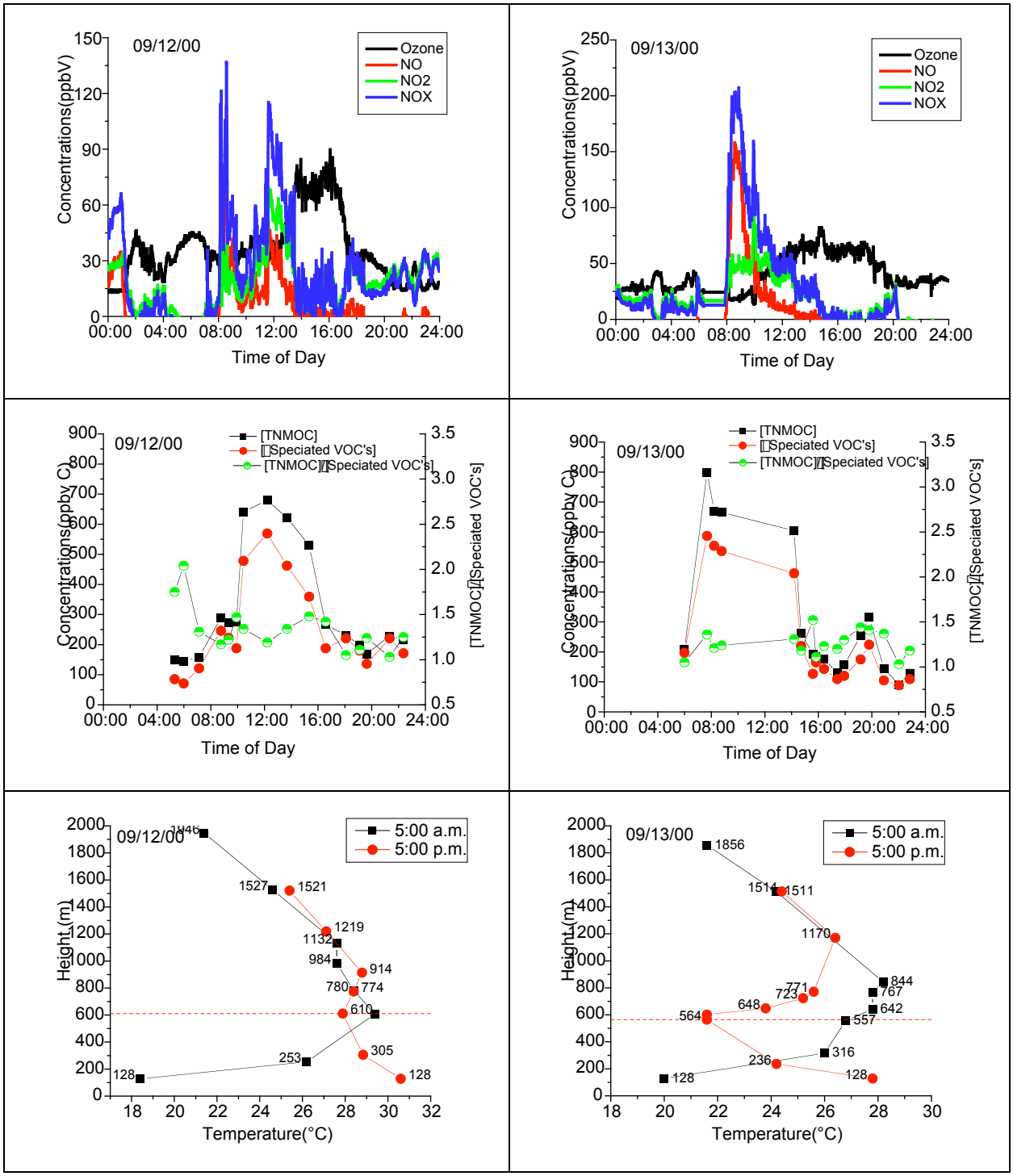

09/14/00 09/15/00

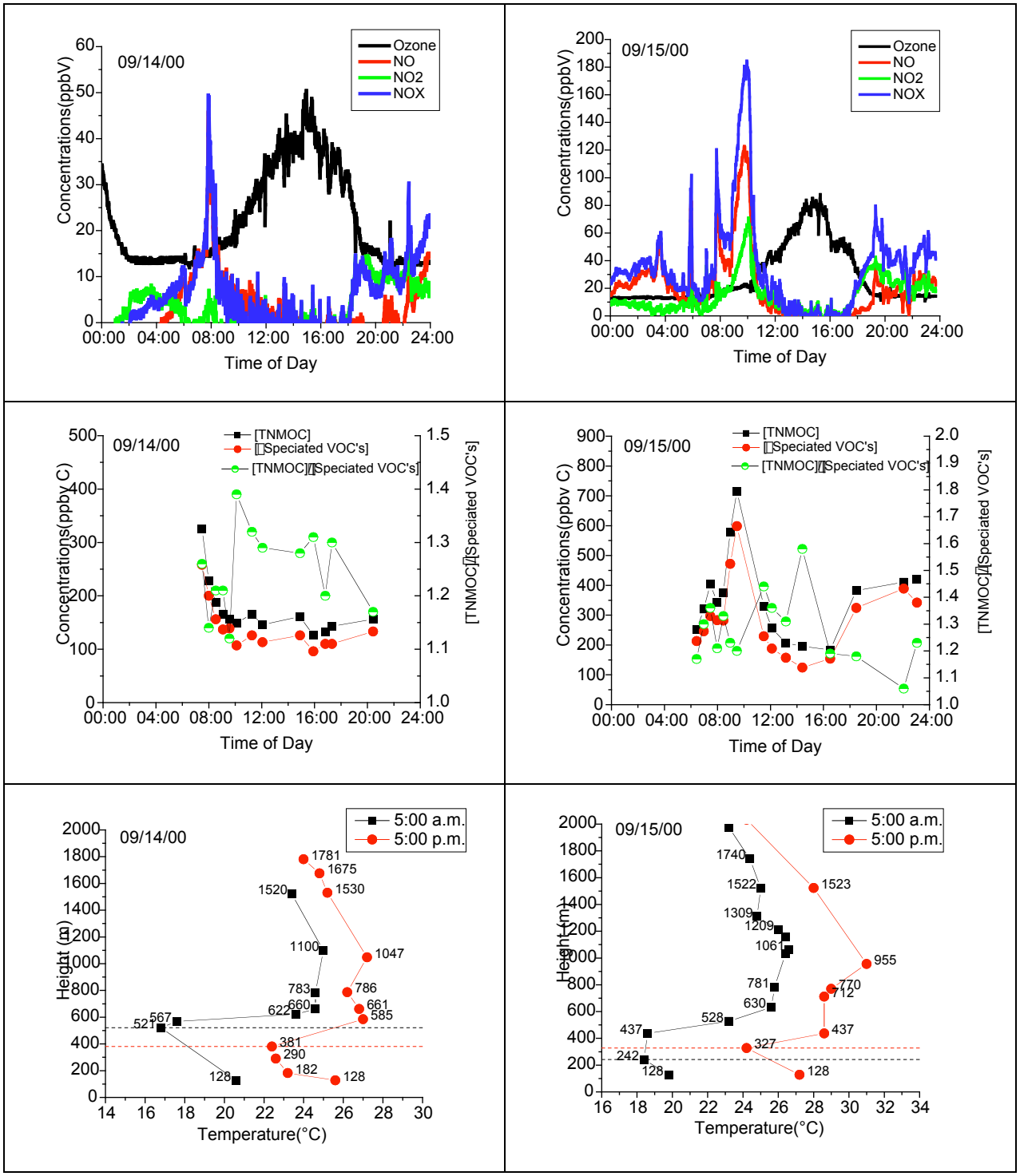

09/16/00 09/17/00

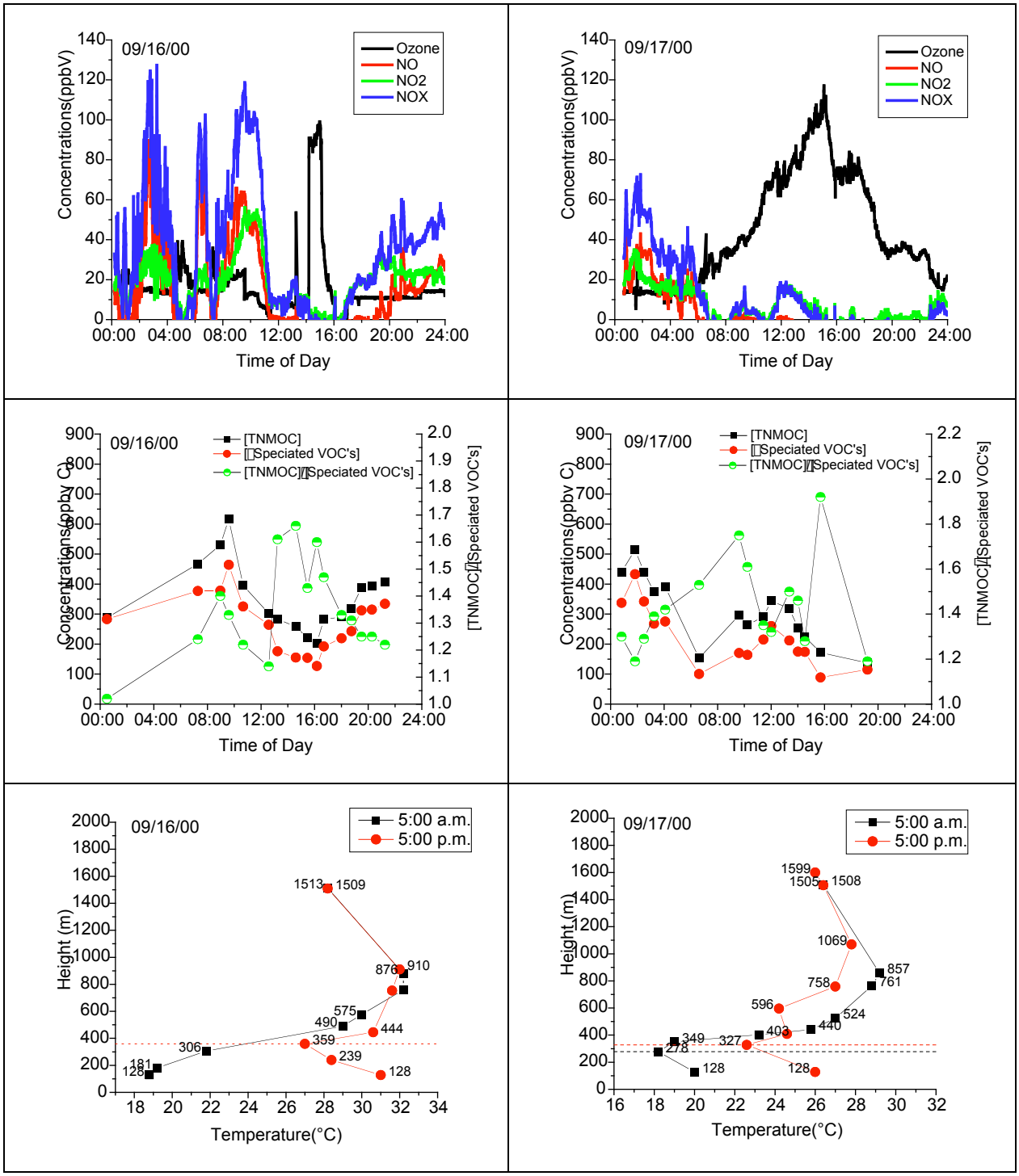

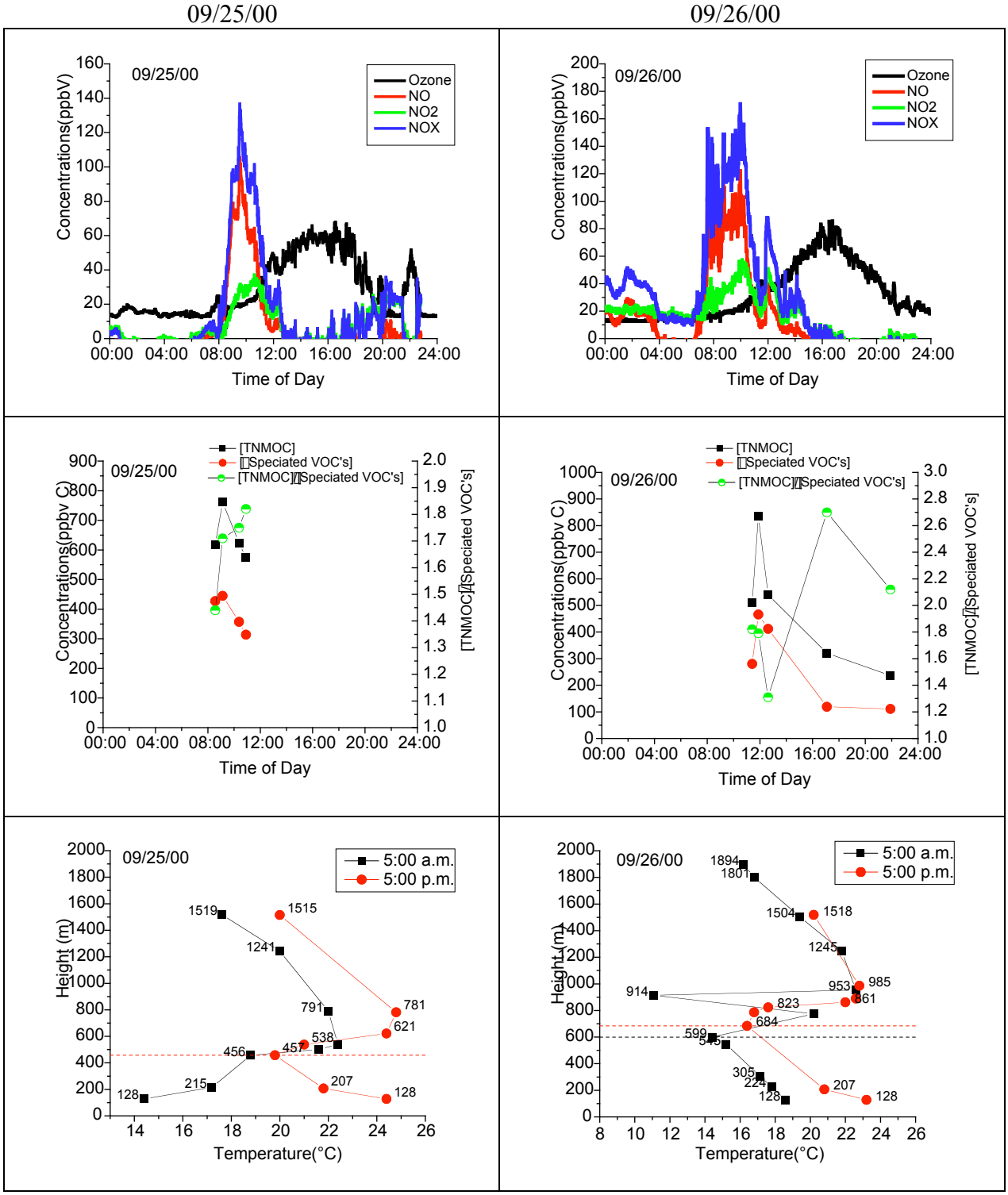

Figure 5.1.1 TNMOC, sum of speciated VOC's, TNMOC/sum of speciated VOC's, NO, NO_2, NO_x, O_3, and the vertical temperature profile from Miramar for clear days in September-October 2000.

Cloudy Days

09/19/00 09/20/00

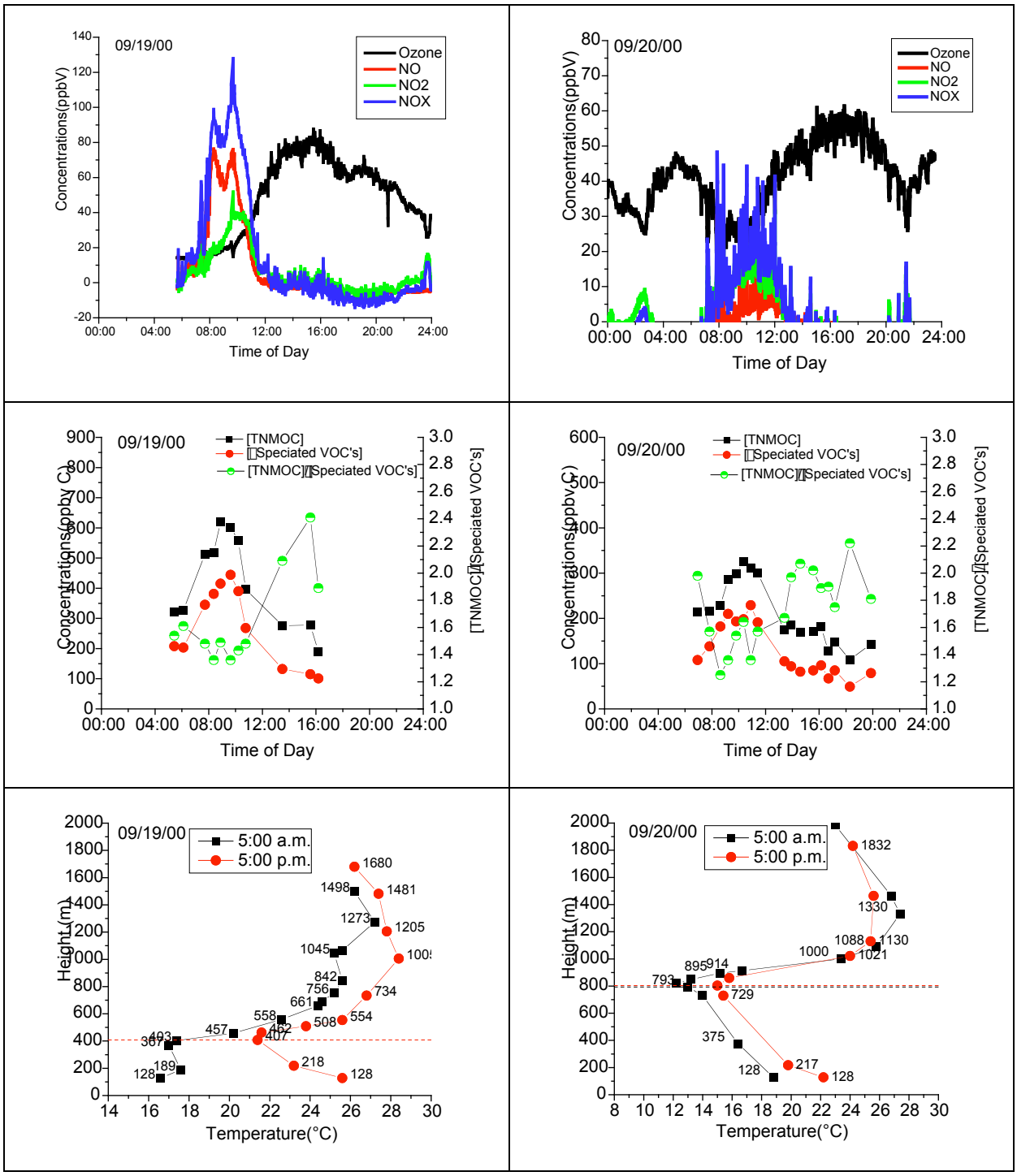

09/22/00 09/23/00

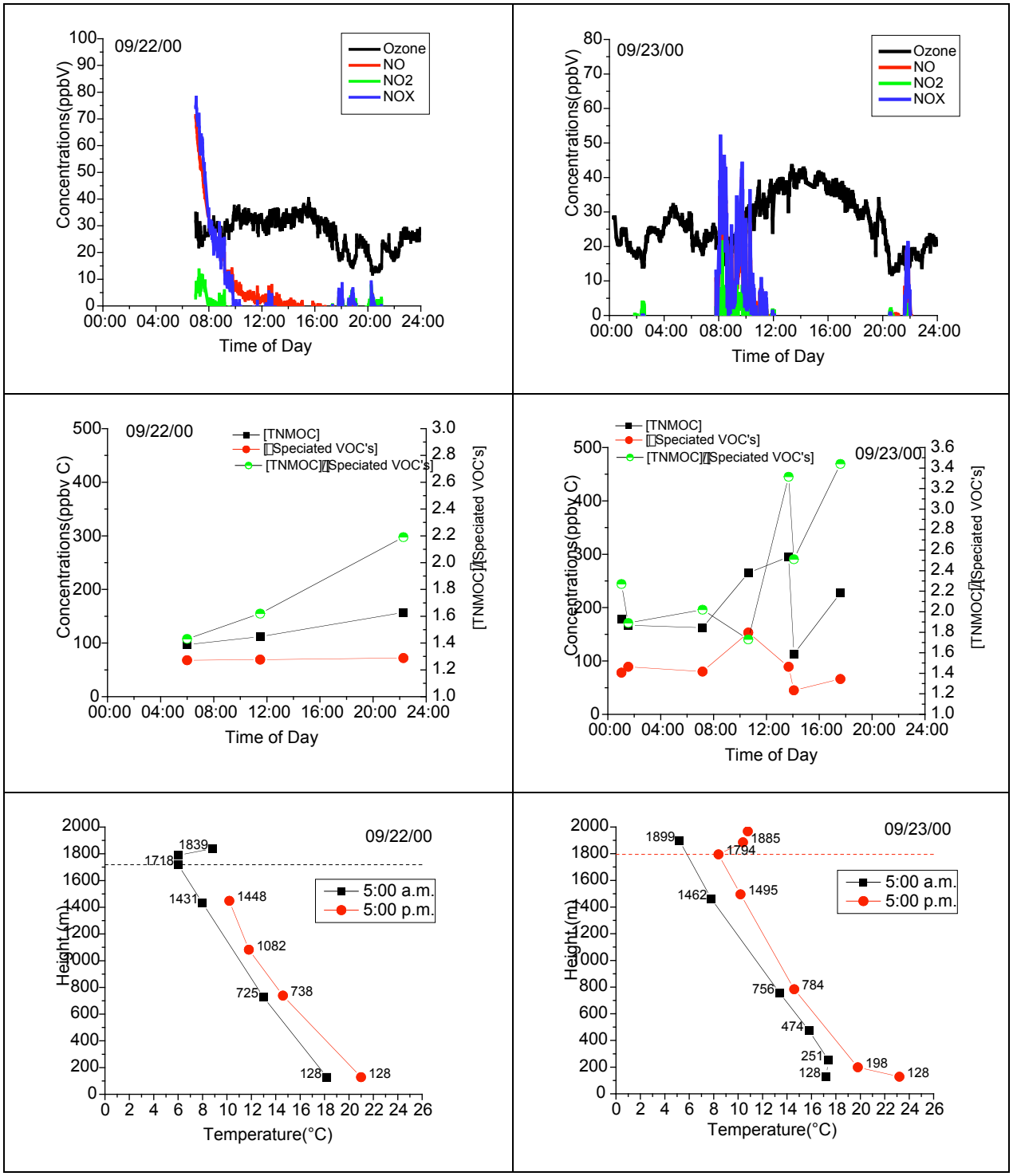

09/27/00 09/28/00

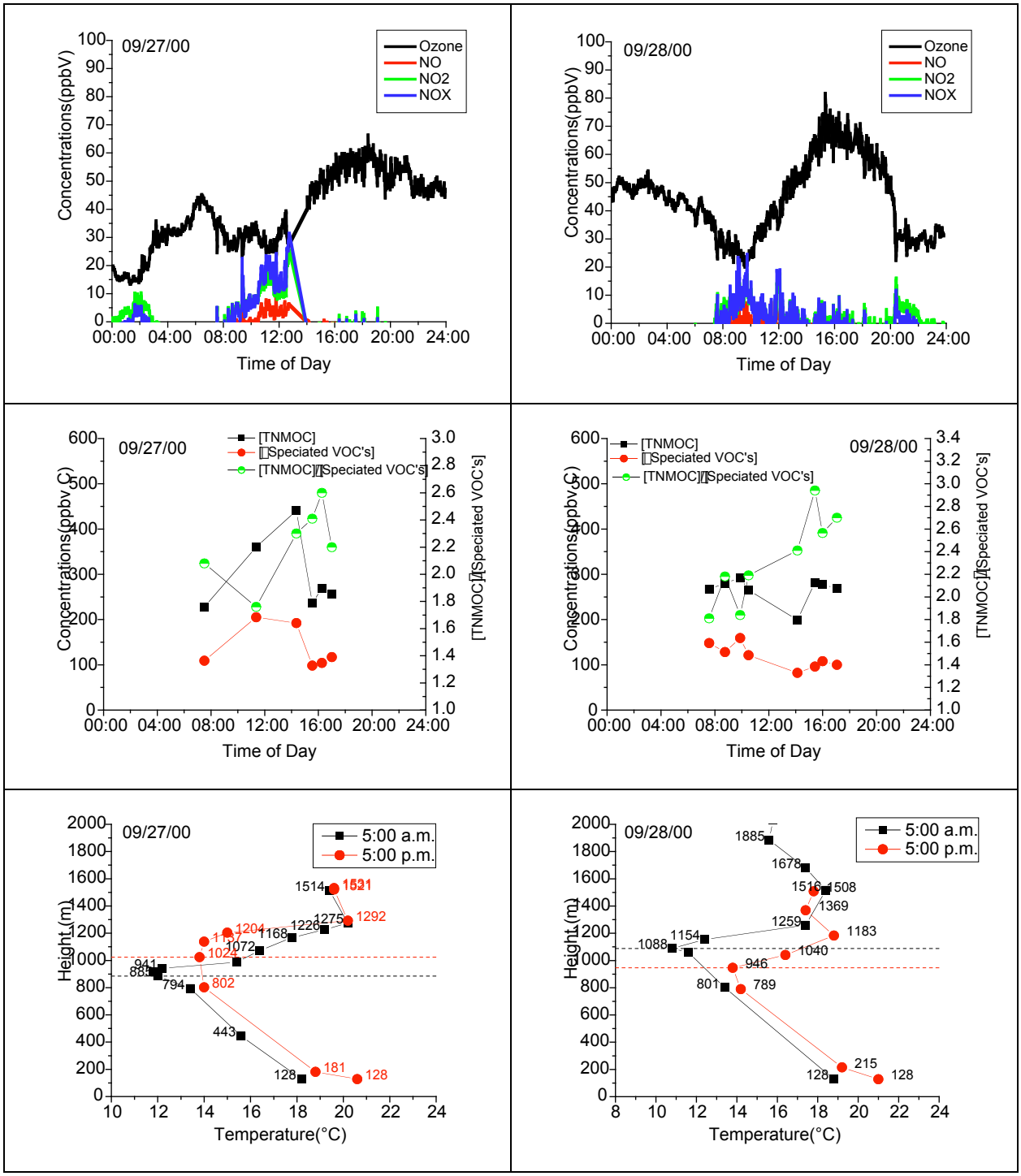

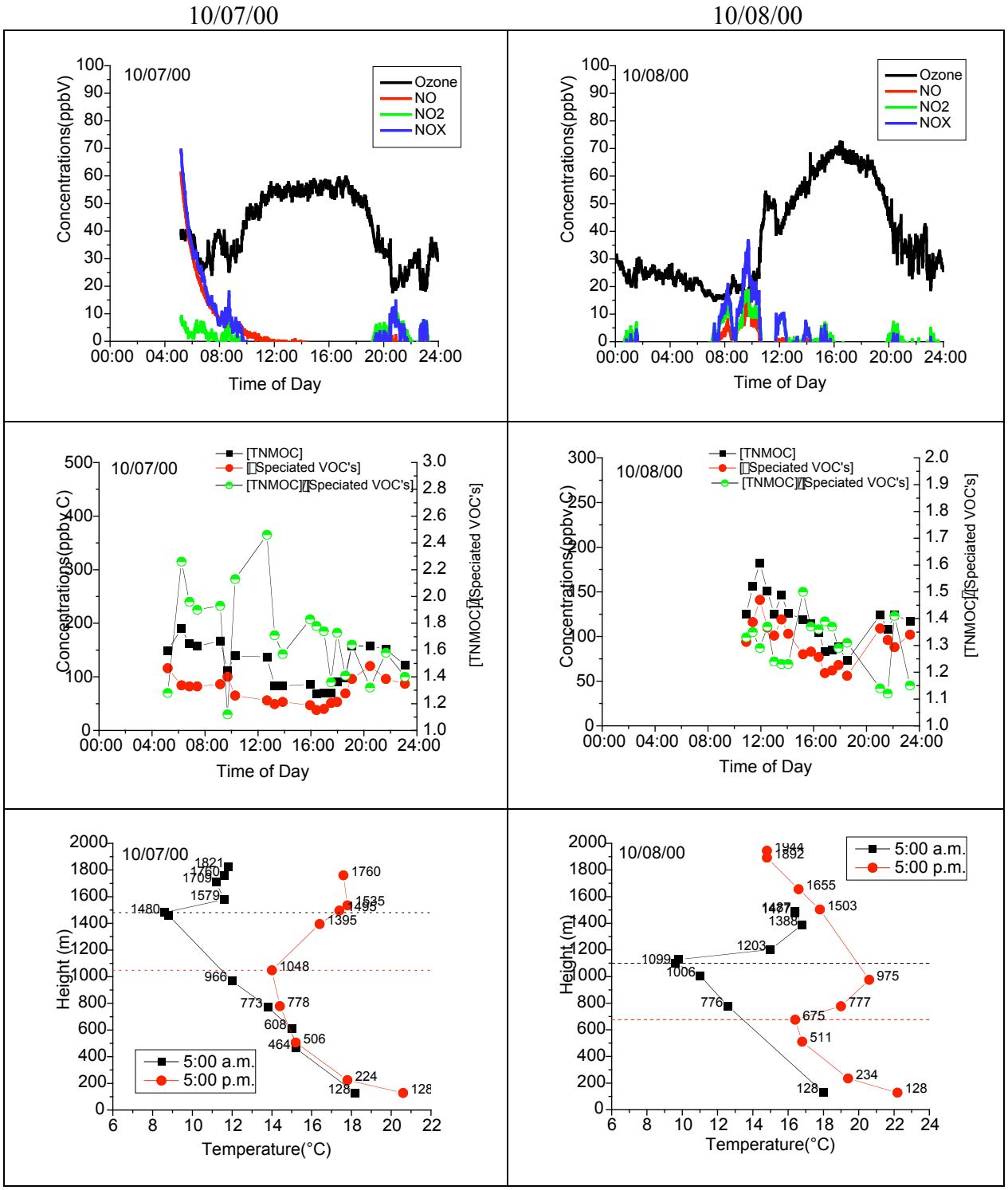

Figure 5.1.2 TNMOC, sum of speciated VOC's, TNMOC/sum of speciated VOC's, NO, NO_2, NO_x, O_3, and the vertical temperature profile from Miramar for cloudy days in September-October 2000.

Figure 5.1.3 shows physical data for clear days, divided into weekdays and weekends. Wind speed, wind direction, and temperature are all very similar for two data sets.

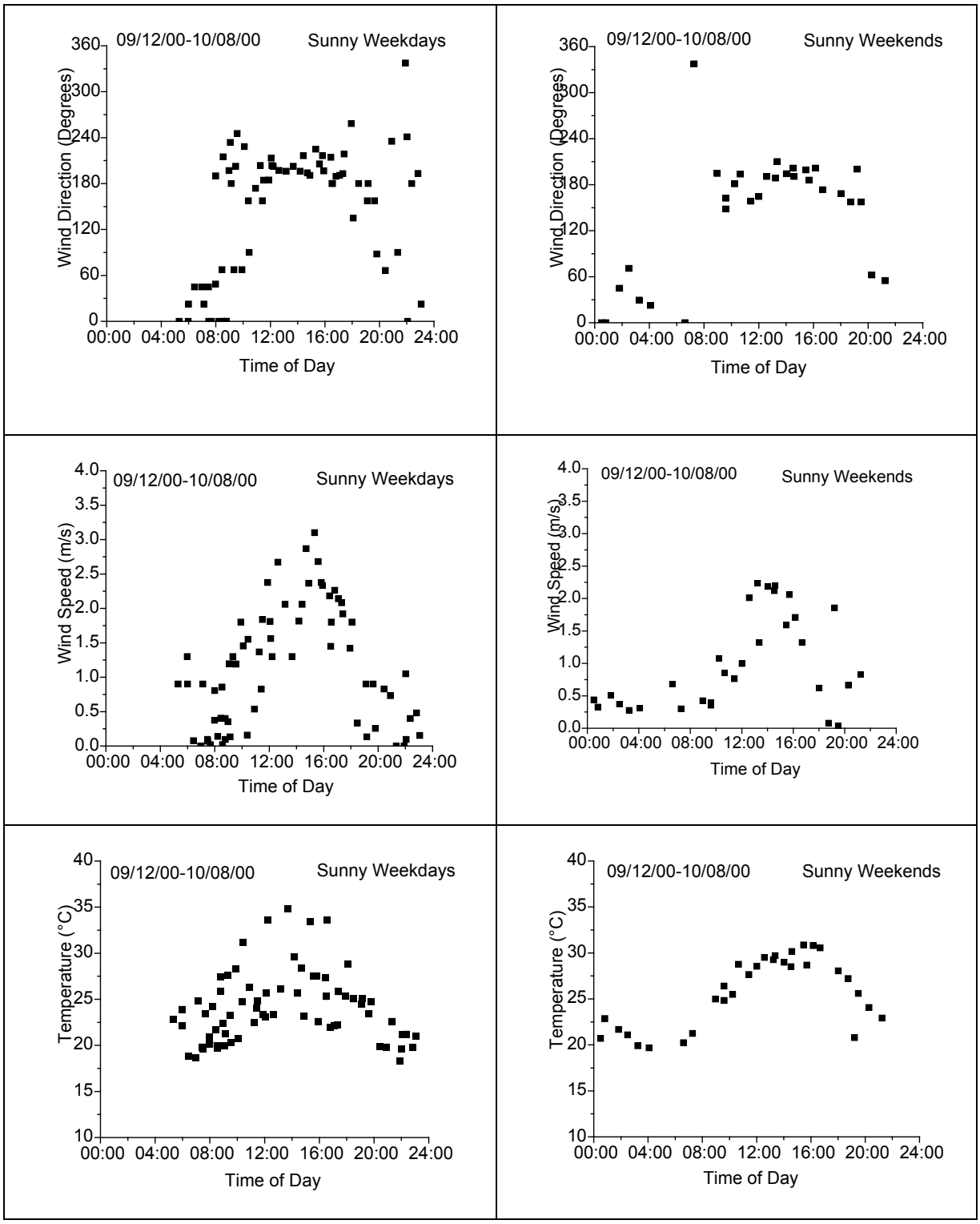

Figure 5.1.3 Comparison of the trends of meteorological data for clear weekdays and weekends.

Figure 5.1.4 shows pollutant data for clear days in September-October. As expected, NO_x concentrations were much lower on the weekends, and lack a clearly defined morning peak. O_3 was more consistently higher on weekdays including at night. The weekend days we sampled had 1 day with no afternoon O_3 peak. TNMOC concentrations span a greater range on weekdays, with both lower and higher levels compared to weekends. The TNMOC/sum of speciated VOC's ratio however, is very similar. The proxy residence time, from the m, p-xylene/ethylbenzene ratio is somewhat longer on the weekends, in spite of the lower O_3 concentrations.

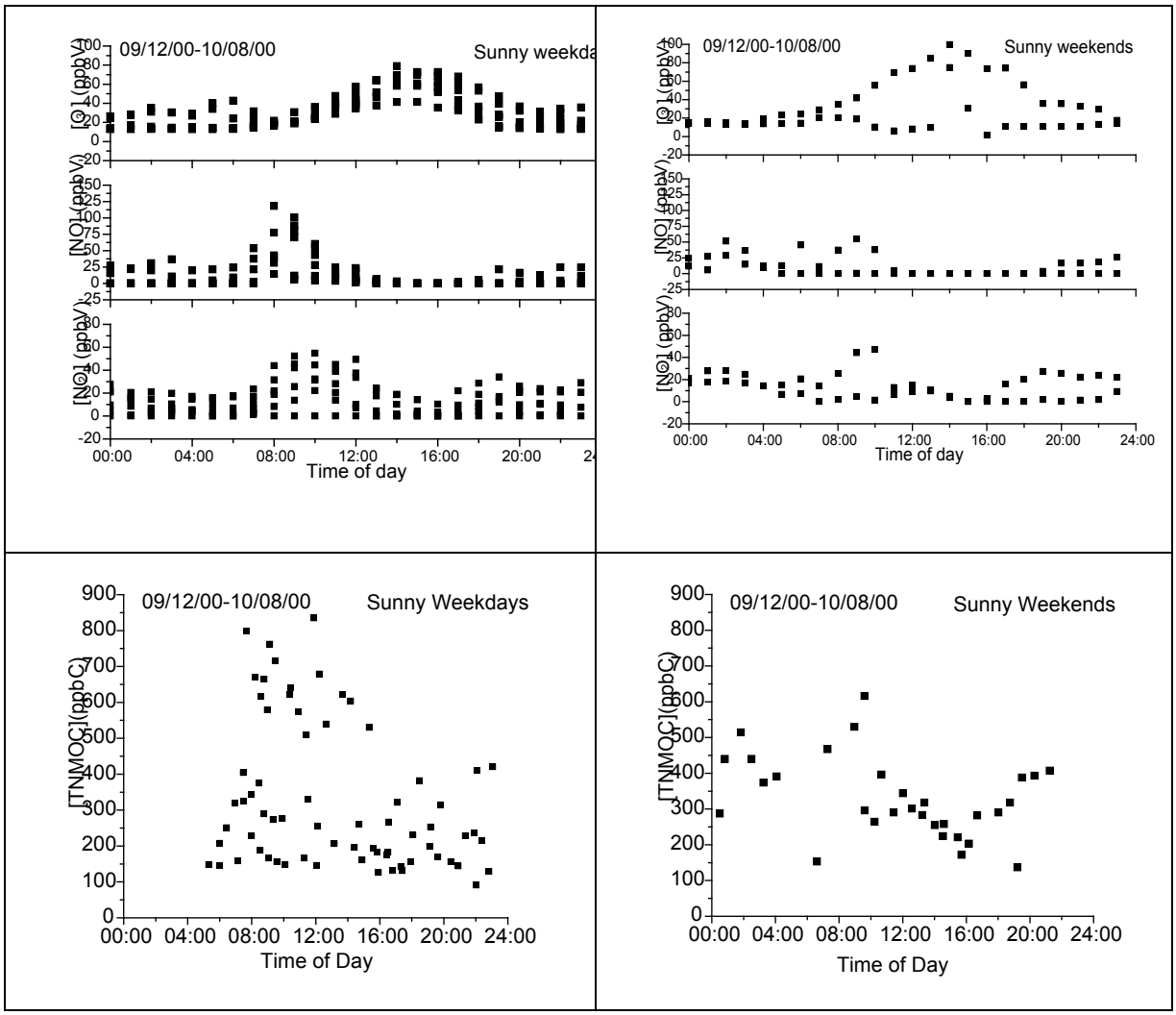

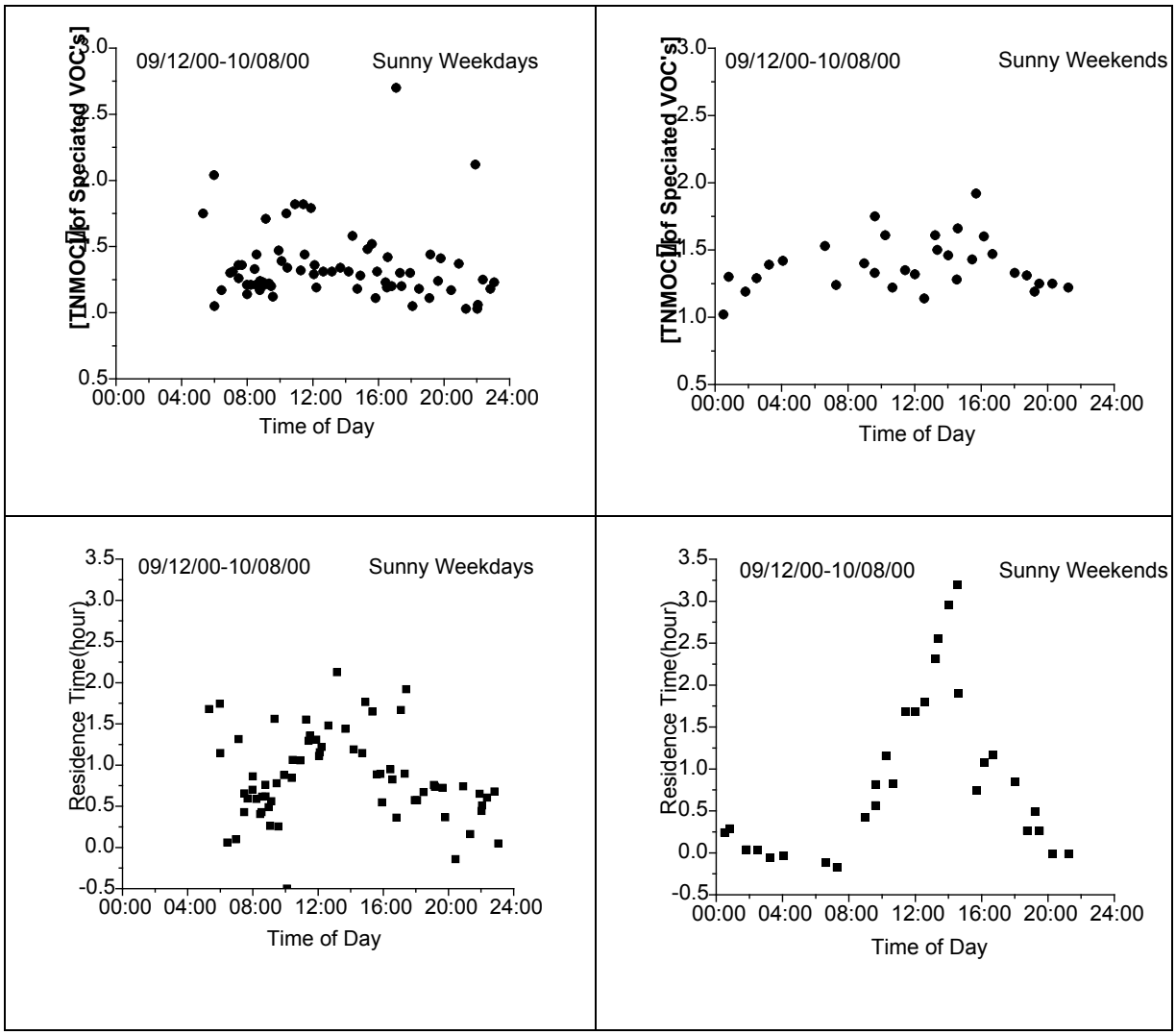

Figure 5.1.4. Trends of O_3, NO_x and total non-methane hydrocarbon concentrations ([TC]), TNMOC/sum of speciated VOC's ratio and residence time (calculated from ln([xylene]/[ethylbenzene])) versus time of day for clear weekdays and weekends.

Figure 5.1.5 shows SCAQMD NO_x and O_3 data for clear weekdays. O_3 maxima are similar, but elevated nighttime O_3 was not observed at AQMD's West Los Angeles site, located in a lightly used parking lot on the Veteran's administration grounds, south of Wilshire Blvd and West of the 405 Freeway. This is reasonable because of the site's close proximity to the 405 freeway and Wilshire Blvd combined with the prevailing wind, which blows from the SSW during mid day but from the North before about 9 AM during September/October. The NO_x concentrations are higher and the morning peaks higher, as expected from the wind pattern.

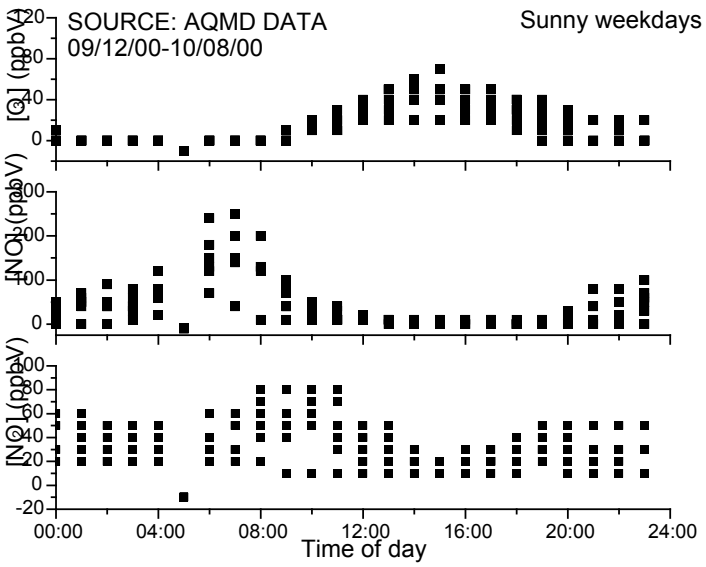

Figure 5.1.5. Trends of O_3, NO_x concentrations (average per hour) versus time of day for clear weekdays in September-October period from AQMD data.

The following plots, Figure 5.1.6 show physical data for cloudy days, divided into weekdays and weekends. Winds are similar for the midday period between 11 AM and 8 PM, and other wise scattered. Wind speeds are quite similar. Several of the weekdays are about 2°C warmer than the weekend days.

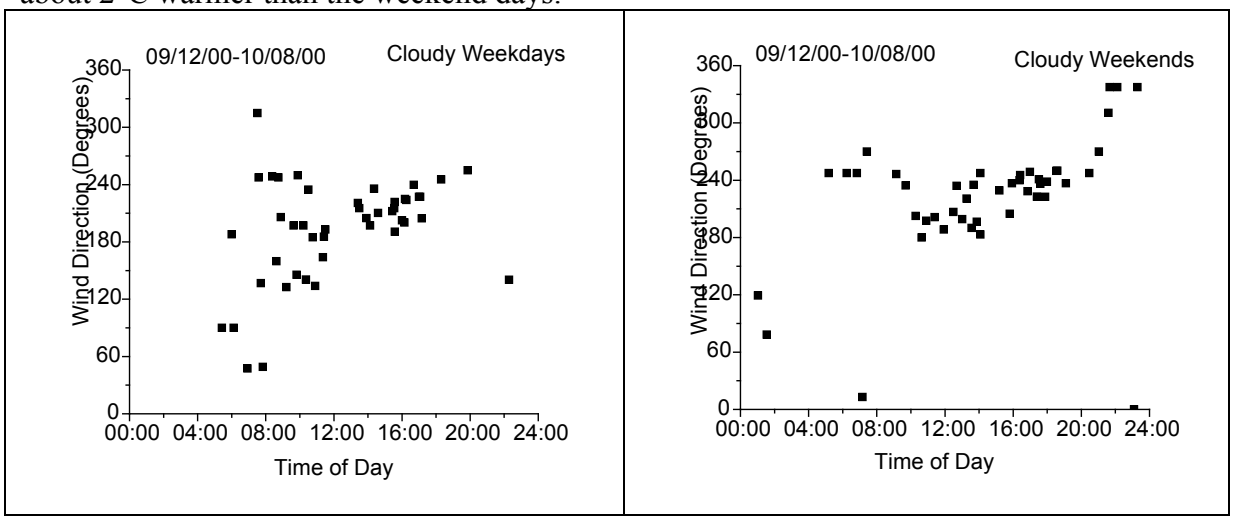

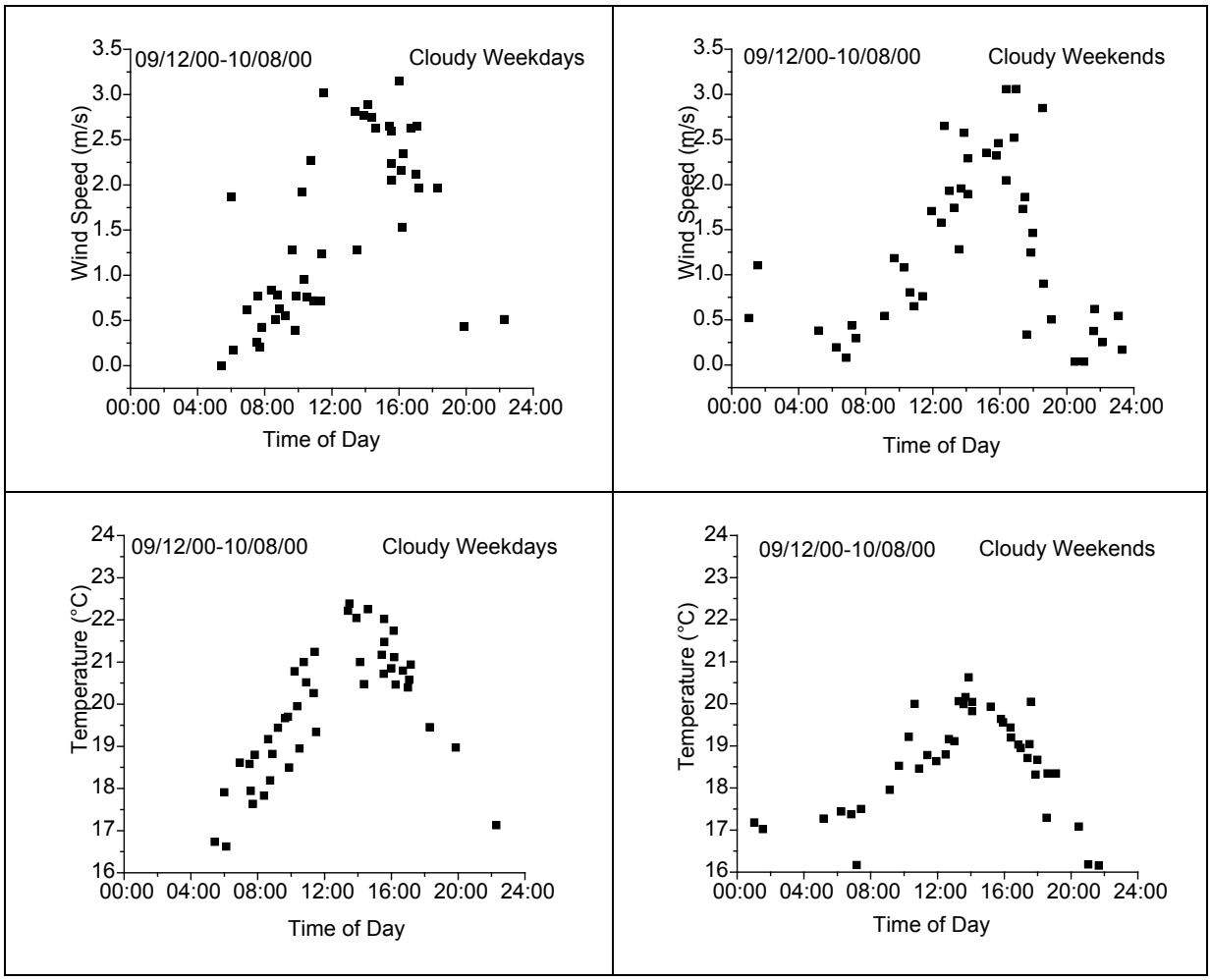

Figure 5.1.6 Comparison of the trends of meteorological data for cloudy weekdays and weekends.

Figure 5.1.7 shows pollutant data for cloudy days. As expected, NO_x concentrations are much lower on the weekends. Afternoon O_3 is similar on the weekdays and weekends, but on this set of days, nighttime ozone is higher on the weekdays. Weekdays had much higher TNMOC concentrations, and the average TNMOC/sum of speciated VOC's ratio is somewhat higher on weekdays (see Sect. 5.3.5). The residence time from m,p,-xylene/ethylbenzene ratio is longer on the weekends. The longest residence time appeared around 2 PM on the weekdays and it shifted about 2 hours on the weekends.

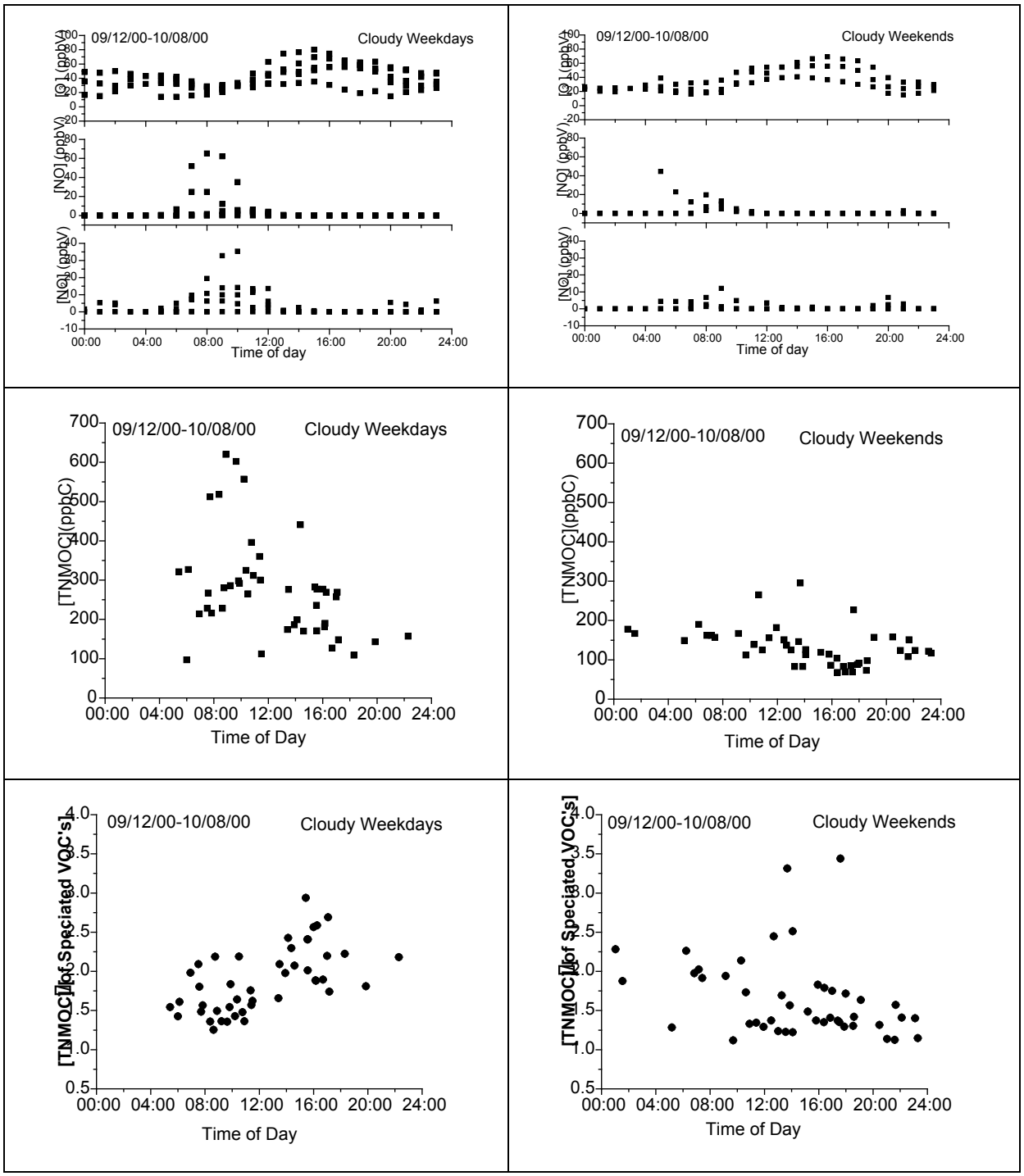
09/12/00-10/08/00
Cloudy Weekdays
[O3] (ppbV)
[NO] (ppbV)
[NO2] (ppbV)
Time of day
09/12/00-10/08/00
Cloudy Weekends
[O3] (ppbV)
[NO] (ppbV)
[NO2] (ppbV)
Time of day
09/12/00-10/08/00
Cloudy Weekdays
[TNMOC](ppbC)
Time of Day
09/12/00-10/08/00
Cloudy Weekends
[TNMOC](ppbC)
Time of Day
09/12/00-10/08/00
Cloudy Weekdays
[TNMOC]/[of Speciated VOC's]
Time of Day
09/12/00-10/08/00
Cloudy Weekends
[TNMOC]/[of Speciated VOC's]
Time of Day

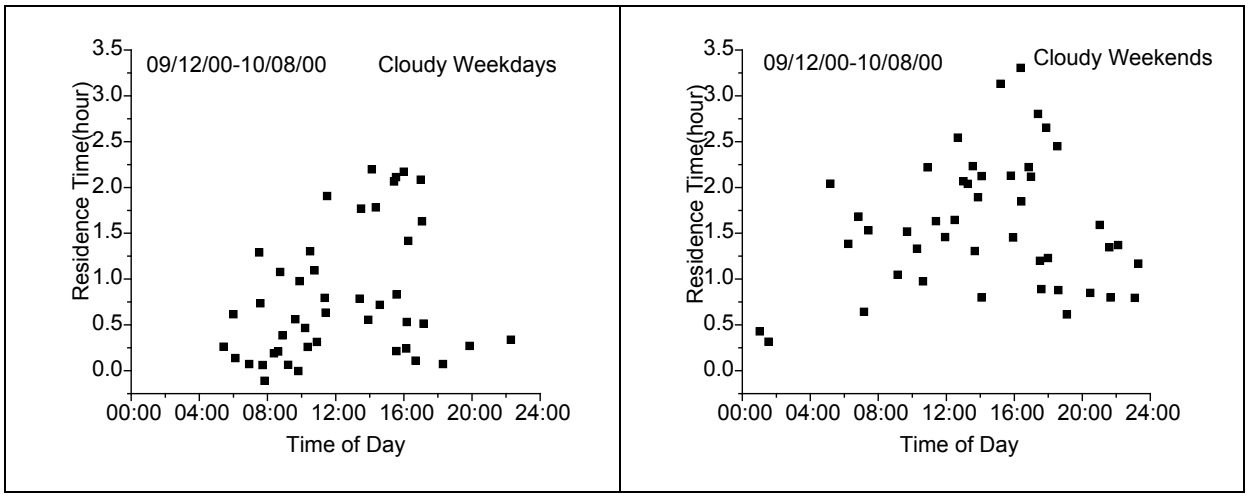

Figure 5.1.7. Trends of O_3, NO_x and total non methane hydrocarbon concentrations ([TC]), TNMOC/sum of speciated VOC's ratio and residence time (calculated from ln([xylene]/[ethy lbenzene])) versus time of day for cloudy weekdays and weekends.

Figure 5.1.8 shows SCAQMD NO_x and O_3 data for cloudy days, divided into weekdays and weekends. The trend of O_3 concentrations is similar to UCLA site and elevated nighttime O_3 is also observed at the AQMD site for both weekdays and weekends, but nighttime O_3 is higher on the weekdays. The higher NO_x concentrations at nighttime are observed at the AQMD site.

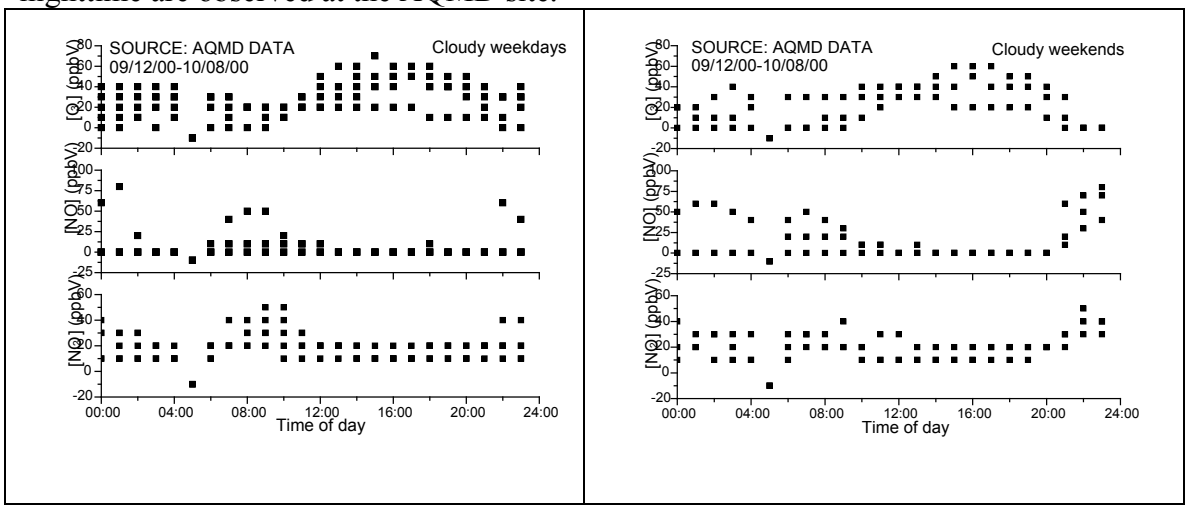

Figure 5.1.8. Trends of O_3, NO_x concentrations (average per hour) versus time of day for cloudy weekdays and weekends in September-October period from AQMD data.

5.2 December Measurements

TNMOC, sum of speciated VOC's, TNMOC/sum of speciated VOC's, NO, NO_2, NO_x, O_3, and the vertical temperature profile from Miramar, CA for each sampling day are shown in the Figure 5.2.1 below. The Miramar site is the closest coastal site that was collecting vertical temperature profiles during this period. As of 2001, vertical profiles have been collected at Los Angeles International Airport (LAX). For 2001 data at elevated heights, LAX and Miramar are similar. The surface temperature variations differ, however, because LAX is beside the ocean, while Miramar is several miles inland. LAX shows little surface temperature variabiltity, while Miramar shows significant variability particularly on clear days. The UCLA site is more similar to Miramar in this regard, although UCLA exhibits somewhat smaller temperature variations. The days we took samples were Sunday and Wednesday and all days had some clouds.

11/30/00 12/03/00

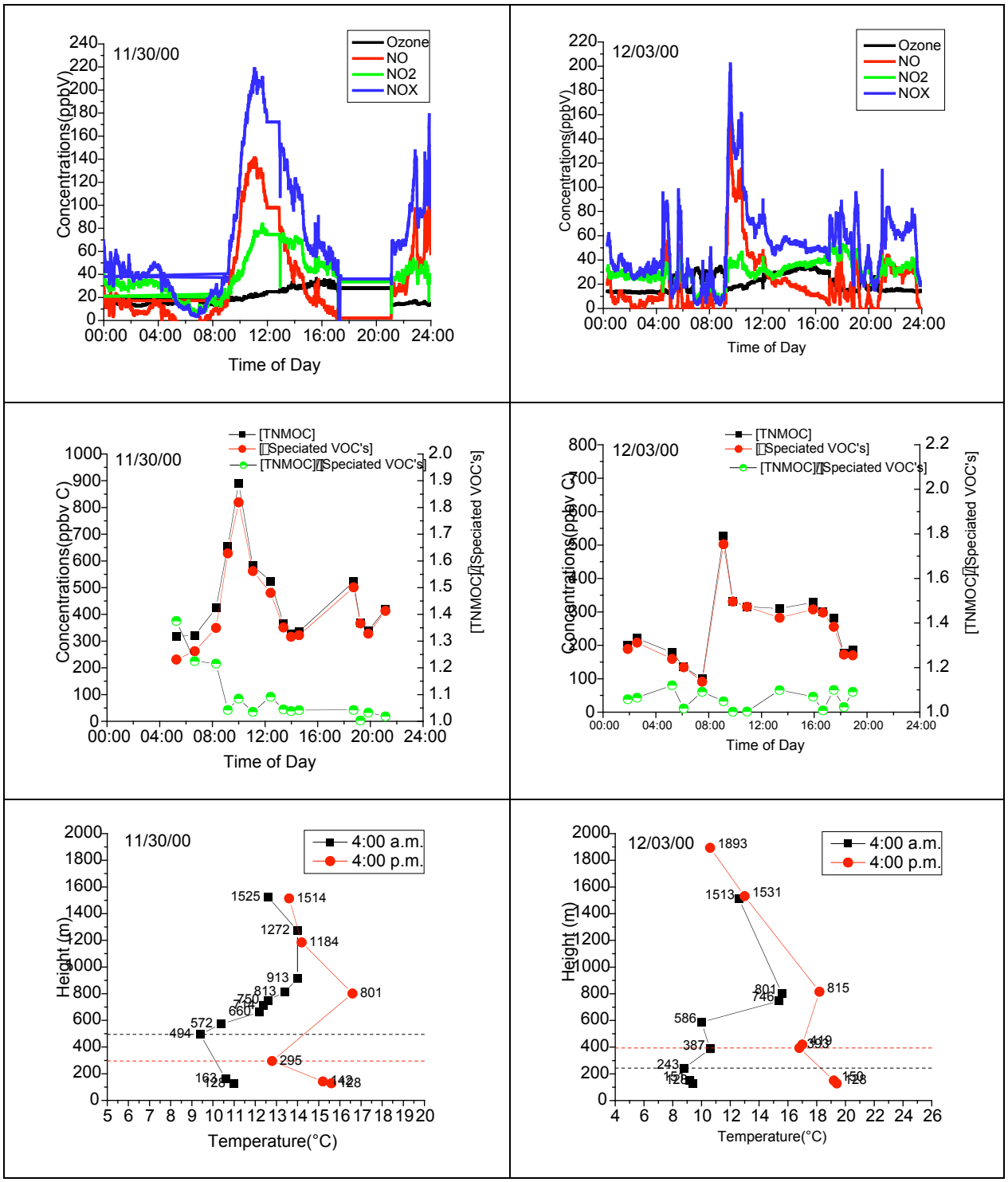

12/06/00 12/10/00

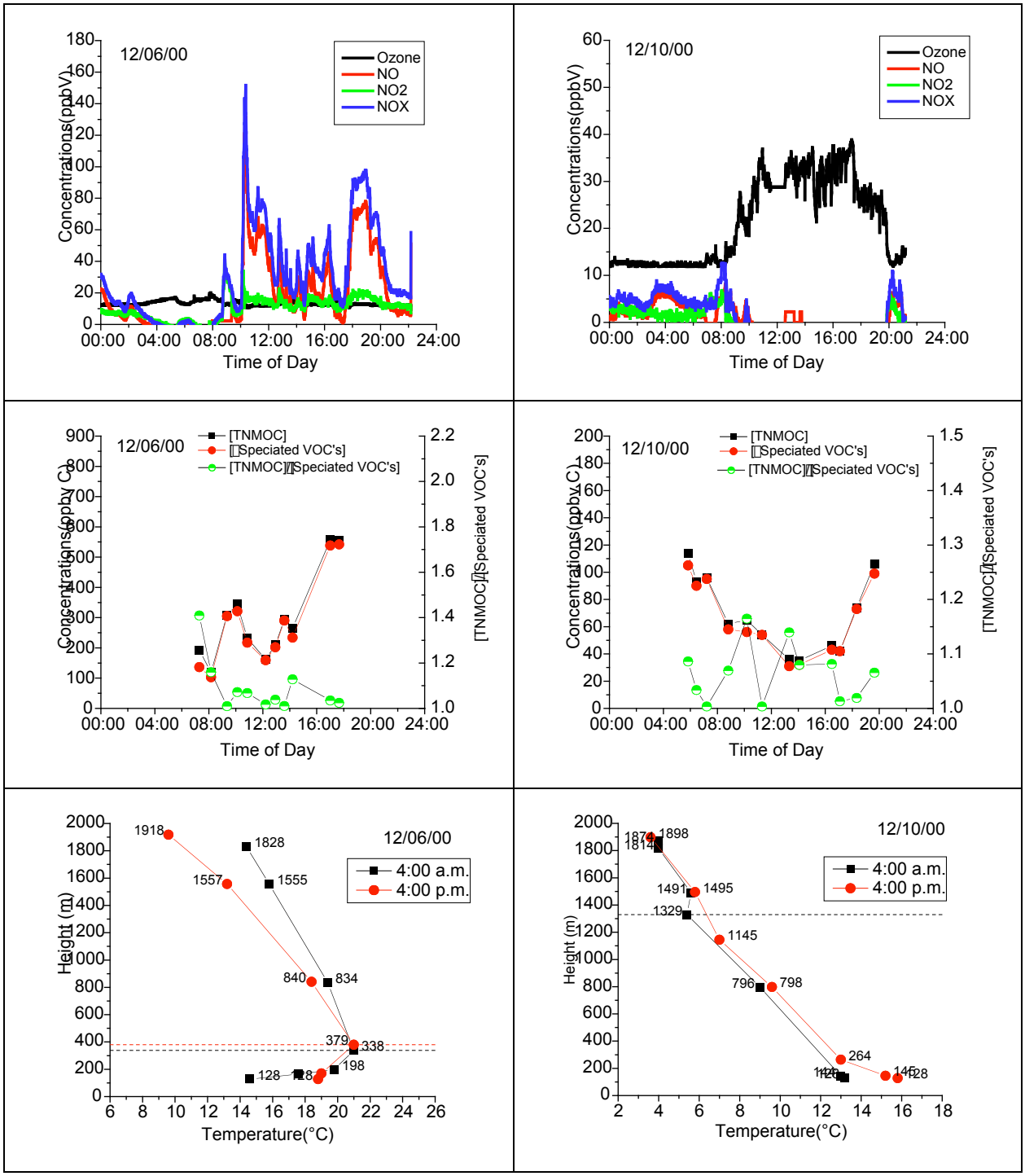

12/13/00 12/17/00

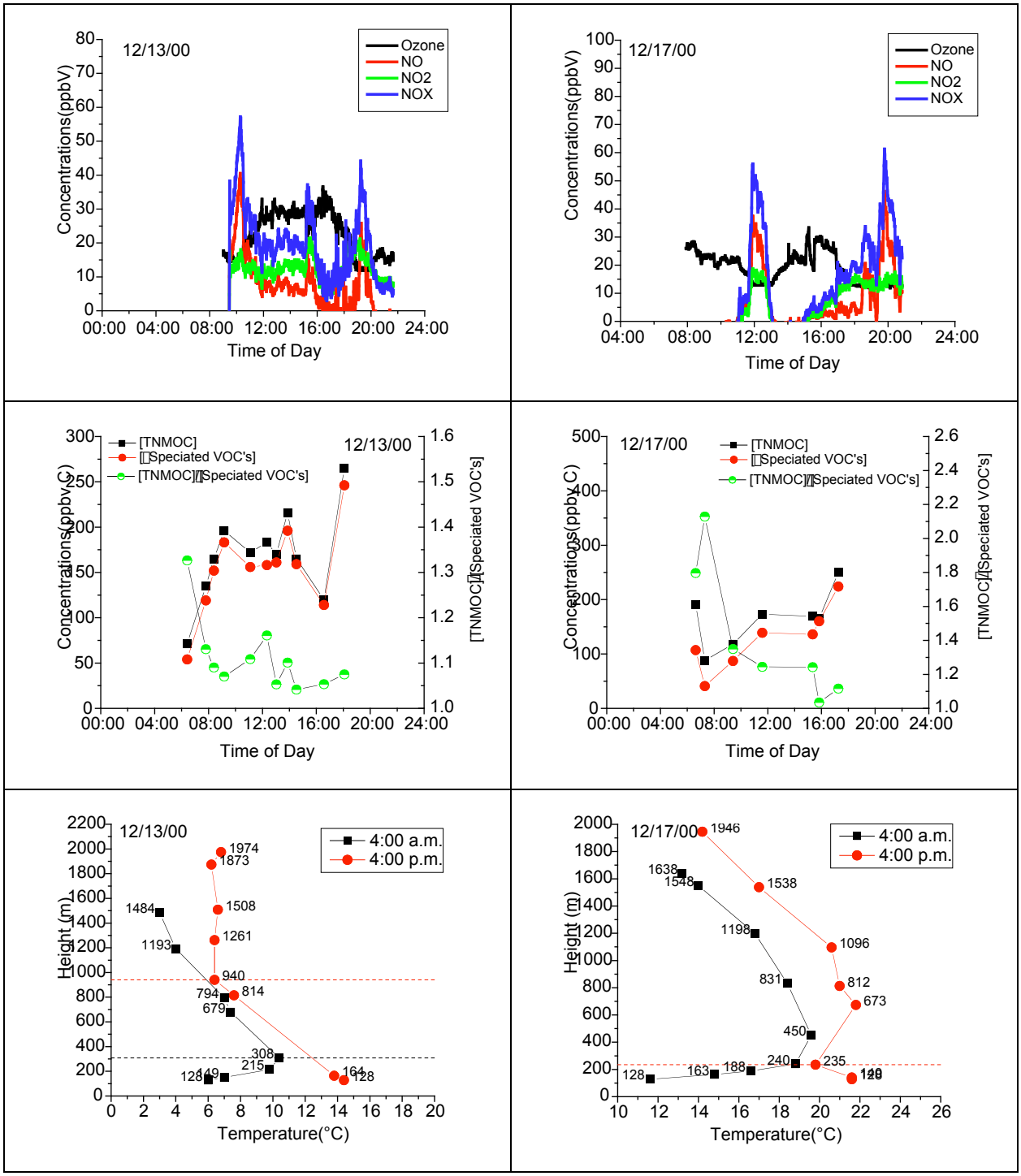

12/20/00

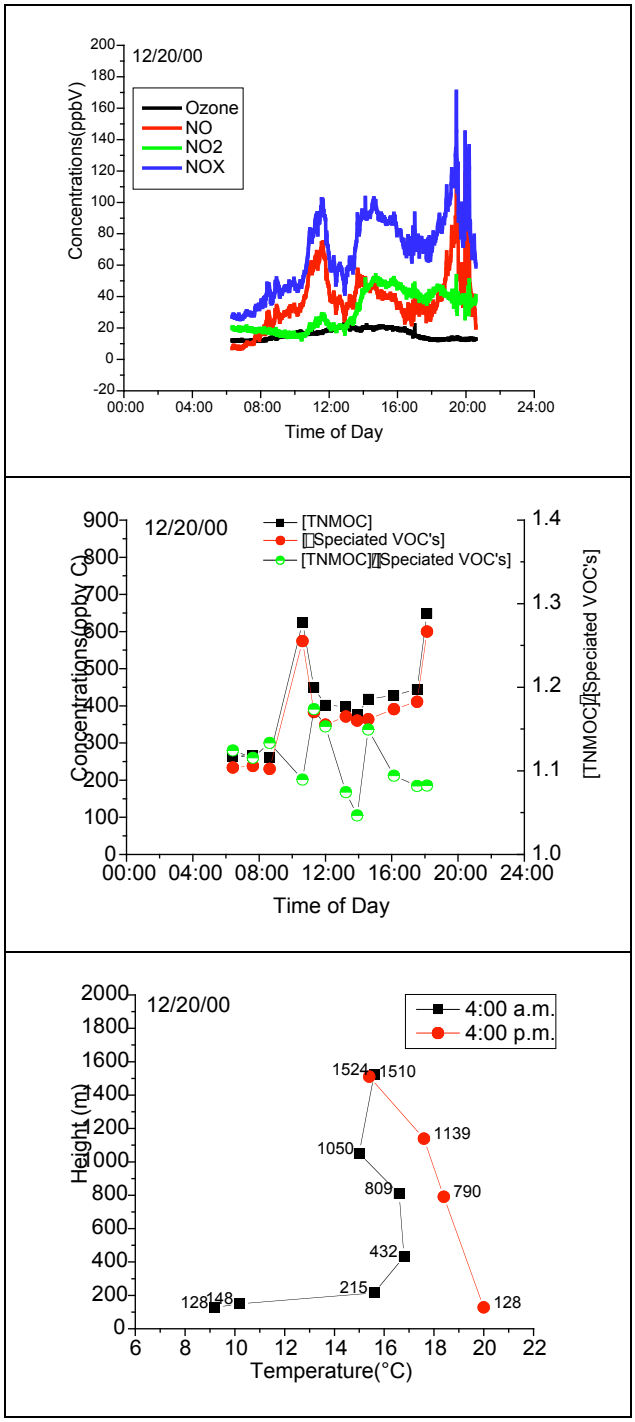

Figure 5.2.1 TNMOC, sum of speciated VOC's, TNMOC/sum of speciated VOC's, NO, NO_2, NO_x, O_3, and the vertical temperature profile from Miramar for Sundays and Wednesdays in November-December 2000.

The following plots show a comparison of physical and chemical parameters for Sundays and Wednesdays during Nov-Dec. The days were fairly similar, although the weekend days are somewhat more extreme, including both the coldest and warmest days. Figure 5.2.2 shows physical data, divided into Wednesdays and Sundays. Wind speed, wind direction, and temperature are quite similar for two data sets.

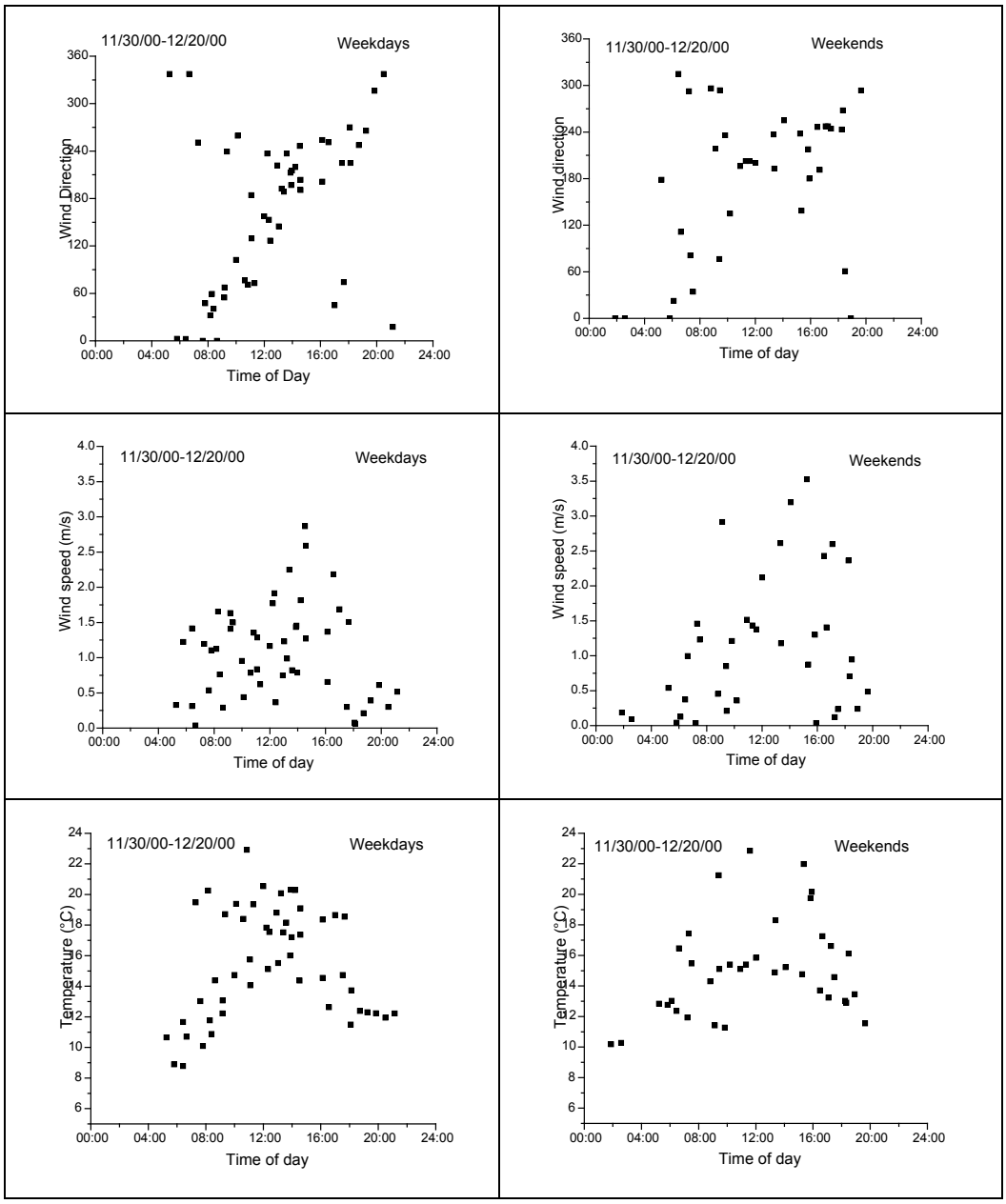

Figure 5.2.2. Comparison of the trends of meteorological data for weekdays and weekends in November-December period.

Figure 5.2.3 shows pollutant data for weekdays and weekends. O_3 and NO_x were also similar for the two data sets. Both Sunday and Wednesday contained one day each with much higher NO_x and O_3 at night. Weekdays had much higher TNMOC

concentrations, and TNMOC/sum of speciated VOC's ratio is slightly higher on weekends except for early in the morning.

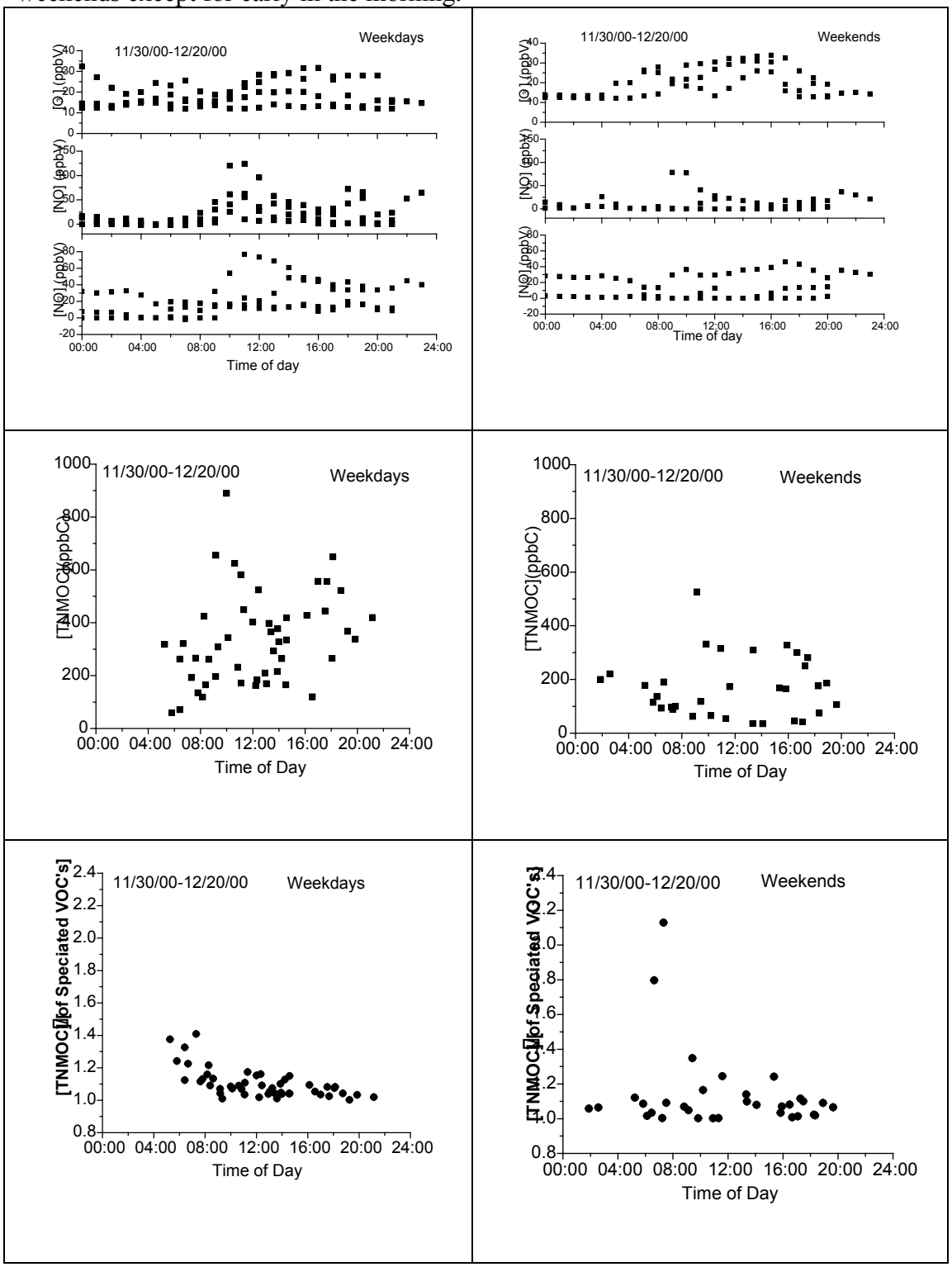

Figure 5.2.3. Trends of O_3, NO_x and total non methane carbon concentrations ([TC]), [TC]/[∑SP] ratio versus time of day for weekdays and weekends in November-December period.

Figure 5.2.4 shows SCAQMD NO_x and O_3 data for weekdays. O_3 maxima are similar, but elevated nighttime O_3 was not observed at the AQMD site. The NO_x concentrations are higher and the morning peaks higher, as expected from the wind pattern.

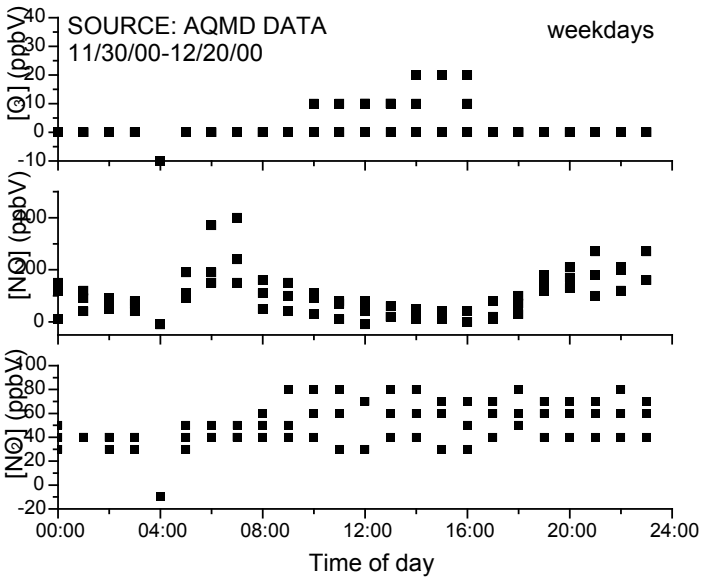

Figure 5.2.4. Hourly averaged AQMD O_3 and NO_x concentrations versus time of day for clear weekdays measurement days in November-December.

5.3 Discussion

Data are presented showing the relationship between excess TNMOC and many parameters below, including photochemical indicators, meteorology, and primary source gasses. For the TNMOC/sum of speciated VOC's ratio, the strongest indicator is meteorology. Additionally, elevated O_3 at night seems to be associated with higher early morning ratios, and higher TNMOC/sum of speciated VOC's ratios are correlated with decreasing trends for longer lived aromatics.

5.3.1 Cloudy and Clear Days

VOC concentrations on clear and cloudy days are qualitatively different. On clear days, VOC concentrations are higher throughout the day. They are high at night, 400-500 ppbC, due to strong nocturnal surface inversions that typically accompany clear weather (Figure 5.1.1). They decrease in the early AM once the sun rises and the inversion begins to break, increase again due to morning rush hour back to 400-500 ppbC, and gradually decrease to around 200 ppbC during the afternoon. In contrast, cloudy conditions bring much higher mixing heights and lower concentrations. Levels stay near 200 ppbC most of

the day, that increasing significantly, to about 400 ppbC, during morning rush hour. Ozone concentrations reach somewhat higher maxima on clear days; 100 vs. 70 ppbV for cloudy days. Cloudy days also tend to have higher O_3 at night, presumably due to carryover aloft and increased vertical mixing that dilutes surface NO emissions.

Average VOC data for cloudy and clear days are given in Table 5.3.1. Standard deviations of the means are a measure of the robustness of the mean value, useful for comparing averages. These are calculated from the expression:

$$\sigma_{mean} = \frac{SD}{\sqrt{n}}$$

where n is the number of observations and SD is the standard deviation of the measurements. For large data sets with a high degree of inherent variability, standard deviations of the means are a realistic way to test for differences. It is an intuitive and theoretical result that, the mean will change little if more data of the same type of points are added. Thus the mean is much more robust than the standard deviation indicates [49]. Comparison of the results indicates that cloudy days have significantly higher TNMOC/sum of speciated VOC's ratios than do clear days, with mean values of 1.37 and 1.77, respectively. These are well outside the respective confidence intervals for the mean values. Our hypothesis for the cause of this behavior is stronger influence from pollutant carryover from air that has been aged for more than a few hours and stored aloft.

Cloudy days are different from clear days primarily in that they have much higher mixing heights lower pollutant concentrations (above). Cloudy days tend to also have somewhat higher humidities, although some clear days also have high humidities. Cloudy days have lower temperature maxima (temperature lows are very similar), somewhat lower peak O_3, and higher nighttime O_3. One potential concern is that higher TNMOC/Sum of speciated VOC's ratios are the result of an artifact in the measurement that appears, or appears more strongly, at the lowest concentrations. Figure 5.3.2 shows the correlation between TNMOC and sum of speciated VOC's for clear and cloudy days. The correlations are very strong, with R^2 values of 0.91 and 0.85 respectively. The plots also show that the highest ratios, seen in this plot as deviations from the average line in the positive direction have no particular trend on clear days. On cloudy days they are clustered at about 100 ppbC in the speciated channel and 200-300 ppbC in the TNMOC channel, well above the lowest concentrations of around 50 ppbC on cloudy days.

There are several points of evidence that corroborate the hypothesis that higher ratios at the UCLA site are due to more influence from pollutants stored aloft for a day or more. It should be noted that between 10 AM and 8 PM at the UCLA site, surface level transport of polluted air will not contribute as it does further inland due to the prevailing winds and close proximity to the ocean. Clearly when pollutant levels are lower there will be more influence from background air, as can be seen from the panel in Section 5.3.3 showing the relationship between both VOC measurements and NO_2, a marker of fresh emissions. This panel shows that NO_2 is linearly related to VOC levels. When mixing heights are higher, greater contributions from pollutant carryover aloft can be expected, thus cloudy days should have higher TNMOC/sum of speciated VOC's ratios, which they do. Higher ratios are not well correlated with O_3 and other short lived tracers, but they are correlate with longer lived tracers. High ratios are never associated with high NO concentrations (Section 5.3.3). Gasoline vapor, a proxy for the dominant source of

VOC's in urban air, has a ratio near 1.0 (Section 7). High TNMOC/sum of speciated VOC's ratios appear to be positively correlated with a higher fraction of oxygenates (5.3.6 and 5.3.7) and with O_3 in the early morning hours when O_3 is a tracer for pollutant transport rather than short term photochemistry. The apparent lack of a weekend effect (Section 5.3.2) is not consistent with this hypothesis, as concentrations are lower on the weekends, and as such more influence from pollutant carryover aloft should be observed. However, but it seems likely that we do not have enough measurement days of each meteorological type to discern such an effect if it occurs.

Table 5.3.1 Averages and Ranges for VOC's and Ozone on Clear and Cloudy Days During September-October

	No. of Obser-vations	TNMOC	Sum of Speciated VOC's	TNMOC/ of Speciated VOC's	Average O_3 (ppbV)	Average Maximum O_3 (ppbV)
Clear	101	329±178 2 mean= 32	245±132 2 mean= 26	1.37±0.26 2 mean=	36±22	75±16
range		91-835	71-598	0.06 1.02-2.7		45-100
Cloudy	90	205±120 2 mean= 26	121±82 2 mean= 18	1.77±0.48 2 mean=	42±17	61±13
range		68-620	38-444	0.10 1.12-3.44		41-79

Clear	Cloudy
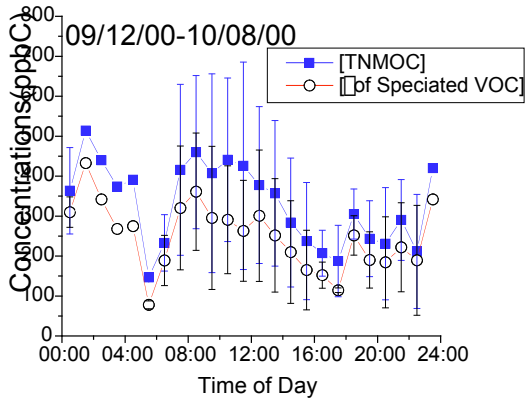	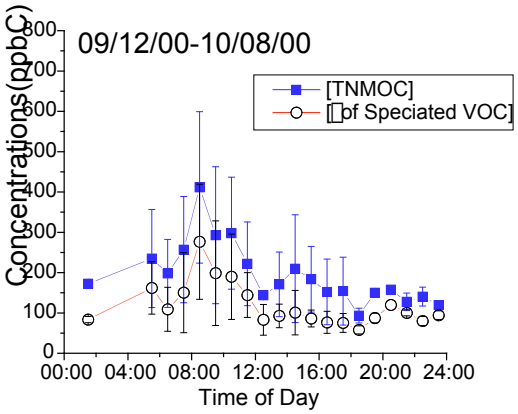

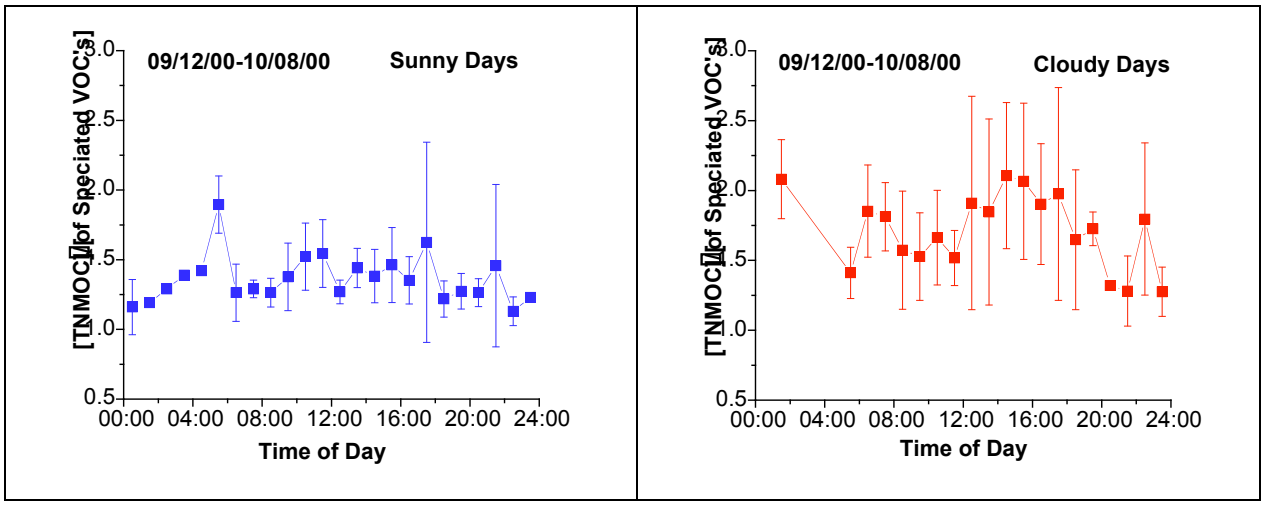

Figure 5.3.1 Diurnal averages for TNMOC/sum of speciated VOC's ratio, TNMOC and sum of speciated VOC's for cloudy and clear days. Error bars show the full range of observations. Points without error bars have only 1 or 2 data points averaged.

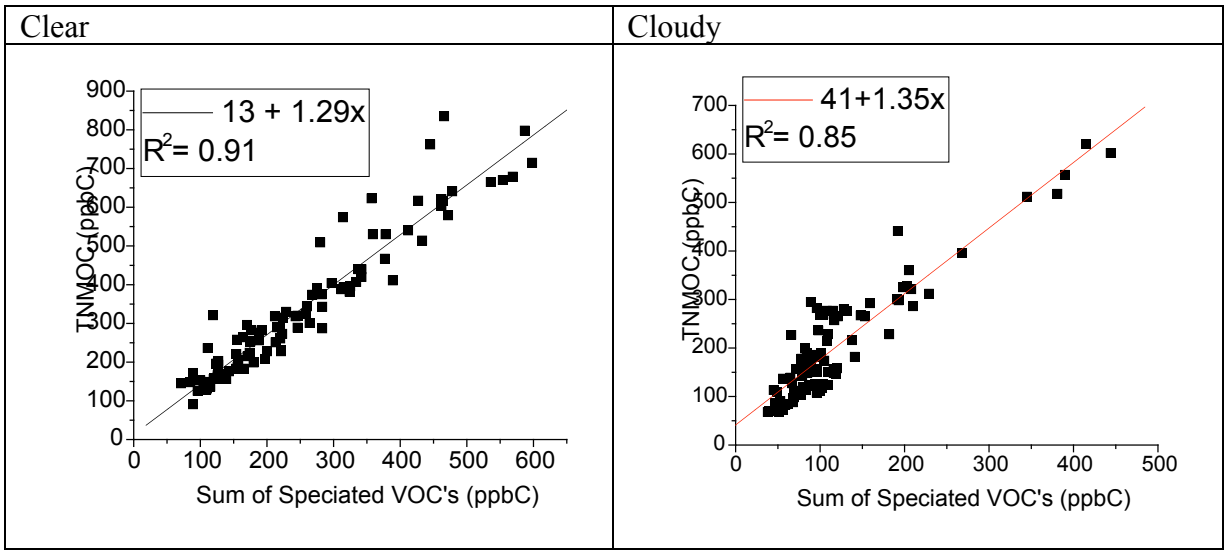

Figure 5.3.2 TNMOC vs. sum of speciated VOC's for clear and cloudy conditions.

5.3.2 Weekend Effect?

Table 5.3.2 shows overall averages and standard deviations for all validated data collected at UCLA during 2000, divided by day of week and meteorology. For each meteorology and day of week there are 2-6 days of sample data, with between 3 and 17 measurements per day. From these data, there appears to be no difference at all between weekdays and weekend days under clear conditions. If anything, on cloudy days, the excess TNMOC is lower than it is on weekends, although this difference is within the 2 standard deviation of the means. During winter, the TNMOC/sum of speciated VOC's ratios are nearly identical on weekdays and weekends, but this is expected since there

appears to be little influence from photochemistry during winter, and the ratio deviates little from 1.0. As shown in Section 5.1 the weekend days during September-October are more extreme than the weekdays. Even if the weekend days had had average meteorology when compared to the weekdays, we likely did not collect sufficiently data to make a statistically robust comparison of weekend and weekdays. Thus while the data do not indicate a weekend effect, they do not rule it out, either.

Table 5.3.2 Average Ratios for Summer and Winter, Weekends and Weekdays, and Clear and Cloudy Conditions

Season	Day of Week/ Weather	Number Of Days	No. of Measure-ments	Average TNMOC (ppbC)	Average TNMOC/sum of speciated VOC's	Average sum of sp. VOC's (ppbC)
Sept-Oct	Weekday Clear	6	69	329 ±201	1.35 ± 0.28 ($2\sigma_{mean}$= 0.08)	245 ±145
	Weekend Clear	2	31	331±113	1.39 ± 0.19 ($2\sigma_{mean}$= 0.2)	247 ± 98
	Weekday Cloudy	5	45	277 ± 127	1.88 ± 0.41 ($2\sigma_{mean}$= 0.14)	159 ± 99
	Weekend Cloudy	3	45	133 ±49	1.66 ± 0.52 ($2\sigma_{mean}$= 0.14)	83 ± 26
Nov-Dec	Weekday Clear	3		337 ± 173	1.10 ± 0.09 ($2\sigma_{mean}$= 0.04)	311 ±165
	Weekend Clear	3		175 ± 120	1.14 ± 0.23 ($2\sigma_{mean}$= 0.1)	154±110

5.3.3 Correlations of TNMOC/sum of speciated VOC's Ratio and VOC's with Winds, O_3, and NO_x

A number of correlation plots are shown in this section. Many show no correlation at all. As above, data are separated by meteorological classification. In all cases, VOC's are strongly correlated with NO_2, much more so than they are correlated with NO or NO_x, as might be expected due to the very short lifetime of NO. High TNMOC/sum of speciated VOC's ratios are never associated with very high NO concentrations. On clear days, the TNMOC/sum of speciated VOC's ratio is weakly correlated with O_3; the correlation coefficient R^2 is 0.1, identical to that observed in 1999 at UCLA (Section 4). On cloudy days the TNMOC/sum of speciated VOC's ratio is uncorrelated to O_3 with the exception of the early morning (Section 5.3.4). Also in the wintertime when the O_3 levels are all below 40 ppbV, there is no correlation between O_3 and TNMOC/sum of speciated VOC's ratio. More high TNMOC/sum of speciated VOC's ratios are associated with winds from the SSW during September-October, but this may result from the fact that most of the data were collected when the wind was coming from that direction. The TNMOC/sum of speciated VOC's ratio is uncorrelated with the wind speed during both seasons and with wind direction in winter.

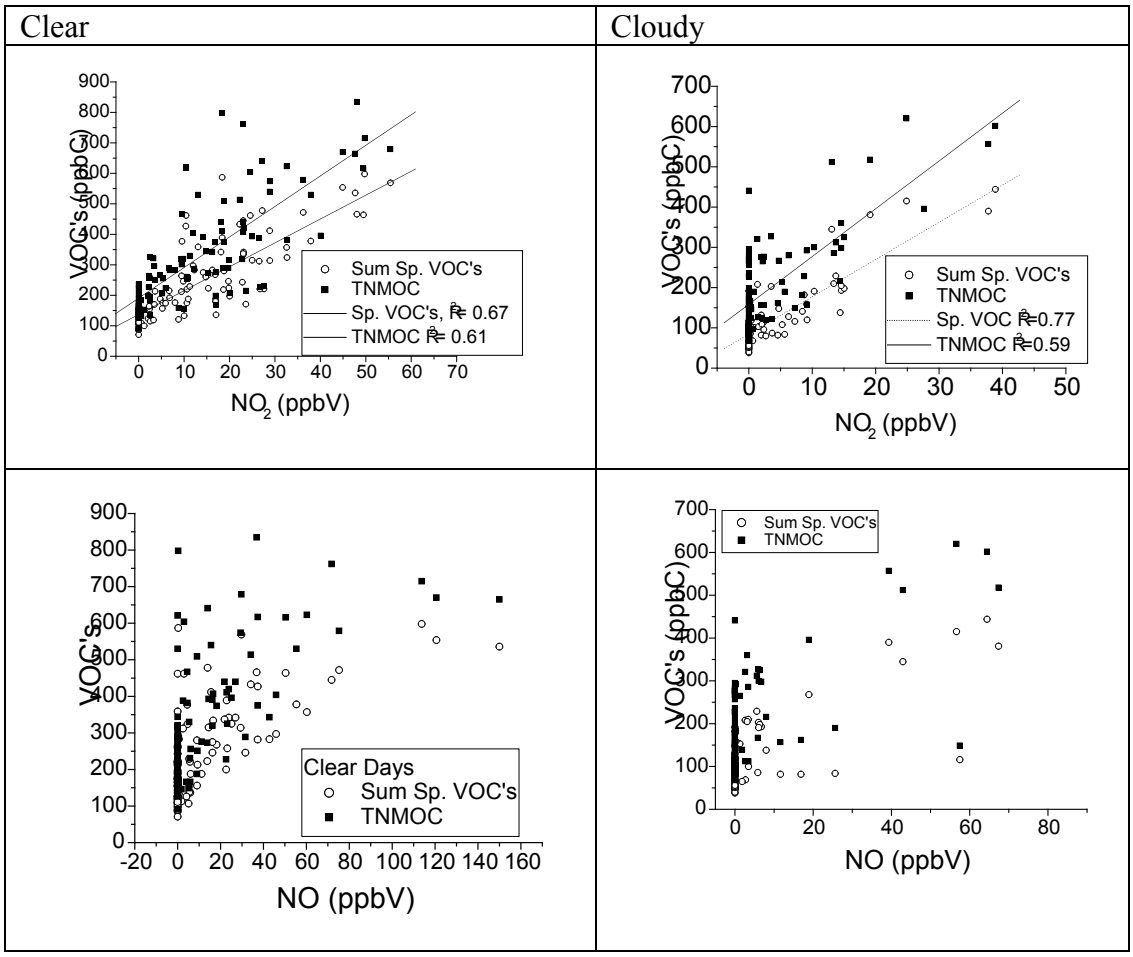

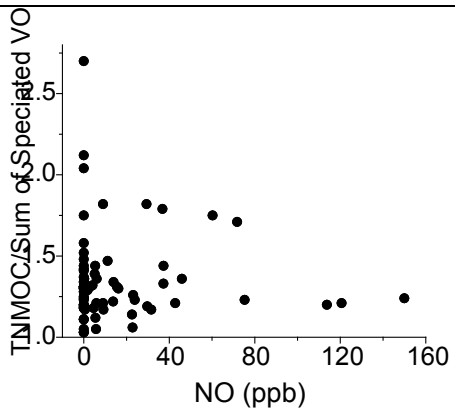
TNMOC/Sum of Speciated VO
NO (ppb)

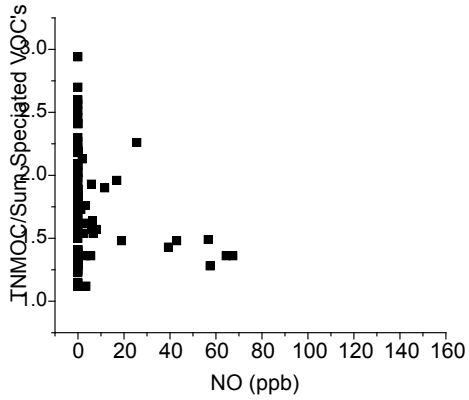
TNMOC/Sum Speciated VOC's
NO (ppb)

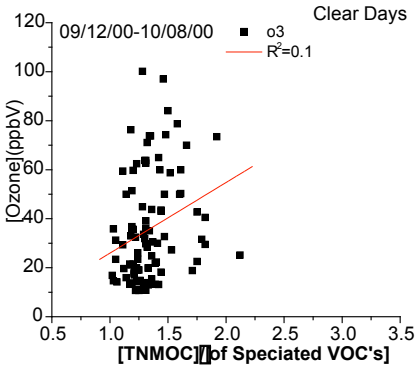
09/12/00-10/08/00
Clear Days
o3
R2=0.1
[Ozone](ppbV)
[TNMOC]/[of Speciated VOC's]

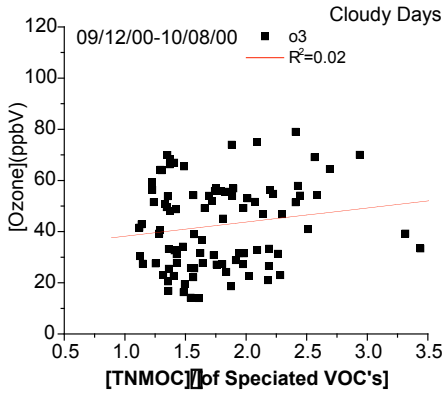
09/12/00-10/08/00
Cloudy Days
o3
R2=0.02
[Ozone](ppbV)
[TNMOC]/[of Speciated VOC's]

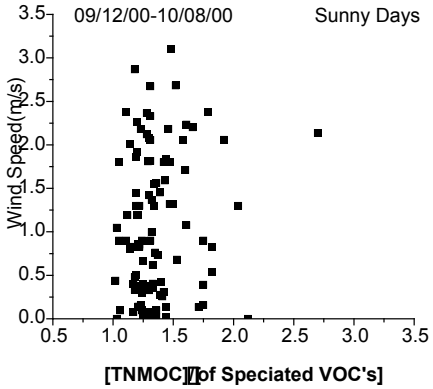
09/12/00-10/08/00
Sunny Days
Wind Speed(m/s)
[TNMOC]/[of Speciated VOC's]

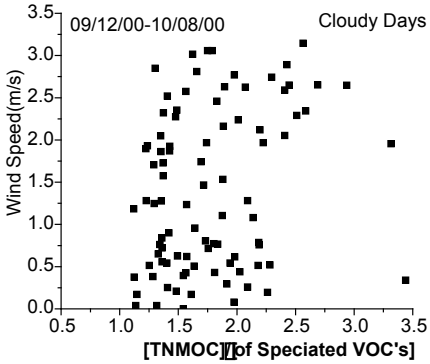
09/12/00-10/08/00
Cloudy Days
Wind Speed(m/s)
[TNMOC]/[of Speciated VOC's]

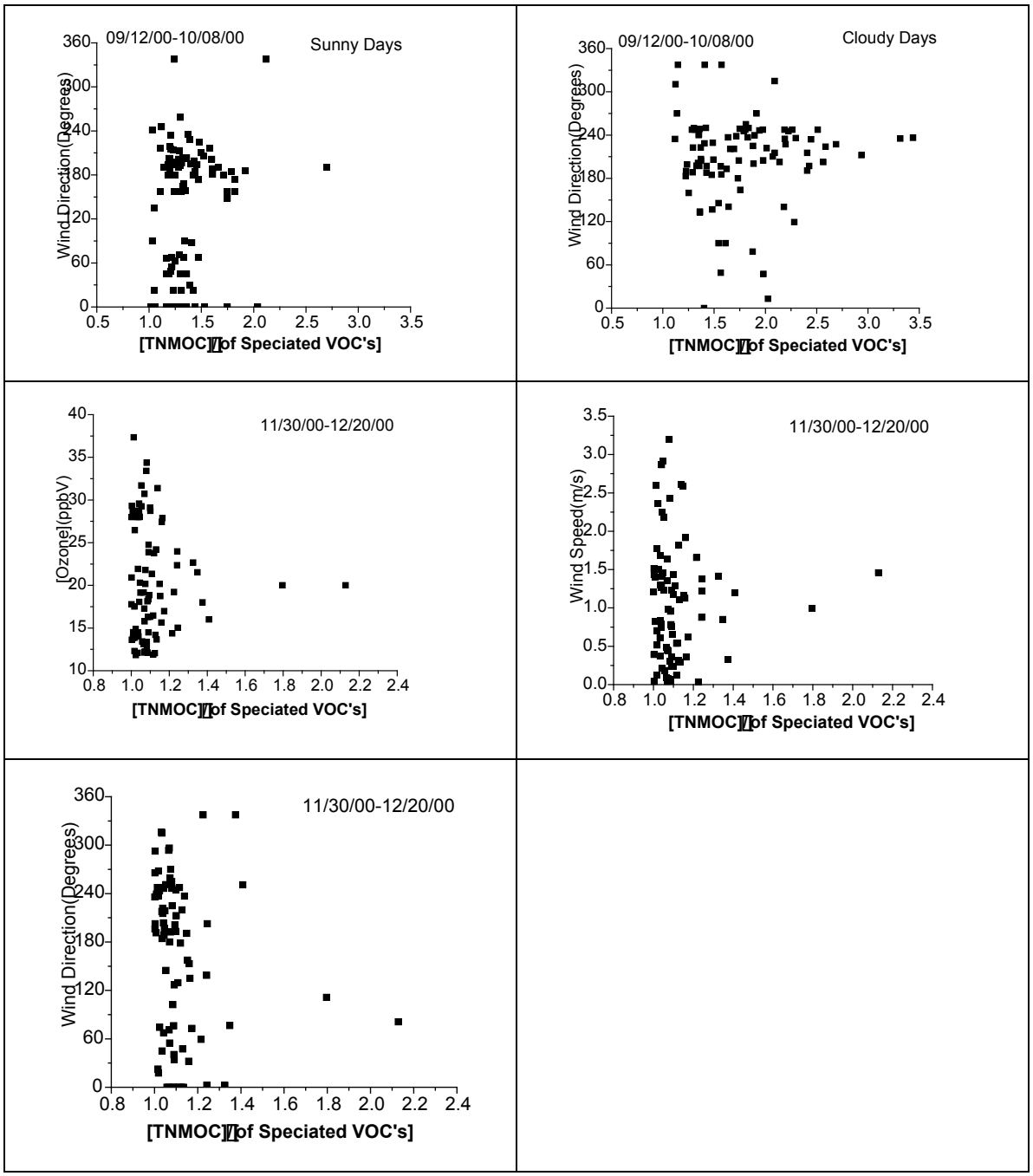

Figure 5.3.3 Correlations between TNMOC/sum of speciated VOC's ratio and O_3, wind direction and wind speed for clear and cloudy days in September-October and all days in November-December.

5.3.4 Nighttime O_3

In the September-October data, there is a correlation between nighttime O_3 and higher TNMOC/sum of speciated VOC's ratios in the early morning, between about 5 and 8 AM before the wind has changed directions and brought significant fresh emissions to the UCLA site. Many of the higher O_3 data correspond to cloudy conditions, and thus may simply represent transport of polluted air. There may also be a contribution from NO_3 chemistry at night. Additionally, examination of the plots in Section 5.2 will show that higher ratios in the winter data, up to 1.4, tend to occur in the early morning, although no correlation between high TNMOC/sum of speciated VOC's ratios and O_3 is observed for this data.

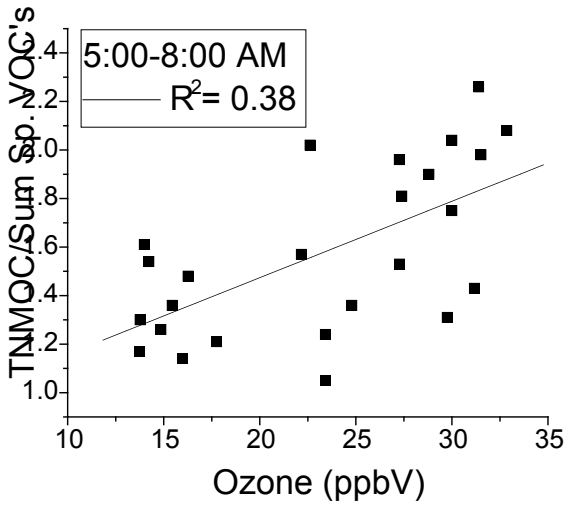

Figure 5.3.4 Relationship between O_3 and TNMOC/sum of speciated VOC's ratio for September-October data collected between 5 and 8 AM.

5.3.5 Aromatic Ratios

Aromatics provide some indication of the photochemical processing of an air mass (see also Section 4). The best aromatic pairs are those that are emitted from the same source at a constant ratio, and for urban air clearly the most robust pair is m&p-xylene/ethylbenzene. This trio of compounds are extremely well correlated with each other (Figure 5.3.5, R^2=0.99). This ratio is not, however, well correlated with the TNMOC/sum of speciated VOC's ratio. The TNMOC/sum of speciated VOC's ratio is better correlated with some of the longer lived aromatics (Tables 5.3.1 and 5.3.2). That the m&p-xylene/ethylbenzene ratio is not well correlated with the quantity of excess TNMOC is not surprising. The TNMOC/sum of speciated VOC's ratio is not well correlated with O_3, while the m&p-xylene/ethylbenzene is correlated with O_3. O_3 has a lifetime in urban air in contact with surface emissions that is similar to the xylenes (several hours, Table 5.3.3), so these two tracers have similar behaviors. More importantly, theory predicts that photochemical processing of fresh emissions should not increase the TNMOC/sum of speciated VOC's ratio much in 4 or 6 hours [50]. Making some assumptions about the OH and O_3 concentrations allows us to calculate the expected degree of increased oxygenation/nitration of the organics. Using the following

assumptions: 1) the average speciated mixture of 100 hydrocarbons from the EPA for 29 cities at 6-9 AM survey [51], 2) rate constants for each hydrocarbon reacting with OH, and for alkenes with ozone, 3) exposure to 0.1 ppt OH and 50 ppbv O_3 for 4 hours, and 4) the following equation:

$$[A]=[A]_0 e^{-(k_A[OH]+k_{O3}[O_3])t}$$

Where A is the concentration of each hydrocarbon, subscript 0 indicates the initial concentration, and k_A and k_{O3} are rate constants with OH and O_3 respectively. Under these conditions, an average of 30% of the hydrocarbons react once with either OH or ozone. Since the organics have an average of 7 carbons [53], and can be expected to add ~1.5 functional groups (primarily alcohol, carbonyl, or nitrate) per reaction, the total mix might increase its heteroatom content relative to the carbon by about 7%. The effect of this modest increase on the TNMOC/sum of speciated VOC's ratio cannot be calculated precisely since the effect of oxygenation/nitration can be to either reduce the FID response or to cause the compound to be lost or broadened in the column so as not to be quantifiable. The latter reduces the sum of speciated VOC's more than the former. It is clear, however, that given the low level of photochemical processing in this data set, the TNMOC/sum of speciated VOC's ratio could be expected to have relatively little dependence on the time of day (above), ozone (Figure 5.3.6), or the ratio of m&p-xylene/ethylbenzene (Figure 5.3.5). Indeed, no trends are observed; each relationship has a correlation coefficient of less than 0.1. We have observed similar results during all of our field measurements including Azusa, Burbank and UCLA during 1999.

Benzene is the longest lived light aromatic (Table 5.3.3), and provides a window into longer timescale processing in the boundary layer. Unfortunately it has multiple sources and different physical properties from many of the other common aromatics. Thus it is not perfectly correlated with the other aromatics; R^2 values are around 0.47. Table 5.3.4 shows that the more poorly pairs of aromatics are correlated with ozone, the more strongly they are correlated with the TNMOC/sum of speciated VOC's ratio. The cloudy day data, which presumably have a greater influence form pollutant carryover due to their much greater mixing heights, generally have lower substituted aromatic/benzene ratios. These correlations indicate that excess TNMOC is associated with air that has been processed for at least a day, and indicates significant influence of carryover emissions.

Table 5.3.3 OH Rate Coefficients and Atmospheric Lifetimes for Common Aromatic Compounds.

Compound	K_{OH} ($\times 10^{-12}$ cm^{3}molecules^{-1}s^{-1})[a]	Atmospheric Lifetime[b]
Benzene	1.23	75 hours
Toluene	5.96	15 hours
Ethylbenzene	7.1	13 hours
m-Xylene	23.6	4 hours
p-Xylene	14.3	6.5 hours
o-Xylene	13.7	6.8 hours

[a]Rate constants with OH radical at 298K [46].

[b]Assuming [OH] = 3×10^6 molecules cm^{-3}, averaged over 24 hours.

Table 5.3.4 Correlation Coefficients for Aromatic Compounds, O_3, and Excess TNMOC.

Aromatic Ratio	R^2 for correlation between aromatics	R^2 for correlation with Ozone	R^2 for correlation with TNMOC/ SP
Ethylbenzene/Benzene	0.48	0.14	0.31
Toluene/Benzene	0.46	0.23	0.27
o-Xylene/Benzene	0.48	0.30	0.26
m,p-Xylene/ Ethylbenzene	0.99	0.48	0.04

Ratio of Toluene to Benzene

Ratio of Ethylbenzene to Benzene

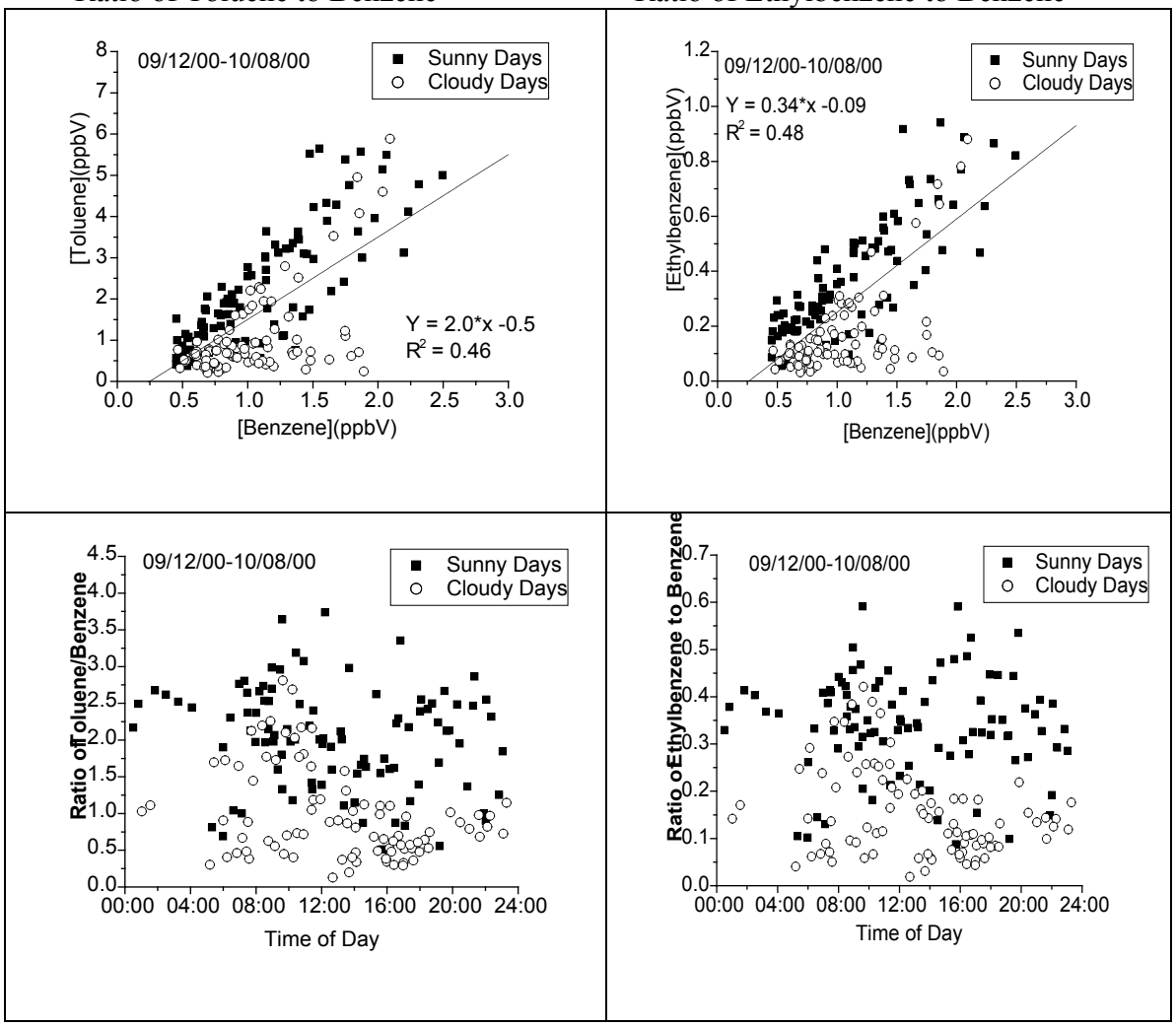

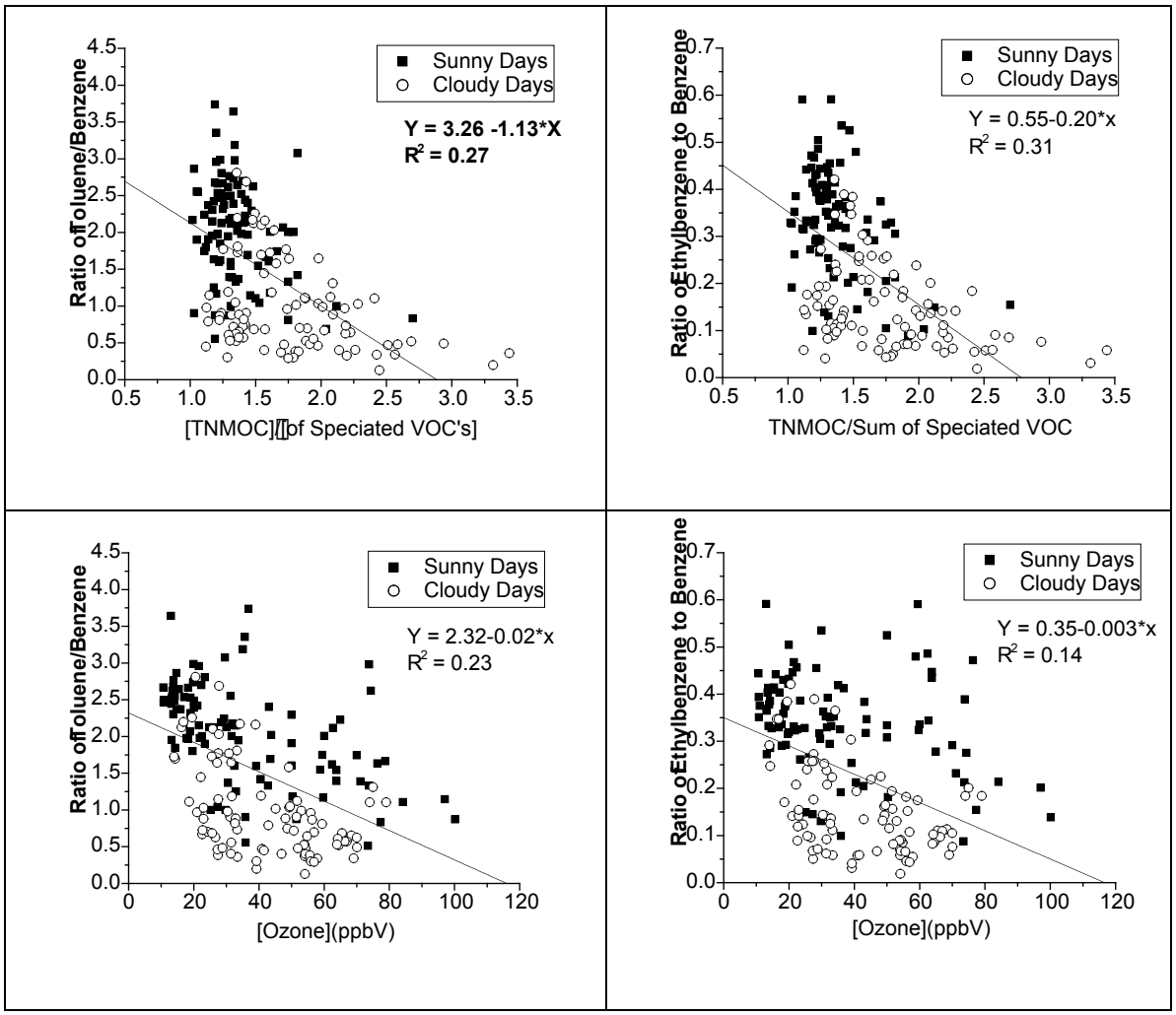

Ratio of o-Xylene to Benzene

Ratio m-p, Xylene to Ethylbenzene

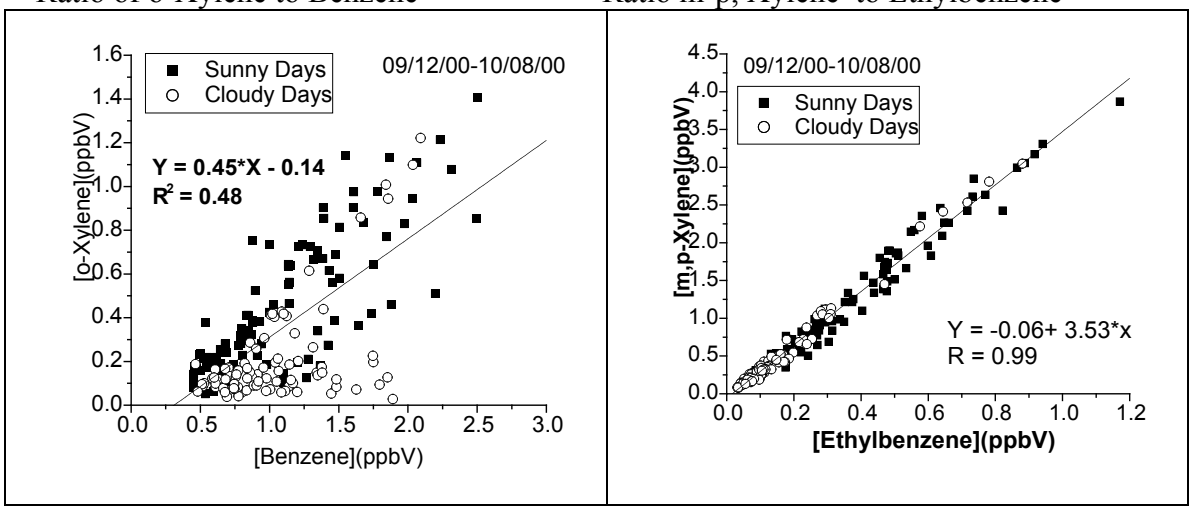

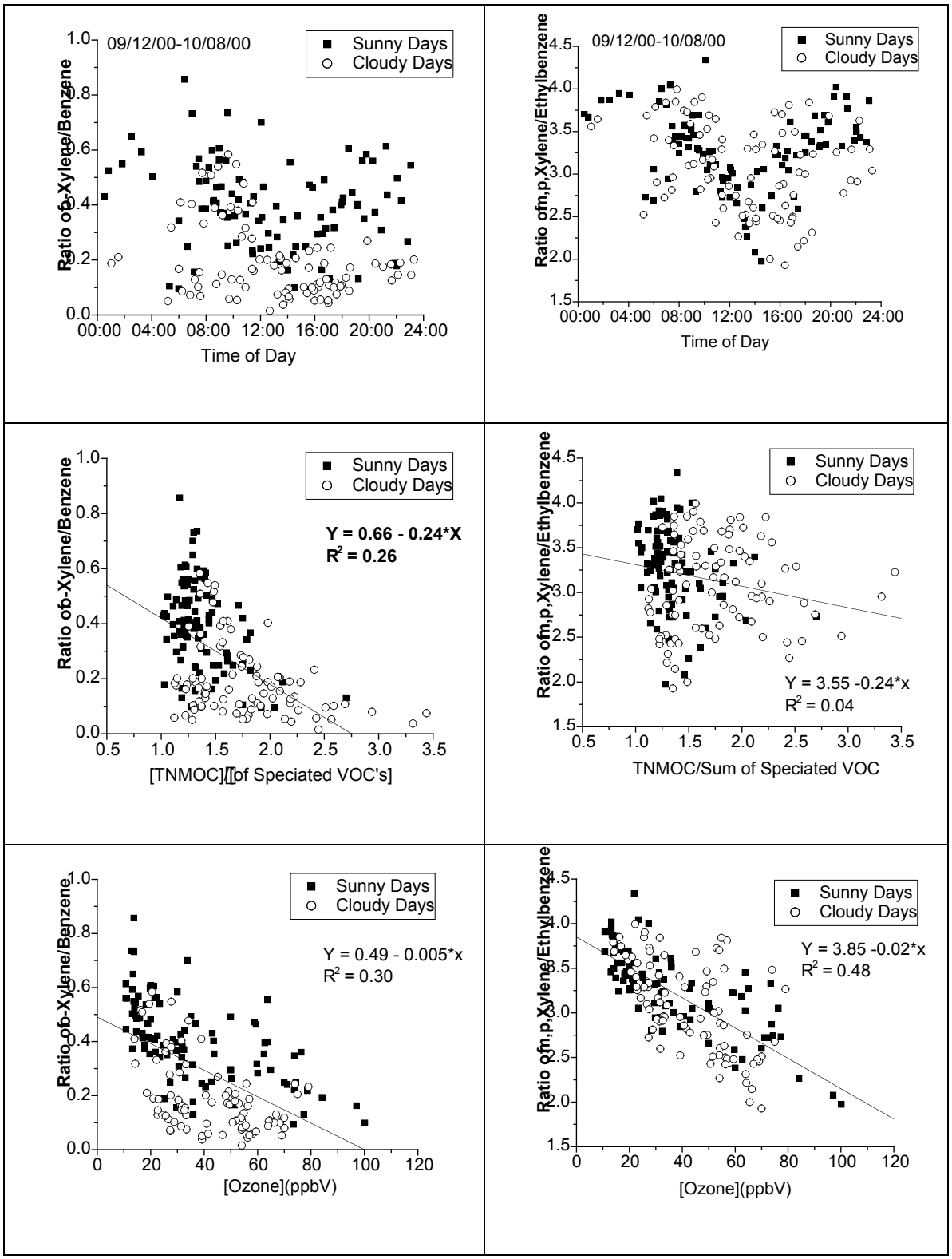

Figure 5.3.5 Correlations for aromatic compounds with themselves, O_3, and Excess TNMOC.

5.3.6 VOC Speciation and [TNMOC]/[SP]

Figure 5.3.6 shows two chromatograms collected on 9/15/00, a clear Friday. The 8:58 chromatogram contained 472 ppbC in the of Speciated VOC's channel and 581 ppbC in the TNMOC channel for a TNMOC/ SP ratio of 1.23. 111 ppbV of NO_x and 20 ppbV of O_3 were measured at this time. 39% of the of Speciated VOC's channel was made up of alkanes, 4% alkenes, 28% aromatics and 7 % oxygenates acetone and propanal. The second chromatogram was collected five and a half hours later at 2:25 PM, and contained 124 ppbC in the of Speciated VOC's channel and 196 ppbC in the TNMOC channel for a TNMOC/ SP ratio of 1.58. 2 ppbV of NO_x and 79 ppbV of O_3 were measured at this time. 40% of the of Speciated VOC's channel was made up of alkanes, 2% alkenes, 19% aromatics and 17 % oxygenates acetone and propanal. Propanal and acetone are the only common oxygenates that we can analyze reliably and which appear consistently in our chromatograms; acetaldehyde and ethanol also occur but the former is difficult to reliably integrate and the latter is not always observed. The later chromatogram contains a much higher fraction of the two oxygenates and a smaller fraction of aromatics. This trend is somewhat reproducible; Figure 5.3.7 shows that the fraction of aromatics do decrease as oxygenates increase, and this phenomenon is correlated with ozone, as shown in Figure 5.3.8 (b). There is a weak correlation between oxygenates and the TNMOC/ SP ratio (Figure 5.3.8 (b)) but no correlation between this ratio and the fraction of aromatics. These figures only contain data the dates shown in Table 5.3.2. This analysis is not quite complete; the other days may well provide a different correlation. Lighter oxygenates such as methanol and formaldehyde are essentially undetected by the FID, but are detected in the TNMOC channel. The oxygen contained in acetone and propanal cannot in and of itself explain much of the difference between the speciated and TNMOC channels; this provides a ratio of 1.08, but additional oxygenated compounds may be expected to increase the ratio somewhat.

Table 5.3.2 Data Analyzed for Oxygenates, Aromatics, Alkanes and Alkenes

Periods	Weather	Days
09/12/00-10/08/00	Clear Days	09/12/00
		09/15/00
		09/16/00
	Cloudy Days	09/19/00
		09/20/00
		09/28/00
		10/08/00
11/30/00-12/20/00		12/06/00
		12/17/00

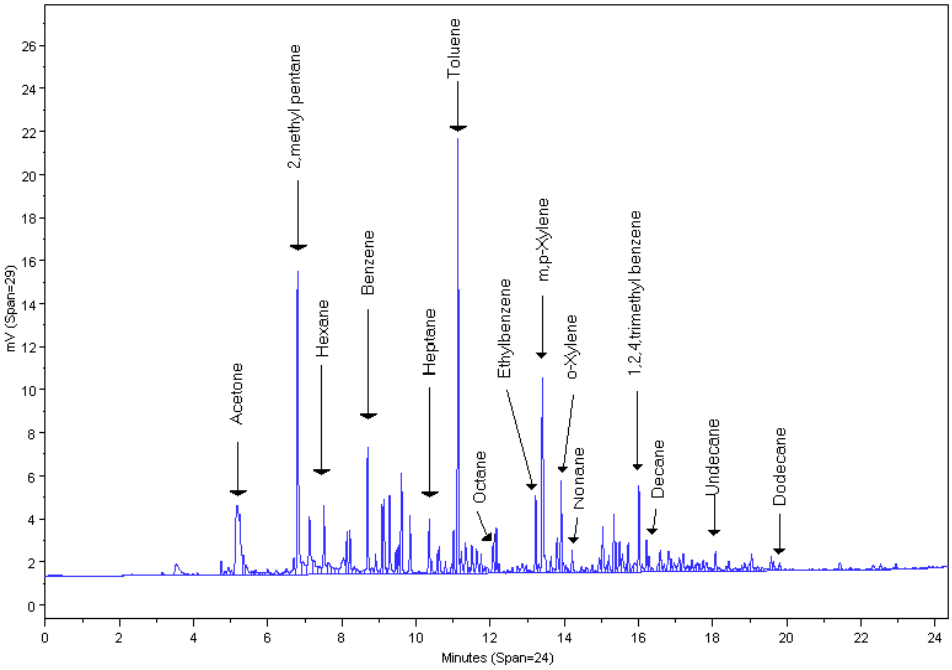
mV (Span=29)
Minutes (Span=24)
Acetone
2,methyl pentane
Hexane
Benzene
Heptane
Toluene
Octane
Ethylbenzene
m,p-Xylene
o-Xylene
Nonane
1,2,4,trimethyl benzene
Decane
Undecane
Dodecane

(a)

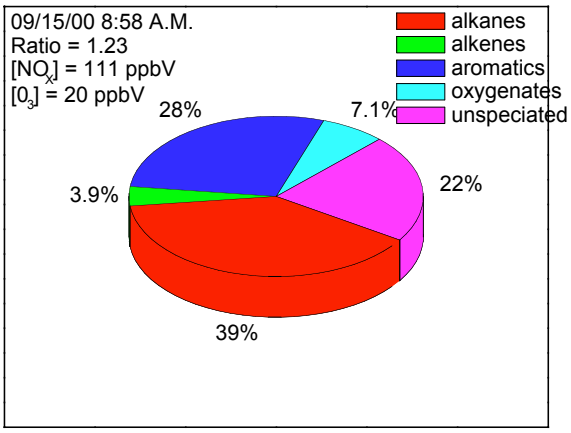
09/15/00 8:58 A.M.
Ratio = 1.23
[NOx] = 111 ppbV
[O3] = 20 ppbV
alkanes
alkenes
aromatics
oxygenates
unspeciated
28%
7.1%
22%
3.9%
39%

(b)

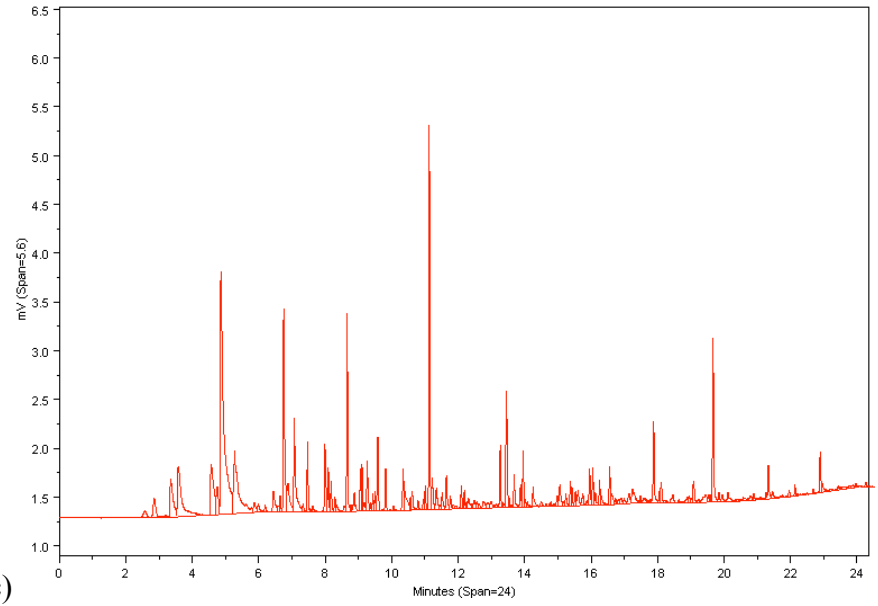

(c)

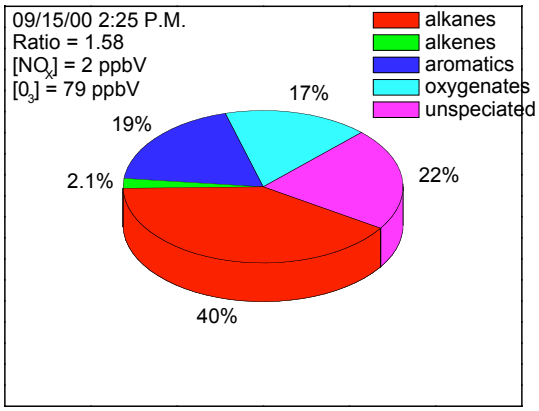

(d)

Figure 5.3.6 a-d. Sample chromatograms and VOC classifications for two measurements on 9/15/00. The two upper plots had sum of speciated VOC's = 472 ppbC, and the lower plots are for sum of speciated VOC's = 124 ppbC.

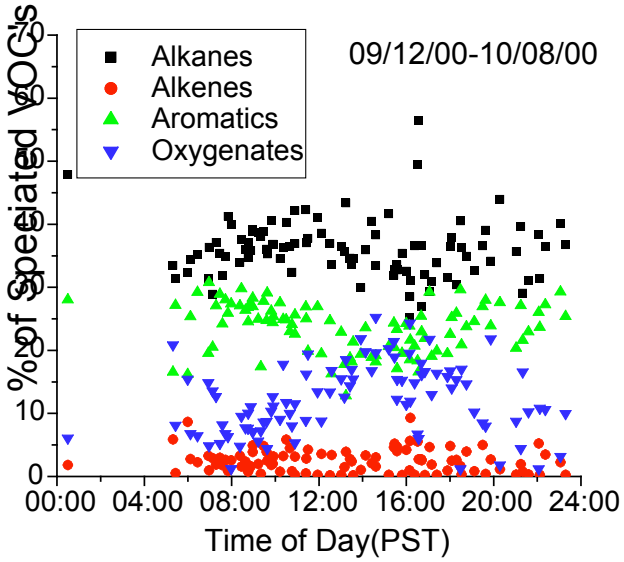

Figure 5.3.7 Evolution of percents of VOC classifications by time of day for high ozone days in Sept. – Oct. 2000.

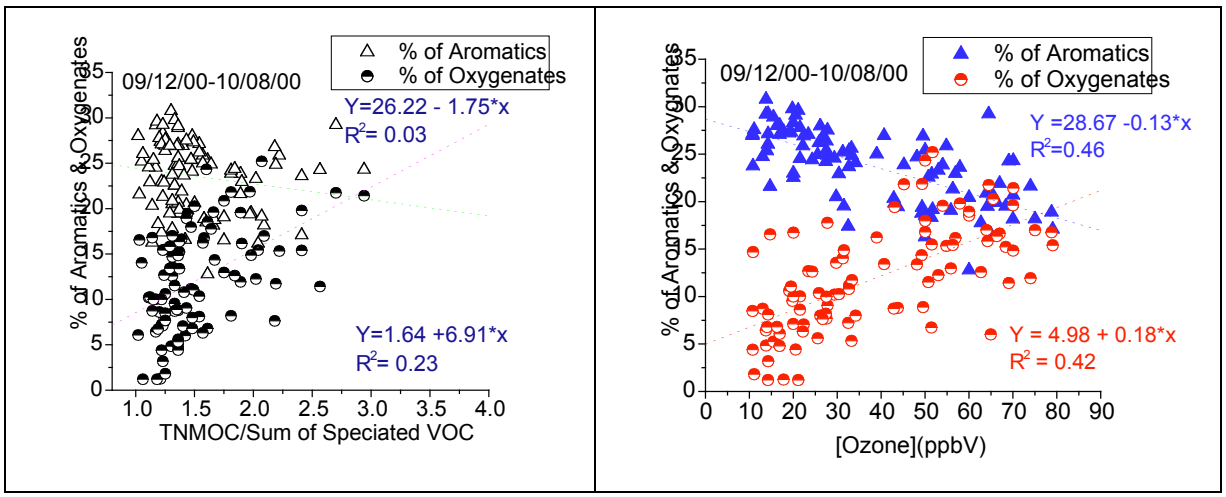

Figure 5.3.8 a) Correlation between percent of aromatics and oxygenates and TNMOC/ sum of speciated VOC's ratio, b) Correlation between percent of aromatics and oxygenates and O_3.

5.3.7 C_2-C_6 Hydrocarbons

Our standard operating procedure involves trapping in Trap 1 at –60°C, a temperature that traps compounds with 5 or fewer carbons at less than 100%. Some samples were collected with trap 1 cooled to –100°C in order to detect C_3-C_5 hydrocarbons. Visual inspection of the chromatograms indicates that for higher TNMOC/sum of speciated VOC's ratios, the quantity of C_3-C_5 hydrocarbons trapped at –100°C tends to be close to C_3-C_5 hydrocarbons trapped at –60°C. At [TC]/[∑SP] ratio

close to 1, C_3-C_5 hydrocarbons detected are mainly alkanes (isopentane, butane, and propane) and carbonyls (acetone, propanal). At [TC]/[SP] ratio higher than 2, carbonyl concentrations increase and alkane concentration decrease, such that the chromatograms at –60°C and –100°C tend to be similar. Figure 5.3.9 shows a negative correlation between the ratio of C_3-C_5 @ -100°C to C_3-C_5 @ -60°C vs. TNMOC/sum of speciated VOC's ratio. This observation is consistent with fairly long time-scale photochemical processing leading to higher TNMOC/sum of speciated VOC's ratios, since alkanes are depleted on timescales of days rather than hours. The oxygenates that are observed with the speciated measurement, acetone, acetaldehyde and propanal, do however build up over timescales of hours.

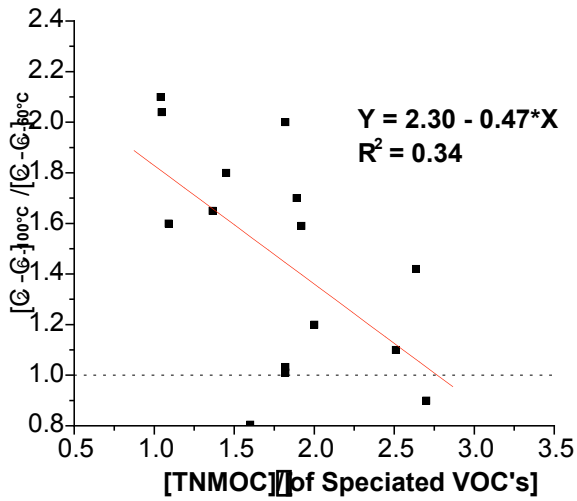

Figure 5.3.9 Ratio of the C_2-C_6 hydrocarbons concentration sampled at –100°C to C_2-C_6 hydrocarbons concentration sampled at –60°C versus TNMOC/sum of speciated VOC's ratio (concentrations are normalized to toluene concentration; each C_2-C_6 hydrocarbon concentration at -60°C is an average of 2 analysis performed before and after the analysis at sampling temperature of –100°C).

5.4 Conclusions

The data presented in this section are the highest quality data we have collected to date and allow a more detailed analysis than do the other data sets. During the September-October smog season, a large fraction of the VOC's at the UCLA site are not measured by the standard GC-FID technique. The unmeasured VOC's averages 30 and 45% of the total airborne organic matter for clear and cloudy days respectively. In wintertime the unmeasured VOC component is much smaller, around 10%. Several lines of evidence point to pollutant carryover as a major source responsible for the unmeasured VOC's. These include the difference between clear and cloudy meteorology--cloudy conditions bring much higher mixing heights than do clear conditions. Higher oxygenates contribute to the higher TNMOC/sum of speciated VOC's ratio chromatograms. Longer lived aromatics and light alkanes are depleted in samples with higher TNMOC/sum of speciated VOC's ratios, while short-lived tracers such as O_3 and fast reacting aromatics

do not have strong positive correlations with the TNMOC/sum of speciated VOC's ratio. High TNMOC/sum of speciated VOC's ratios are positively correlated with O_3 in the early mornings when O_3 is a tracer of transport rather than photochemistry. Although a weekend effect might be expected due to the fact that higher TNMOC/sum of speciated VOC's ratios tend to be associated with lower VOC concentrations, our data does not indicate a weekend effect. This is likely due to the small number of sample days which happened to have somewhat different meteorology.

6. Diesel Bus Study

6.1. Introduction

During the third week of April 2001, we acquired samples at the California Air Resources Board (CARB) Heavy Duty Dynamometer Testing Facility located at the Metropolitan Transit Authority (MTA) Headquarters in downtown Los Angeles. An in-service bus fueled by Arco ECD 1, a low sulfur fuel (less than 5 ppm) that is used in the Los Angeles area was tested. The exhaust of the bus was connected to a constant velocity dilution tunnel. The bus was run on a series of standard drive cycles as well as at idle and in steady state.

This steady state aims to 1) determine the hydrocarbon emissions from heavy-duty diesel running on contemporary fuel, and 2) investigate the source of the excess TNMOC compared to sum of speciated VOC's that is observed in urban air. The ratio of TNMOC/sum of speciated VOC's can be as high as three under some conditions, and averages 1.4 during summer at UCLA. The unmeasured VOC's are either primary or secondary in nature, and diesel, with its large component of semi volatiles and carbonyls [52] [11], is a candidate primary source.

6.2. Sample Collection

The majority of samples were collected via a 10 m□0.25" OD FEP Teflon line heated to approximately 60 °C and equipped with a filter. The 47 mm Teflon filter in a Teflon holder was heated to about 30° C, also with heating tape. Filters were changed every two or three samples. The inlet of the sampling line was connected via a stainless steel reducing union to the dilution tunnel at the same point where samples for most of the particle measurements were withdrawn, located in the middle of the test bay. Flow through the sampling line was maintained at 40 Lpm using a Gast rotary vane pump, resulting in a residence time in the tube of less than 1 s. From this flow 56 mL/min was sampled into the TNMOC instrument.

In parallel with our sample collection, the Emissions Testing Group from CARB-El Monte headed by Dr. Leo Zefonte collected samples in Tedlar bags for light and mid-range hydrocarbon analysis. These samples were collected from a point a few meters up stream from our sample collection point in the dilution tunnel and were passed through a fiber filter before collection. We analyzed two of these bags after the Emissions Group was finished with them, and these results are also discussed below.

6.3. Results and Discussion

The results are divided into four sections; calibration with a CARB hydrocarbon retention time/concentration standard, unburned diesel vapor, *in situ* drive cycle results, and CARB Tedlar bag results.

6.3.1 Calibration Standard

The CARB Emissions Testing Group allowed us to run two samples of their multi-component retention time/calibration standard cylinder from Matheson Gas Products. Results are shown in Table 6.1. Almost all compounds are recovered at the 95%-100% level. Our values for this test cylinder are an average of about 5% lower than the measurement of this cylinder made on 1.23.01 by the CARB Emissions Testing Group. The most likely explanation for this slight bias is a difference in our calibration standards. The second and third columns contain data for a sample that was collected at –60 °C, which is our normal operational temperature. This temperature is chosen so that we do not trap much CO_2 from the sample. Trapping VOC's at –60 °C means that light hydrocarbons are not trapped, and the data in Table 6.1 show this; n-butane and n-pentane are not trapped completely at these temperatures. We ran another sample at –100 °C, and as expected, these two compounds (as well as some of the lighter hydrocarbons not listed) are completely trapped. The other compounds that are not recovered completely are the C_{12} and C_{13} alkanes dodecane and tridecane. Our value for tridecane is nearly identical to that of the CARB Emissions Group measurement [53], indicating that some of the tridecane may be lost in the cylinder or in the regulator. This may also explain the apparent loss of some of the C_{12} compound, although the CARB group measurements returned 105% for this compound. Tests in our laboratory show that n-hexadecane, a C_{16} alkane is recovered completely by our standard procedure.

Table 6.1 Results from CARB Emissions Testing Group Matheson Gas Products (MGPI) Cylinder.

	MPGI Cylinder Concentration	4.20.01, Trap Temperature = -60° C		4.18.01, Trap Temperature = -100° C	
Compound	ppbC	ppbC	Percent Recovery	ppbC	Percent Recovery
n-Butane	1015	894	88	1068	105
n-Pentane	1025	619	60	984	96
n-Hexane	1042	1008	97	1001	96
Benzene	1572	1508	96	1485	94
2,2,4-Methylpentane	1004	965	96	958	95
n-Heptane	1025	974	95	974	95
Toluene	989	965	98	981	99
n-Octane	971	932	96	940	97
m-, p-Xylene	944	943	100	937	99
o- Xylene	931	913	98	920	99
Nonane	975	911	93	931	96
1,2,4-Trimethylbenzene	664	649	98	648	98
Decane	944	897	95	891	94
Undecane	869	833	96	819	94
Dodecane	730	646	88	645	88
Tridecane	431	241	56	350	81

6.3.2.1 Unburned Diesel Fuel

Figure 6.3.1 shows the speciated chromatogram for unburned diesel fuel vapor, and the concentration data for the major peaks is shown in Tables 6.3 and 6.4, last columns. A 0.2 μL volume of ECD1 was evaporated into a 240 L Teflon bag. Because the evaporation vessel and the bag were not heated, it appears that some of the heavier hydrocarbons, larger than C_{11} (the tallest peak, at 33 minutes) were depleted. The heavier alkanes are under represented compared to the drive cycle samples, which likely contain a significant fraction of unburned fuel (Table 6.4 below). As expected [52] the vast majority of the hydrocarbons in diesel vapor fall between C_8 and C_{17} (22 and 49 minutes respectively). The chromatogram derived with our standard ambient air method is very congested due to numerous peaks in this region. This type of chromatogram is particularly difficult to integrate, as the thick "forest" of peaks renders the baseline rather undefined. Of all of the samples we have ever tested, those from unburned diesel are the worst in this respect; typical ambient air chromatograms have nearly flat baselines even under highly polluted conditions. The baseline we used (shown), and was chosen such that the lowest valleys define the baseline. The total carbon channel (not shown) provides a well-defined single peak that introduces relatively little uncertainty, however the speciated integration for diesel has a fairly large error, which renders the TNMOC/μ of speciated VOC's for the unburned diesel samples relatively uncertain.

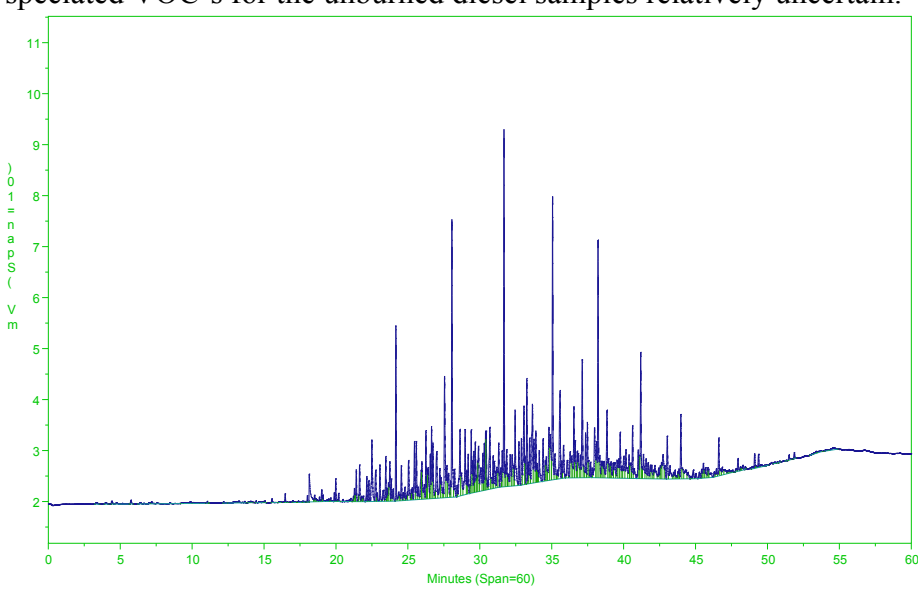

Figure 6.3.1 Unburned diesel vapor chromatogram.

6.3.3 Drive Cycle Results

Table 6.2 provides a summary of the results for the baseline bus tested at MTA. Both direct measurements and the calculated concentration in the exhaust stream after correction for dilution are shown. Because we must subtract CO_2 trapped from the sample from our TNMOC channel results, the CARB staff kindly re-ran each test cycle for us so that we could acquire an additional matched sample necessary to determine the CO_2

background (no oxidation in the TNMOC channel). Precise sampling times and intervals are shown below (Table 6.2). The first day of testing, expecting higher concentrations in the diluted exhaust samples, we used a dilution system. The dilution system did not work properly, and resulted in elevated concentrations in both channels on 4/17/01. Relative values for both TNMOC and Σ of speciated VOC's should be reliable however, since dilution introduces the same conversion factor for both samples. After the initial runs, we did not dilute samples, and believe the concentrations to be reliable.

6.3.3.1 TNMOC and sum of speciated VOC's

Total non-methane organic carbon and the sum of speciated VOC's are shown in Table 6.2. The sum of speciated VOC's is calculated by taking the sum of all peaks recognized by the integration program, after adjusting the baseline by hand as described in Section 4.2 above. The raw measurements were converted to concentrations in the exhaust stream using dilution factors provided by Dr. Zafonte, and the measured tunnel blanks.

Table 6.2 Summary of TNMOC and sum of speciated VOC's measurements from the 1998 New Flyer Transit Bus, MTA#3007; Detroit Diesel EC50 Engine; License#1017104, running with ECD1 fuel, tested at the CARB Heavy Duty Diesel Testing Facility located at the MTA in downtown Los Angeles.

Date 2001	Time Begin	Sample Interval (Min.)	Drive Cycle	TNMOC (ppmC)	Corrected[1] TNMOC (ppmC)	Σ Sp. VOC's (ppmC)	Corrected[1] Σ Sp. VOC's (ppmC)	Raw Ratio[2]	Corrected[1] Ratio[2]
4/17	2:01 P	18	Tunnel blank[3]	-	-	-	-	1.29	-
4/17	3:31P	18	Idle 1[3]	-	-	-	-	1.62	-
4/17	4:58 P	17:44	Idle 2[3]	-	-	-	-	1.34	-
4/18	5:44 P	12	Steady State[3]	-	-	-	-	1.60	1.60[4]
4/18	2:24 P	10	New York	0.86	26.4	0.73	25.7	1.17	1.03
4/18	4:50 P	5	Tunnel blank	0.31	-	0.20	-	1.55	-
4/19	10:40	17:40	UDDS 1	1.03	25.3	0.92	23.0	1.12	1.10
4/19	2:28 P	17:40	UDDS 2	0.76	17.4	0.64	14.4	1.20	1.21
4/19	3:50 P	17:40	Tunnel blank	0.19	-	0.16	-	1.19	-
4/20	10:57	18:57	CBD 1	0.81	19.3	0.71	18.5	1.15	1.04
4/20	1:50 P	18	CBD 2	0.79	18.6	0.61	15.5	1.30	1.20
4/20	4:25 P	9:30	Tunnel blank	0.19	-	0.10	-	1.81	-
5/20	-	-	Diesel fuel 1	-	-	-	-	1.44	-
5/20	-	-	Diesel fuel 2	-	-	-	-	1.39	-
	Average (Excluding Tunnel Blanks, Idle cycles, and Diesel Fuel)							1.26	1.20

[1]Corrected for the tunnel blank that was measured on the same day, and for the dilution factor as provided in the file HDETL GC Test Log-2R0102 provided by Dr. Zafonte.

[2] The dominant source of uncertainty in these ratios is the integration of the speciated chromatogram, as discussed above. Because we have made a conservative (high) estimate of the concentration of the sum of speciated VOC's, the ratios should be considered lower limits. The average corrected ratio (last line) could be as high as 1.4. Other sources of uncertainty include the tunnel blank, which contributes a larger than anticipated uncertainty due to the high dilution rates.

[3]No absolute concentrations are reported for these runs because we were using a dilution system that was not functioning properly. Because the samples for TNMOC and speciated VOC's are drawn in parallel from the same point in the diluted air stream, the relative quantities of TNMOC and Sum of speciated VOC's remain accurate.

[4]Because this run had a relatively low dilution factor (12 vs. 30-50 for the other runs), the correction for the tunnel blank is negligible.

In general, the excess VOC's; the material collected by the TNMOC channel but not by the speciated channel, is small, thus the TNMOC/Σ sp. VOC's ratios (last two columns, Table 6.2) are quite close to one. The only exception is the steady-state test, for which only about 60% of the VOC's made it through the column to be quantified by the FID. The idle ratios are higher, but because these tests had particularly high dilution rates, the ratios likely represent dilution air rather than the diesel exhaust [53]. All of the TNMOC/Σ sp. VOC's ratios should be considered lower limits because we set our speciated chromatogram baselines rather low, so as to maximize this value and make a conservative estimate of the unmeasured VOC's. It should also be emphasized that our inlet is designed with minimizing losses of semi-volatile VOC's as a primary focus, and we recover hydrocarbons up to C_{16} well. A GC with a different inlet may not be as successful in recovering as much semi-volatiles VOC's in the speciated channel.

6.3.2.3 Speciated Hydrocarbon Concentrations

Table 6.3 shows the speciated hydrocarbon concentrations for the five test cycle samples collected between 4/18 and 4/20. Both the actual concentrations in the sample, labeled "direct", and the calculated concentration in the exhaust stream, after correction for the tunnel blank (Table 6.4) for that day and the dilution factor ("corr.") are shown. Calculated concentrations in the exhaust stream below 50 ppbC, are not reported. The identified VOC's are between 23 and 33% of the TNMOC levels (Table 6.1). This is reasonable because we have a limited capability to identify peaks, reporting only simple alkanes and aromatics plus acetone. Diesel exhaust contains significant fractions of carbonyls, complex branched alkanes and aromatics [52]. Also shown in Table 6.3 are results from two samples of unburned diesel fuel vapor (Figure 6.3.1).

The speciated tunnel blank data from 4/18-4/20 are shown in Table 6.4. The three tunnel blank samples indicate that the individual hydrocarbon concentrations in the dilution air were fairly variable. To the degree that the single samples are not representative of the dilution air over the course of the day, some additional uncertainly is introduced to the results. The tunnel blank dilution air is primarily ambient air, which typically has decreasing hydrocarbon levels throughout the day. Because the tunnel blank samples were collected at the end of each day, they may have underestimated the late morning and early afternoon levels. This might also explain a portion of the difference between the first and second UDDS and CBD test cycles on 4/19 and 4/20. In both cases, the first test cycle has both a higher TNMOC concentration and a relatively larger contribution from light compounds C_8 or less (Tables 6.3 and 6.5).

Table 6.5 shows the relative abundances of speciated hydrocarbons in each sample; all peaks were normalized to the decane peak, one of the primary diesel fuel constituents. This Table includes data from several additional tests, including the idle and steady state cycles. The idle and first steady state cycles were not included in Table 6.3 because of the dilution system discussed above. The steady state test conducted on 4/23 is not included because we do not know the dilution factor for that day. As expected, the diesel vapors contain little carbon lighter than C_8, while the drive cycle results indicate significant contributions from lighter hydrocarbons, which comprise 20 to 50% of the total. The tunnel blanks (second column, and Table 6.4) consist almost entirely of VOC's smaller than C_8. Consistent with a possible under correction for the contribution of light

hydrocarbons from the dilution air (above), the earlier UDDS and CBD samples are more enriched in the light VOC's than are the later replicates. With the exception of the two idle runs, the contributions of light vs. heavy hydrocarbons (with an arbitrary cutoff at octane) are not very reproducible.

Table 6.3 Speciated Hydrocarbon Concentrations in Diesel Exhaust Samples

Test Cycle	**New York**		**UDDS 1**		**UDDS 2**		**CBD 1**		**CBD 2**		**Diesel Fuel**	**Diesel Fuel**
Date	**4/18**		**4/19**		**4/19**		**4/20**		**4/20**		**5/16**	**5/16**
Cutoff (ppbC)[1]		*75*		*50*		*50*		*50*		*50*		
	Concentration (ppbC)											
	Direct	Corr.[2]	Direct	Corr.[2]	Direct	Corr.[2]	Direct	Corr.[2]	Direct	Corr.[2]	**Vapor**	**In bag**
Acetone +	30.7	1475	47.4	1130	26.6	518	29.51	708	19.21	391	1.3	1.2
Pentane	11.2	536									1.8	1.6
Cyclopentane	2.0	95	2.9	85			1.7	53			1.1	1.0
2-Methylpentane	5.1	246	23.1	574	7.3	105	9.1	289			2.3	1.4
3-Methylpentane			11.4	248	7.4	131	7.0	224	1.5	50	1.0	0.7
Hexane	4.3	204	7.0	120			6.4	157			1.4	0.6
Methylcyclopentane	6.5	314	8.1	104			4.7	151	2.4	80		0.7
Benzene	18.9	907	24.5	543	21.1	448	22.1	541	20.7	510	0.6	1.5
Cyclohexane	2.6	124	3.7	69			6.6	210			0.6	0.7
3-Methylhexane			4.1	77			1.6	52				
2,2,4,trimethylpentane	2.3	110	6.2	135			3.8	123				0.7
heptane	1.9	91	4.2	79			2.8	89	2.1	69		0.7
methylcyclohexane			8.7	163			3.3	106			1.4	1.4
toluene	25.2	659	26.2	428			3.3	107	1.7	58	3.6	3.3
2,methylheptane			2.6	71			12.4	190			2.4	2.2
Octane	2.7	130	4.4	106	2.6	55	3.3	105	2.5	81	7.7	7.5
ethyl benzene	2.0	95	3.8	57			2.1	66	2.6	85	10.5	10.5
m,p,xylene	8.1	268	11.6	266	6.5	117	6.9	219	5.6	186	36.5	36.5
o,xylene			5.7	142	2.6	51	3.6	114	2.5	82	17.7	17.5
nonane	8.8	421	12.7	369	10.3	303	11.1	353	10.9	359	58.0	58.2
1,3,5,trimethylbenzene			2.4	73	1.7	52	1.7	54			16.7	17.0
1,2,4,trimethylbenzene	5.7	272	9.3	277	6.9	210	6.2	198	6.4	212	58.3	58.7
decane	13.2	636	18.6	554	17.3	525	16.1	515	19.0	624	106.9	106.6
Undecane	12.8	612	24.4	726	19.2	581	15.7	500	19.8	651	127.9	128.2
dodecane	10.3	494	16.5	492	14.0	423	13.1	418	16.6	548	104.7	104.7
tridecane	9.0	430	16.5	490	11.6	351	13.5	432	14.1	465	87.6	88.6
tetradecane	7.5	360	15.5	463	9.3	282	9.4	301	11.0	362	62.0	49.4
pentadecane	6.7	322	16.7	496	8.0	242	8.7	278	9.9	324	39.0	28.2
hexadecane	12.2	585	10.3	278	3.9	88	6.7	214	6.1	199		17.0
Dilution Factor	**48.0**		**29.8**		**30.3**		**31.9**		**32.9**			

[1]Peaks with areas that resulted in corrected concentrations in the exhaust stream of less than 50 or 75 ppbC are not reported.

[2]These values are corrected for the tunnel blank collected on the same day (Table 6.3), and the dilution factor.

[3]Acetone tails somewhat and at a least two other compounds come out on the tail. We have attempted to remove these from the integration, but acetone is particularly prone to interferences of this type. This peak was not corrected for its reduced FID response factor.

Table 6.4 Tunnel blank results for 4/18-4/20

Tunnel Blank	4/18	4/19	4/20
acetone		9.8	7.5
2-methylpentane		3.9	
3,methylpentane	14.6	3.2	
hexane	0.9	3.1	1.5
Methylcyclopentane		4.8	
2,4,dimethylpentane		1.2	
benzene		6.6	5.3
cyclohexane		1.5	
2,methylhexane		1.6	
3,methylhexane		1.6	
2,2,4,trimethylpentane		1.7	
heptane		1.6	
methylcyclohexane		3.3	
toluene	11.7	12.2	6.6
2,methylheptane		0.3	
3,methylheptane		0.4	
Octane		0.8	
ethyl benzene	1.1	2.0	
m,p,xylene	2.6	2.7	
o,xylene	2.2	0.9	
Nonane		0.3	
hexadecane		1.0	

Table 6.5 Speciated Hydrocarbon Concentrations Normalized to Decane

Test Cycle	Tunnel blank	Idle 2	Idle 2	Steady State 1	New York	UDDS 1	UDDS 2	CBD 1	CBD 2	Steady State 2	Diesel 1	Diesel 2
Date	4/17	4/17	4/17	4/18	4/18	4/19	4/19	4/20	4/20	4/23	5/16	5/16
acetone	825	113	156	151	232	204	99	138	63	79	1	1
pentane	583	96	100	35	84					25	2	1
Cyclopentane	72	10		11	15	15		10		5	1	1
2,methylpentane	388	25	27	59	39	104	20	56		14	2	1
3-methylpentane	122	8	11	42		45	25	44	8	18	1	1
hexane	181	8	14	64	32	22		31		12	1	1
Methylcyclopentane	105	9	23	50	49	19		29	13	19		1
benzene	382	89	95	146	143	98	85	105	82	91	1	1
cyclohexane	54	3	4	23	20	12		41		10	1	1
3,methylhexane	137	5	4	24	0	14		10		6		0
2,2,4,trimethylpentane	209	15	17	51	17	24		24		8		1
heptane	95	7	12	36	14	14		17	11	7		1
methylcyclohexane	193	23	19	40	0	30		21		10	1	1
toluene	640	63	72	173	104	77		21	9	44	3	3
2,methylheptane	94	6	22	31		13		37		0	2	2
Octane	127	21	101	64	20	19	10	20	13	10	7	7
ethyl benzene	115	22	25	37	15	10		13	14	7	10	10
m,p,xylene	323	63	67	107	42	48	22	42	30	29	34	34
o,xylene	163	32	36	59		26	10	22	13	30	17	16
Nonane	145	59	71	101	66	67	58	69	57	76	54	55
1,3,5-trimethylbenzene	53	21	18	25		13	10	11		0	16	16
1,2,4-trimethylbenzene	174	102	72	87	43	50	40	38	34	31	55	55
decane	100	100	100	100	100	100	100	100	100	100	100	100
Undecane	705	99	138	155	96	131	111	97	104	93	120	120
dodecane		126	107	103	78	89	81	81	88	78	98	98
tridecane			102	112	68	89	67	84	74	53	82	83
tetradecane			104	412	57	84	54	59	58	49	58	46
pentadecane			161	96	51	90	46	54	52	61	36	26
hexadecane				78	92	50	17	42	32	38	0	16

6.3.4 Tedlar Bag Measurements

We made several analyses of the UDDS 1 test cycle collected by the CARB Emissions Testing Group in a Tedlar bag on 4.18.01. These are summarized in Table 6.6. Our initial intent was to analyze all of the bag samples in the week following their collection, but the samples were found to be too unstable (below).

Table 6.6 Summary of UDDS Tedlar bag and *in situ* analyses, shown in Figure 6.3.2.

Sample	Sample	Fill	Age	Bag Temperature	sum of speciated VOC's (ppbC)
In-situ	UDDS-I	Exhaust 4.19.01	10 minute sample	--	843
Bag	UDDS-I	Exhaust 4.19.01	7 hrs	~ 25° C	1140
Bag	UDDS-I	″	8 hrs	Heated to 60°C	1250
Bag	UDDS-I	″	6 days	Heated to 60°C	2070
Bag	Blank	Nitrogen	1 week	Heated to 60°C	

The UDDS bag sample was analyzed three times: the first time without heating as soon as it became available (7 hours after collection and immediately after CARB analyzed it), and then subsequently with heating 8 hours after collection, and again 6 days later (Figure 6.3.2b-d). Figure 6.3.2a shows the results of our sample collected through our "*in situ*" sample line in parallel with the bag sample (during the UDDS cycle). The general shape of the chromatograms in Figures 6.3.2a. and 6.3.2b. (fresh, unheated bag) is in good agreement, however the total of the *in-situ* measurement is only about 74% of those from the bag. The *in-situ* chromatogram is uniformly smaller, except that the C_{14} and larger hydrocarbons are recovered somewhat more successfully with the *in-situ* sample than the unheated bag. Heating this bag, Figure 6.3.2c., results in much larger peaks, especially at the heavy end, above C_9. Unless these compounds are somehow lost between the two sampling points, which seems unlikely, it seems that some of the compounds are lost in our sampling line, most likely on our filter. The light hydrocarbons, before C_9 at 24 min, are reasonably well behaved; in particular heating the bag makes little difference in this area of the chromatogram. Figure 6.3.2-d, which shows the chromatogram that resulted after allowing the bag to sit for 6 days, shows many *new* peaks. A possible explanation for this phenomenon is reactions in the bag. NO_x concentrations in the samples were very high, and nitric acid was measured in the bags collected under similar conditions, possibly indicative of OH in the bags [53].

Figure 6.3.3 shows the result for the bag blank, run 4. This bag, filled with N_2, revealed one very large peak at about 27 minutes, together with a number of smaller peaks primarily in the 28-47 minute range. The very large peak is not observed in the bag samples; we have no explanation for this behavior.

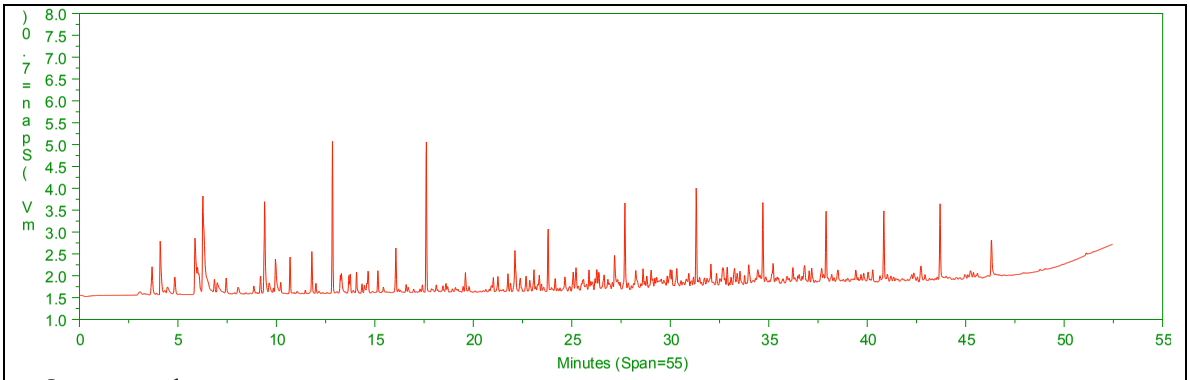

a. *In situ* sample.

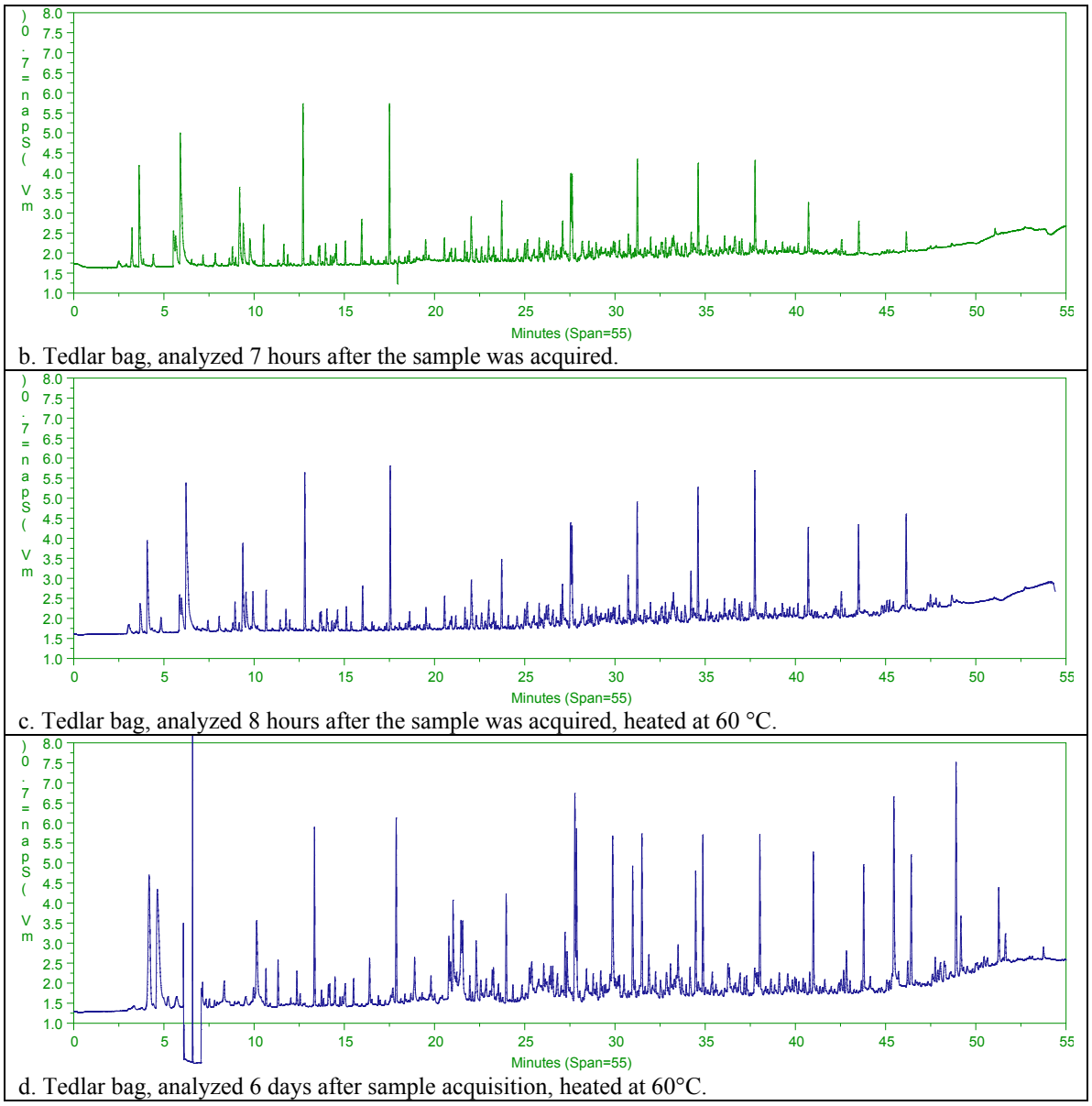

b. Tedlar bag, analyzed 7 hours after the sample was acquired.

c. Tedlar bag, analyzed 8 hours after the sample was acquired, heated at 60 °C.

d. Tedlar bag, analyzed 6 days after sample acquisition, heated at 60°C.

Figure 6.3.2 Chromatograms from Urban Dynamometer Driving Schedule 1 collected on 4.19.01; real time sample (panel a), Tedlar bag sample (panels b-d).

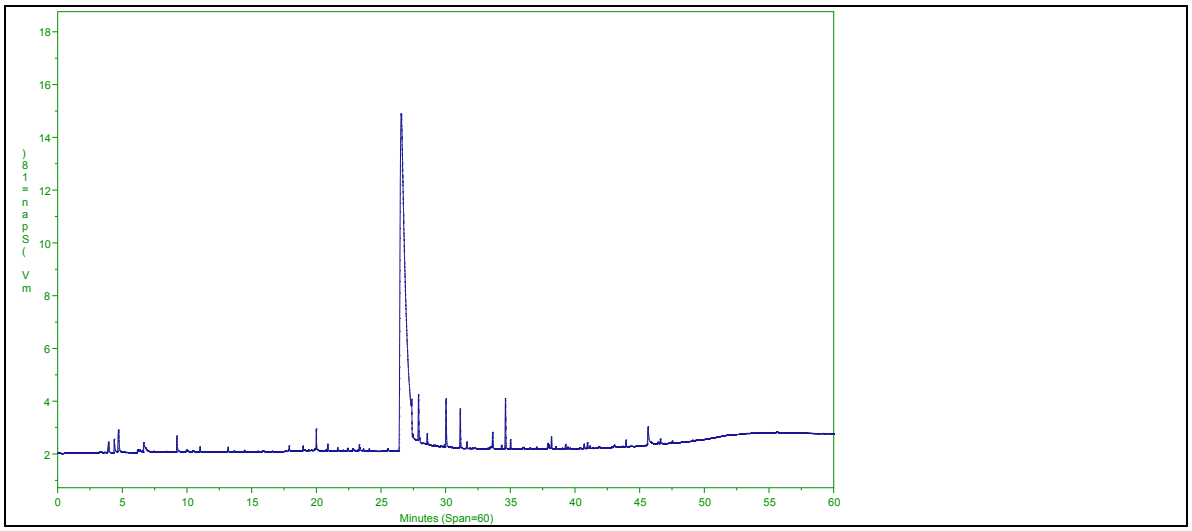

Figure 6.3.3 Bag blank (1) chromatogram. This was an empty bag filled with N_2 by the emissions group. It was measured 1 week after it was filled and was heated to 60°C during sampling.

6.4 Conclusions

- A future study of this type would be improved by: lower exhaust dilution rates, better sampling acquisition protocols for recovering semi-volatiles, a longer chromatographic method designed to separate heavy hydrocarbons, and more replicates.

- While there are several sources of uncertainty in this study, we conclude that diesel exhaust is not able to explain much of the excess TNMOC observed in ambient air, for three reasons: a. diesels make a modest contribution to total VOC's, b. the ratio we measured was only somewhat greater than 1.0, and c. the conclusion is consistent with our field measurements. The most important factor is that diesel contributes less than 10% of VOC's in urban air; often much less. For example, at Azusa during summer 2000 and 2001 field studies, the Desert Research Institute apportioned between 0.7 and 7% of NMHC's to diesel exhaust [54]. On freeways with heavy truck traffic the contribution of diesel exhaust to NMHC's during the same period was still only 27% [54]. To make a convincing case that diesel contributes significantly to the excess VOC's, given its small contribution to the overall NMHC loadings, it would need to register a large quantity of excess VOC's, which it did not.

  A minor additional point is that while the average TNMOC/sum of speciated VOC's ratio was 1.2, 5 of 6 of the tests returned ratios between 1.03 and 1.20, with an average of 1.12, while one test had a much higher ratio, of 1.6. We have no reason to exclude the high value, however the data suggest that the average of 1.2 may have been somewhat positively skewed. We reiterate however that this conclusion should be regarded as tentative, primarily due to the ambiguous integration of the speciated chromatograms and the loss of

semivolatile hydrocarbons in PAMS type GC's. Our instrument likely detects more semivolatile hydrocarbons in the speciated channel as well as the TNMOC channel than instruments designed for the C_2-C_{10} hydrocarbons. Even so, since the contribution of diesel to total VOC's is so small, it is unlikely that the TNMOC/sum of speciated VOC's ratio could be large enough that diesel could be a large contributor to the excess VOC's observed in urban air under photochemically active conditions.

Finally, the observation that diesel exhaust does not make a large contribution to excess VOC's is consistent with our field data. The diesel contribution has a much smaller seasonal variation than does photochemistry, and thus could not explain the TNMOC/sum of speciated VOC's ratios observed at UCLA during summer and ratios close to 1.0 for UCLA during December. The site that likely has the largest contribution from diesel is Burbank due to its close proximity to freeways and local truck traffic. This site also has an average TNMOC/sum of speciated VOC's ratio of only 1.11 during the summer.

7. Gasoline Vapor

Chevron regular unleaded gasoline was purchased in a gas station in Westwood. Small quantities of gasoline were injected into the 240L Teflon bag while zero grade air was filling in the bag. Three measurements were made for each bag. The results indicate that, as might be expected, the speciated channel does a good job of measuring VOC's in gasoline vapor; the average ratio is 1.06. PAMS and GC measurements were designed to effectively measure morning emissions, of which gasoline vapor is a major component, thus it is not surprising that the speciated GC approach works well on this type of sample.

Table 7.1 Gasoline Vapor Measurements

Experiment	Volume of Gasoline Liquid(μL) in 240L	[TNMOC](ppbC) ± SD	[Σ Speciated VOC's](ppbC) ± SD	[TNMOC]/ [Σ Speciated VOC's] ± SD
Exp 1	3	10291 ± 49	9985 ± 39	1.031 ± 0.004
Exp 2	1	4919 ± 204	4569 ± 174	1.076 ± 0.004
Exp 3	1	3779 ± 0	3499 ± 56	1.08 ± 0.02

Retention Indices were calculated by following equation based on **Kovats index** which is a logarithmic scale on which the adjusted retention time of a peak is compared with those of linear alkanes. The Kovats index, *I*, for the unknown is calculated from the formula:

$$I = 100\left[n + (N - n)\frac{\log t_r'(unknown) - \log t_r'}{\log t_r'(N) - \log t_r'(n)}\right]$$

Where n is the number of carbon atoms in the *smaller* alkane

N is the number of carbon atoms in the *larger* alkane

t'_r (n) is the adjusted retention time of the *smaller* alkane

t'_r (N) is the adjusted retention time of the *larger* alkane

This definition makes the Kovats index for a linear alkane equal to 100 times the number of carbon atoms. For octane $\underline{I}$ = 800, and for nonane $\underline{I}$ = 900. A sample chromatogram and the resulting peak identities and quantification are shown in Figure 7.1 and Table 7.2.

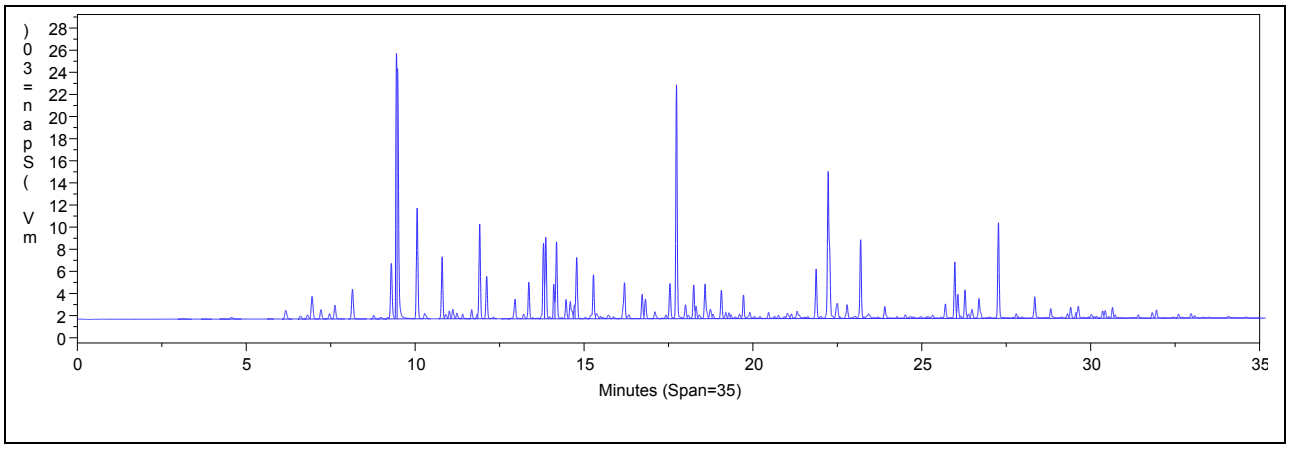

Figure 7.1 Gasoline vapor chromatogram.

Table 7.2 Peak Identification

Gasoline liquid 3ul, Oven temperature program:5°C/min				
Peak Number	*Retention time (min)*	*Name*	*Retention Index*	*Concentration (ppbC)*
1	3.134			4.90
2	3.81			1.85
3	4.259			2.55
4	4.426			1.94
5	4.557	butane	400.00	10.68
6	5.719		453.83	1.43
7	6.17	2.methylbutane	471.82	40.18
8	6.605	1-pentene	487.97	12.46
9	6.817		495.45	17.16
10	6.949	pentane	500.00	94.86
11	7.212	trans-2-pentene	508.42	36.52
12	7.465		516.24	21.42
13	7.627	2. methyl-2-butene	521.11	53.14
14	8.145	2, 2, dimethylbutane	536.01	118.83
15	8.776		552.94	12.90
16	8.996		558.55	8.39
17	9.191	cyclopentane	563.41	5.29
18	9.295	2, 3, dimethylbutane	565.97	207.42
19	9.447	MTBE	569.65	710.14
20	9.477	2.methylpentane	570.36	770.00
21	10.06	3-methylpentane	583.90	377.17
22	10.281	1-hexene	588.83	25.75
23	10.8	hexane	600.00	197.54
24	10.905		602.79	17.12
25	11.013	trans-2-hexene	605.63	24.53
26	11.114	3-methyl-trans-2-pentene	608.26	34.82
27	11.235	2-methyl-2-pentene	611.38	21.05
28	11.407	cis-2-hexene	615.76	14.94
29	11.674	3-methyl-cis-2-pentene	622.43	28.33
30	11.838		626.45	12.40
31	11.912	methylcyclopentane	628.24	306.37
32	12.118	2,4,dimethylpentane	633.18	143.00
33	12.323		638.02	6.66
34	12.661		645.82	1.33
35	12.958	benzene	652.50	77.92
36	13.214		658.14	17.12
37	13.366	cyclohexane	661.43	118.15
38	13.481		663.90	4.71
39	13.625		666.96	2.61
40	13.8	2methylhexane	670.64	246.65
41	13.868	2,3,dimethylpentane	672.06	260.95
42	13.985		674.48	7.09
43	14.103		676.90	102.01
44	14.186	3,methylhexane	678.59	258.63
45	14.345		681.80	4.59
46	14.468	cis, 1,3,dimethylcyclopentane	684.26	61.57
47	14.594	trans-1-3-dimethylcyclopentane	686.76	77.85
48	14.719		689.22	37.46
49	14.783	2,2,4,trimethylpentane	690.47	215.10
50	15.043		695.50	5.17
51	15.28	heptane	700.00	152.45
52	15.369		702.28	23.73
53	15.493		705.43	7.23
54	15.571		707.40	4.59
55	15.721		711.15	16.70

56	15.872	714.90	8.50
57	16.198 methylcyclohexane	722.87	146.20
58	16.329	726.03	17.53
59	16.532	730.87	2.00
60	16.722 2,5,dimethylhexane	735.35	82.00
61	16.819 2,4,dimethylhexane	737.62	68.10
62	17.099 1,2,4,trimethylcyclopentane	744.09	28.67
63	17.331	749.38	2.26
64	17.426	751.52	12.68
65	17.544 2,3,4,trimethylpentane	754.16	124.72
66	17.737 toluene	758.45	736.40
67	18.004 2,3,dimethylhexane	764.31	50.71
68	18.085	766.07	13.93
69	18.247 2,methylheptane	769.57	110.94
70	18.317	771.07	37.73
71	18.413	773.12	16.35
72	18.583 3,methylheptane	776.72	132.98
73	18.74	780.02	37.93
74	18.819	781.67	15.26
75	19.066 2,2,5,-trimethylhexane	786.78	97.10
76	19.196	789.44	21.30
77	19.29	791.36	18.95
78	19.351	792.60	13.14
79	19.48	795.20	6.84
80	19.605	797.71	17.03
81	19.72 octane	800.00	75.29
82	19.908	804.93	28.53
83	20.037 2,4,4,trimethylhexane	808.29	7.86
84	20.207	812.68	8.08
85	20.464 2,3,5,trimethylhexane	819.25	20.78
86	20.64	823.70	9.83
87	20.755 2,4,dimethylheptane	826.59	11.80
88	20.937	831.13	8.00
89	21.02	833.19	25.17
90	21.138	836.10	15.90
91	21.308 3,5,dimethylheptane	840.26	42.61
92	21.52	845.41	6.00
93	21.633	848.13	8.55
94	21.871 ethylbenzene	853.82	159.76
95	22.01	857.11	9.48
96	22.227 m,p, xylene	862.21	657.45
97	22.497 2,methyloctane	868.49	73.92
98	22.789 3,methyloctane	875.19	51.95
99	23.028 styrene	880.61	13.41
100	23.188 o,xylene	884.21	254.99
101	23.422	889.43	31.12
102	23.573	892.77	3.91
103	23.698	895.52	8.74
104	23.903 nonane	900.00	46.09
105	24.084	905.00	1.79
106	24.265	909.97	6.99
107	24.38	913.10	2.27
108	24.513 I-propylbenzene	916.71	13.22
109	24.647	920.33	11.17
110	24.758	923.31	6.12
111	24.964	928.80	9.95
112	25.131	933.23	4.44
113	25.187	934.70	7.83
114	25.326	938.35	15.05
115	25.422	940.86	2.45
116	25.571	944.74	5.63
117	25.696 n-propylbenzene	947.97	50.87
118	25.976 1-ethyl-3-methylbenzene	955.16	180.20
119	26.066 1-ethyl-4-methylbenzene	957.45	78.26
120	26.277 1,3,5,trimethylbenzene	962.80	95.34
121	26.38 4,methylnonane	965.39	14.75
122	26.484	968.00	35.23
123	26.69 1,ethyl-2-methylbenzene	973.14	83.77
124	26.924 3-methylnonane	978.93	3.76
125	27.009	981.02	6.64
126	27.267 1,2,4,trimethylbenzene	987.33	314.69
127	27.554	994.27	2.92
128	27.698	997.73	4.21
129	27.793 c10	1000.00	16.28
130	27.967	1005.11	5.32
131	28.342 1,2,3,trimethylbenzene	1016.02	83.66
132	28.602	1023.50	3.15
133	28.708	1026.52	3.68
134	28.815 indan	1029.57	38.33
135	29.142	1038.81	9.04
136	29.309 1,3,diethylbenzene	1043.49	15.29
137	29.406 1-methyl-3-propylbenzene	1046.20	39.01
138	29.564	1050.58	17.42
139	29.63 1,2,diethylbenzene	1052.41	46.79
140	29.779	1056.52	5.74
141	29.934	1060.77	4.38
142	30.015 1,-methyl-2-propylbenzene	1062.98	15.72
143	30.173	1067.28	6.66
144	30.352 1,4,-dimethyl-2-ethylbenzene	1072.12	26.87

146	30.534	1077.02	4.96
147	30.642 1.2.-dimethyl-4-ethylbenzene	1079.91	35.95
148	30.722	1082.05	11.04
149	30.897	1086.70	2.53
151	31.172	1093.95	1.37
152	31.275	1096.66	3.07
153	31.403 c11	1100.00	13.22
155	31.581	1105.82	1.80
156	31.82 1.2.4.5.-tetramethylbenzene	1113.58	19.69
157	31.945 1.2.3.5.-tetramethylbenzene	1117.62	31.12
158	32.28	1128.36	1.52
159	32.45	1133.77	4.60
160	32.597	1138.42	14.64
161	32.702	1141.73	3.80
162	32.791	1144.53	2.36
163	32.889	1147.60	1.28
164	32.967	1150.04	16.56
165	33.075	1153.41	12.01
166	33.326	1161.19	5.73
167	33.517	1167.08	6.35
168	33.764	1174.64	4.05
169	33.935	1179.84	2.92
170	34.064	1183.75	10.92
171	34.244	1189.17	3.88
172	34.32	1191.46	2.01
173	34.397	1193.76	1.35
174	34.606 c12	1200.00	8.90
176	34.921		2.54
178	36.337		1.36
179	37.375		1.23
180	40.457		4.00

[TNMOC](ppbC)	10258
[Sspeciated VOC's](ppbC)	10001.47
[TNMOC]/[Sspeciated VOC's]	1.02565
Alkanes(ppbC)	4891.325
Alkenes(ppbC)	251.5651
Aromatics(ppbC)	3094.693
Oxygenates(ppbC) (MTBE)	710.1419
Unspeciated(ppbC)	1053.745
Alkanes (%)	48.90606
Alkenes(%)	2.515281
Aromatics(%)	30.94238
Oxygenates(%)	7.100376
Unspeciated(%)	10.53591

8. Conclusions

The technique to measure TNMOC centers on a cryogenic separation (on an inert surface) of reactive carbon from the carbon oxides and methane. After separation, the isolated organic material is oxidized to carbon dioxide, allowing quantification. The sample comes in contact only with a sampling tube and heated valve before passing through the primary trap. The target TNMOC condenses, while carbon monoxide, methane and most of the carbon dioxide pass through. Next, the primary trap is briefly purged with helium to remove residual carbon oxides and methane. In the second step, the trap is rapidly heated; and a helium/oxygen mix sweeps the desorbed TNMOC into an oxidation catalyst where it is converted to carbon dioxide. The carbon dioxide is focused in a second trap, desorbed, reduced to methane and quantified with a flame ionization detector. Assuring that all relevant classes of compounds are detected at 100% is crucial to a TNMOC analyzer. Under an earlier contract, we determent that under normal operating conditions all aldehydes and alcohols tested trap at 100%; including formaldehyde, and that there is no interference from water. During this contract period, we established that the organic carbon in the particulate phase (which we do not filter) contributes less than 2% to the TNMOC.

A second air sample is collected simultaneously in a parallel trap under identical conditions, and this sample is analyzed for individual hydrocarbons and a few other organic components. Taken together, these individual compounds make up the "volatile organic compounds" (VOC's) that are measured by standard techniques. This sample is transferred directly to the focusing trap, and from there it is directed into a gas chromatograph. The speciated channel may also be used to determine individual VOC concentrations. This analysis is very similar to the Photochemical Assessment Monitoring Station (PAMS) hydrocarbon analysis, and it has performed well in intercomparisons with PAMS type measurements.

Dozens of smog chamber experiments have been carried out to investigate the oxidation chemistry and ozone formation from hydrocarbons. Few of these experiments can account for 100% of the reacted carbon as products, and less than 40% is common. As the starting hydrocarbons become oxidized, their products become progressively less volatile and more polar. Some of the products may deposit on the walls of the reactor, form aerosols, or deposit in the gas chromatograph or inlet. In a sense, measuring total carbon in a smog chamber experiment is the "acid test" for a TNMOC analyzer. Results show that the TNMOC measurement works well, in detecting greater than 90% of the oxidized products from both m-xylene (C_9), and isoprene (C_5), and it detects roughly 75% of α-pinene (C_{10}) photooxidation products.

The TNMOC analyzer was deployed to make five measurements series during 1999-2001, and the results are shown in Table 8.1. Three series were collected at the University of California at Los Angeles (UCLA) during August 1999, September-October and November-December 2000, one was collected at Burbank during September 1999, and a final set of measurements were made at the California Air Resources Board's heavy duty truck dynamometer during April 2001. At UCLA and Burbank, nitrogen oxides, ozone, and meteorological data were logged simultaneously with the VOC analyses. Gasoline vapor was also investigated. For the gasoline vapor, a dominant source of VOC's in ambient air, the speciated measurement not surprisingly does an excellent job of detecting most VOC's; the TNMOC/sum of speciated VOC's ratio is only about 1.06 ± 0.02. The TNMOC/sum of speciated VOC's ratio observed for diesel exhaust was 1.2 ± 0.16. The Burbank site, which is located near the intersection of several freeways and in a light industrial area dominated by auto body shops, had an average ratio of 1.1 ± 0.08. Measurements made at UCLA during winter had a

TNMOC/sum of speciated VOC's ratio of 1.1 ± 0.06. The excess TNMOC (that portion unmeasured by the speciated channel) was much higher at UCLA during the smog season, averaging 1.41 ± 0.14 and 1.37 ± 0.06 on clear days in 1999 and 2000 respectively and 1.77 ± 0.10 on cloudy days, during 2000. All confidence intervals are twice the standard deviations of the means. In an earlier study we reported a TNMOC/sum of speciated VOC's ratio of 1.3 ± 0.3 for Azusa.

Table 8.1 Summary of TNMOC/sum of speciated VOC's Ratios for All Measurement Series

Site/Source	Meteorology	TNMOC (ppbC)	Sum of Speciated VOC's(ppbC)	TNMOC/ of Speciated VOC's
Gasoline Vapor	—	—	—	1.06 2 $_{mean}$= 0.02 1.02-1.10
Diesel Exhaust range	—	—	—	1.2 ± 0.2 2 $_{mean}$= 0.16 1.0-1.6
Burbank 8/99	Clear	2300 ± 640 2 $_{mean}$= 250 740-4000	2070 ± 510 2 $_{mean}$= 200 730-3000	1.11 ± 0.18 2 $_{mean}$= 0.08 0.8-1.4
UCLA 8-9/99 range	Clear	380 ± 170 2 $_{mean}$= 60 120-880	260 ± 99 2 $_{mean}$= 35 80-520	1.41 ± 0.41 2 $_{mean}$= 0.14 0.8-2.4
UCLA 9-10/00 range	Clear	329±178 2 $_{mean}$= 32 91-835	245±132 2 $_{mean}$= 26 71-598	1.37±0.26 2 $_{mean}$= 0.06 1.02-2.7
UCLA 9-10/00 range	Cloudy	205±120 2 $_{mean}$= 26 68-620	121±82 2 $_{mean}$= 18 38-444	1.77±0.48 2 $_{mean}$= 0.10 1.12-3.44
UCLA 11-12/00 range	Cloudy	269±172 2 $_{mean}$= 38 35-889	248±164 2 $_{mean}$= 36 31-819	1.1 ± 0.16 2 $_{mean}$= 0.04 1.0-2.13
Azusa* 1997	Clear	530 ± 200 2 $_{mean}$= 44 150-1250	410 ± 150 2 $_{mean}$= 33	1.29 ± 0.27 2 $_{mean}$= 0.06 0.6-2.2

* During these measurements, TNMOC and sum of speciated VOC's ratio analyses were made sequentially, so much of the variability may be due to real differences between airmasses.

The pattern that emerges form these data is as follows. The source materials, the site dominated by fresh emissions, and wintertime data have ratios close to 1.0, indicating little unmeasured or "excess" VOCs.; the speciated measurements seem to underestimate the total organics by 20% or less. This group of measurements includes gasoline vapor, Diesel exhaust, and data from Burbank and UCLA during late November-December. Sites influenced by photochemistry with a smaller contribution from fresh emissions have higher levels of excess organics relative to the standard measurements. This group includes UCLA during August-October and Azusa. but the excess organics appear to be associated with air that has been aged for longer periods than the 4-8 hours associated with diurnal ozone formation.

For the data that are influenced by photochemistry, lower average ratios are associated with higher average VOC concentrations. Examination of the NO_x data confirms the contribution of fresh emissions to high VOC concentrations. This together with several other results seems to indicate that much of the excess VOC's comes from carryover from pollutants that have been aged for a day or more. The result that cloudy days have much higher TNMOC/sum of speciated VOC's ratios than do clear days is consistent with this hypothesis because mixing heights are several times higher on cloudy summer and fall days than clear days, thus pollutants stored aloft can mix down to the surface. The aromatics data from the speciated channel show that the TNMOC/sum of speciated VOC's ratio is positively correlated with increased depletion of aromatics with lifetimes longer than several hours. The TNMOC/sum of speciated VOC's ratio is also positively correlated with an increased contribution of oxygenates, and with O_3 in the early morning when O_3 is a tracer for pollutant carryover rather than surface emission control of the VOC concentrations. Pollutant carryover would be expected to make a larger contribution on weekend days than on weekdays, but we do not have a sufficient number of days of data during the smog season to determine a weekend effect.

In summary, the standard measurements significantly underestimate VOC concentrations during the smog season except near fresh emission sources and thus underestimates the VOC/NO_x ratio. The identity and importantly, the reactivity of this unmeasured organic carbon is still to be determined.

9. References

1. Ridley, B.A., J.D. Shetter, J.G. Walega, S. Madronich, C.M. Elsworth, C.M. Grahek, F.C. Fehsenfeld, R.B. Norton, D.D. Parrish, G. Hubler, M. Buhr, E.J. Williams, E.J. Allwine, and H.H. Westburg, *The behavior of some organic nitrates at Niwot Ridge, Colorado.* J. Geophys. Res., 1990. **95**: p. 13949-13961.
2. Bakwin, P.S., S.C. Wofsy, and S.M. Fan, *Measurements of reactive nitrogen oxides (NOy) within and above a tropical forest canopy in the wet season.* J. Geophys. Res., 1990. **95**: p. 16765-16772.
3. Stillman, S., J.A. Logan, and S.C. Wofsy, *The sensitivity of ozone to nitrogen oxides and hydrocarbons in regional ozone episodes.* J. Geophys. Res., 1990. **95**: p. 1837-1851.
4. Carroll, M.A. and A.M. Thompson, *NOx in the non-urban troposphere*, in *Current Problems and Progress in Atmospheric Chemistry*, J. Barker, Editor. 1996, World Scientific Publishing Co. p. 198-255.
5. Hubler, G., D.D. Montzka, R.B. Norton, P.C. Murphy, F.C. Fehsenfeld, S.C. Liu, B.A. Ridley, J.G. Walega, E. Atlas, F.E. Grahek, L.E. Heidt, J. Merrill, B.J. Huebert, and B.A. Bodhaine, *Total reactive nitrogen (NO_y) in the remote pacific troposphere and its correlation with O_3 and CO: Mauna Loa observatory photochemistry experiment 1988.* J. Geophys. Res., 1992. **97**(D10): p. 10427-10447.
6. Fahey, D.W., G. Hubler, D.D. Parrish, E.J. Williams, R.B. Norton, B.A. Ridley, H.B. Singh, S.C. Liu, and F.C. Fehsenfeld, *Reactive nitrogen species in the troposphere: measurements of NO, NO_2, HNO_3 , particulate nitrate, peroxyacetyl nitrate (PAN), O_3, and total reactive odd nitrogen (NO_y) at Niwot Ridge, Colorado.* J. Geophys. Res., 1986. **91**: p. 9781-9793.
7. Singh, H.B., *Reactive nitrogen in the troposphere.* Environ. Sci. Technol., 1987. **21**: p. 320-327.
8. Atlas, E., *Evidence for >= C_3 alkyl nitrates in rural and remote atmospheres.* Nature, 1988. **331**(6155): p. 426-428.
9. Ghosh, T.K. and A.L. Hines, *Adsorption of acetaldehyde, propionaldehyde, and butyraldehyde on molecular seive 13x.* Separation Sci. Technol., 1991. **26**: p. 931-945.
10. Sigsby, J.E., D.L. Dropkin, and R. Snow, *Resolution of apparent underestimation in flame ionization detector hydrocarbon analysis.* Environ. Sci. Technol., 1990. **24**: p. 818-821.
11. Zielinska, B., J.C. Sagebiel, G. Harshfield, A.W. Gertler, and W.R. Pierson, *Volatile organic compounds up to C20 emitted from motor vehicles; measurement methods.* Atmos. Environ., 1996. **30**: p. 2269-86.
12. Cao, X.-L. and C.N. Hewitt, *Build-up of artifacts on adsorbents during storage and its effect on passive sampling and gas chromatography-flame ionization*

detection of low concentrations of organice compounds in air. J. Chrom. A, 1994. **668**: p. 368-74.

13. Kelly, T.J., P.J. Callahan, J. Piell, and G.F. Evans, *Method development and field measurements for polar volatile organic compounds in ambient air.* Envir. Sci. Tech., 1993. **27**: p. 1146-1153.
14. Madronich, S. and J.G. Calvert. *Theoretical study of tropospheric oxidation of Hydrocarbons: oxidant generation and organic product distribution.* in *Proc. Int'l. Conf. Global and Regional Envir. Atmos. Chem.* 1989.
15. Kwok, E., S. Aschmann, J. Arey, and R. Atkinson, *Product formation from the reaction of the no3 radical with isoprene and rate constants for the reactions of methacrolein and methyl vinyl ketone with the NO3 radical.* Int'l J. Chem. Kinet., 1996. **28**: p. 925-34.
16. Carter, W.P.L. and R. Atkinson, *Development and evaluation of a detailed mechanism for the atmospheric reactions of isoprene and NO_x.* Intl. J. Chem. Kinet., 1996. **28**: p. 497-530.
17. Paulson, S.E., R.C. Flagan, and J.H. Seinfeld, *Atmospheric Photooxidation of Isoprene. Part 1: The Reactions of Isoprene with Hydroxyl Radical and Ground State Atomic Oxygen.* Intl. J. Chem. Kinet., 1992. **24**: p. 79-102.
18. Roberts, J.M., S.B. Bertman, T. Jobson, H. Niki, and R. Tanner, *Measurement of total nonmethane organic carbon (C-y): Development and application at Chebogue Point, Nova Scotia, during the 1993 North Atlantic Regional Experiment campaign.* J. Geophys. Res. Atmos., 1998. **103**: p. 13581-92.
19. Alastair, C., N. Carslaw, P. Marriott, R. Kinghorn, P. Morrison, A. Lee, K. Bartle, and M. Pilling, *A larger pool of ozone-forming carbon compounds in urban atmospheres.* NATURE, 2000. **405**: p. 778-781.
20. Howe, G.B., S.K. Gangwal, and R.K.M. Jayanty, *Validation and improvement of EPA reference method 25-determination of gaseous nonmethane organic emissions as carbon.*, . 1983, U.S. EPA.
21. Jayanty, R., S. Tompkins, R. Fuerst, T. Logan, and D.J. VonLehmden, *Performance audit results using EPA method 25 during source compliance tests.* J. Air & Waste Manage. Assoc., 1990. **40**(1): p. 38-41.
22. Salo, A.E., W.L. Oaks, and R.D. MacPhee, *Measuring the organic carbon content of Source emissions for air pollution control.* J. Air Poll. Cont. Assoc., 1975. **25**(4): p. 390-393.
23. Finlayson-Pitts, B.J. and J. Pitts, *Atmospheric Chemistry: Fundamentals and Experimental Techniques.* 1986, New York: Wiley-Interscience.
24. Mayrsohn, H., M. Kuramoto, J.H. Crabtree, R.D. Sothern, and S. Mano, *Atmospheric hydrocarbon concentrations, June-Sept., 1974*, . 1975, Report to State of California Air Resources Board.
25. Nelson, P.F. and S.M. Quigley, *Non-methane hydrocarbons in the atmosphere of Sydney, Australia.* Env. Sci. Tech., 1982. **16**: p. 650-655.
26. Sexton, K. and H. Westberg, *Nonmethane hydrocarbon composition of urban and rural atmospheres.* Atmos. Environ., 1984. **18**: p. 1125-1132.
27. Jorgensen, A.D., K.C. Picel, and V.C. Stamoudis, *Prediction of gas chromatography flame ionization detector response factors from molecular structures.* Anal. Chem., 1990. **62**: p. 683-689.

28. Fujita, E.M., B.E. Croes, C.L. Bennett, D.R. Lawson, F.W. Lurmann, and H.H. Main, *Comparison of emission inventory and ambient concentration ratios of CO, NMOG, and NOx in California's South Coast Air Basin.* J. Air. Waste. Manage. Assoc., 1992. **42**: p. 264-276.
29. Blake, N.J., S.A. Penkett, K.C. Clemitshaw, P. Anwyl, P. Lightman, A.R.W. Marsh, and G. Butcher, *Estimates of atmospheric hydroxyl radical concentrations from the observed decay of many reactive hydrocarbons in well-defined urban plumes.* J. Geophys. Res., 1993. **98**: p. 2851-2864.
30. Guenther, A., P. Zimmerman, L. Klinger, J. Greenberg, C. Ennis, H. Westberg, G. Allwine, and C. Geron, *Estimates of regional natural volatile organic compound fluxes from enclosure and ambient measurements. J. Geophys. Res*, 1996. **101**: p. 1345-1359.
31. Oliver, K.D., J.R. Adams, J.E.H. Daughtrey, W.A. McClenny, M.J. Young, and M.A. Pardee, *Technique for monitoring ozone precursor hydrocarbons in air at photochemical assessment monitoring stations-sorbent preconcentration, closed cycle cooler cryofocussing, and GC-FID analysis. Atmos. Environ*, 1996. **15**: p. 2751-2757.
32. Fraser, M.P., G.R. Cass, B.R.T. Simonet, and R.A. Rasmussen, *Air quality model evaluation data for organics. 4. C2-C36 non-aromatic hydrocarbons.* Envir. Sci. Technol., 1997. **31**: p. 2356-67.
33. Guenther, A., C.N. Hewitt, D. Erickson, R. Fall, C. Geron, T. Graedel, P. Harley, L. Klinger, M. Lerdau, W. McKay, T. Pierce, B. Scholes, R. Steinbrecher, R. Tallamraju, J. Taylor, and P. Zimmerman, *A global model of natural volatile organic compound emissions.* J. Geophys. Res., 1995. **100**(5): p. 8873-92.
34. Bierbach, A., I. Barnes, K.H. Becker, B. Klotz, and E. Wiesen. *OH-Radical initiated degradation of aromatic hydrocarbons*. in *Physio-Chemical Behaviour of Atmospheric Pollutants*. 1993. Varese, Italy: European Commission.
35. Paulson, S.E. and J.H. Seinfeld, *Atmospheric photooxidation of 1-Octene: OH, O_3, and $O(^3P)$ reactions.* Env. Sci. Technol., 1992. **26**: p. 1165-1173.
36. Kwok, E.C., R. Atkinson, and J. Arey, *Observation of hydroxycarbonyls from the OH radical initiated reaction of isoprene.* Envir. Sci. Tech., 1995. **29**: p. 2467-9.
37. Griffin, R.J., D.R. Cocker, and J.H. Seinfeld, *Incremental aerosol reactivity: application to aromatic and biogenic hydrocarbons.* Envir. Sci. Tech., 1999. **33**: p. 2403-8.
38. Klotz, B., I. Barnes, and K. Becker, *New results on the atmospheric photooxidation of simple alkylbenzenes.* Chem. Phys., 1998. **231**: p. 289-301.
39. Griffin, R.J., D.R. Cocker, J.H. Seinfeld, and D. Dabdub, *Estimate of global atmospheric organic aerosol from oxidation of biogenic hydrocarbons.* Geophys. Res. Lett., 1999. **26**: p. 2721-2724.
40. Wangberg, I., I. Barnes, and K.H. Becker, *Product and mechanistic study of the reaction of NO3 radicals with a-pinene.* Env. Sci. Tech., 1997. **31**: p. 2130-5.
41. Kavouras, I., N. Mihalopoulos, and E.G. Stephanou, *Secondary organic aerosol formation vs. primary organic aerosol emission: in situ evidence for the chemical coupling between monoterpene acidic photooxidation products and new particle formation over forests.* Environ. Sci. Tech., 1999. **33**: p. 1028-1037.

42. Singh, H.B., ed. *Composition, Chemistry and Climate of the Atmosphere*. . 1995, Van Nostrom Reinhold: New York.
43. Seinfeld, J.H. and S. Pandis, *Atmospheric Chemistry and Physics*. 1997, New York: Wiley Interscience.
44. Roberts, J.M., F.C. Fehsenfeld, S.C. Lui, M.J. Bollinger, C. Hahn, D.L. Albritton, and R.E. Sievers, *Measurements of aromatic hydrocarbon ratios and NOx concentrations in the rural troposphere: observation of air mass photochemical aging and NOx removal.* Atmos. Environ., 1984. **18**: p. 2421 - 32.
45. Nelson, P.F. and S.M. Quigley, *The m,p-xylenes:ethylbenzene ratio. A technique for estimating hydrocarbon age in ambient atmospheres.* Atmos. Environ., 1983. **17**(3): p. 659-62.
46. Atkinson, R., *Gas-Phase Tropospheric Chemistry of Volatile Organic Compounds: 1. Alkanes and Alkenes.* J. Phys. Chem. Ref. Data, 1997. **26**(2): p. 215.
47. Kramp, F. and S.E. Paulson, *On the uncertainties in the rate coefficients for OH reactions with hydrocarbons, and measurement of rate coefficients of the 1,3,5-trimethylbenzene and m-xylene reactions with OH radicals in the gas-phase.* J. Phys. Chem., 1998. **102**: p. 2685-90.
48. Connor, T.L., W.A. Lonneman, and R.L. Seila, *Transportation related volatile hydrocarbon source profiles measured in Atlanta.* J. Air & Waste Manag. Assoc., 1995. **45**: p. 383-394.
49. Taylor, J.R., *An Introduction to Error Analysis*. first ed. 1982, Mill Valley, CA: University Science Books. 270.
50. Paulson, S.E., R. Meller, and M. Chung, *Final Report: Total non-methane organic carbon: Development and validation of a new instrument, and measurements of total non-methane organic carbon and C2-C7 hydrocarbons in the south coast air basin.*, . 1999, California Air Resources Board Report No. 95-335.
51. Jeffries, H.E., *Composition, Chemistry and Climate of the Atmosphere*, ed. H.B. Singh. 1995: VNR.
52. Schauer, M. Kleeman, Cass G.R., and B. Simoneit, *Characterization and Control of Organic Compounds Emitted from Air Pollution Sources*, . 1998, California Air Resources Board contract 93-329.
53. Zafonte, D.L., . 2001.
54. Fujita, E., W. Stockwell, and D. Campbell. *Weekend/weekday ozone study in the South Coast air basin.* in *Weekend Effect Work Group*. 2002. California Air Resources Board, Sacramento, CA: California Air Resources Board.

10. Glossary

Channel 1	TNMOC analysis channel
Channel 2	VOC analysis channel
FID	Flame Ionization Detector
GC	Gas Chromatograph
PAMS	Photochemical Assessment Monitoring Stations
SCAQMD	South Coast Air Quality Management District
TNMOC	Total Non-Methane Organic Carbon
VOC	Volatile Organic Compound
ARB	Air Resources Board